Fall 1-1-2017

The neonatal anti-viral response fails to control measles virus spread in neurons despite interferon-gamma expression and a Th1-like cytokine profile

Priya Ganesan

THE NEONATAL ANTI-VIRAL RESPONSE FAILS TO CONTROL MEASLES VIRUS

SPREAD IN NEURONS DESPITE INTERFERON-GAMMA EXPRESSION AND A

TH1-LIKE CYTOKINE PROFILE

A Dissertation

Submitted to the Graduate School of Pharmaceutical Sciences

Duquesne University

In partial fulfillment of the requirements for

the degree of Doctor of Philosophy

By

Priya Ganesan

December 2017

THE NEONATAL ANTI-VIRAL RESPONSE FAILS TO CONTROL MEASLES VIRUS

SPREAD IN NEURONS DESPITE INTERFERON-GAMMA EXPRESSION AND A

TH1-LIKE CYTOKINE PROFILE

By

Priya Ganesan

Approved November 12, 2017

Lauren A. O'Donnell, Ph.D.
Associate Professor of Pharmacology
Graduate School of Pharmaceutical Sciences
Duquesne University, Pittsburgh, PA
(Committee Chair)

Paula A. Witt-Enderby, Ph.D.
Professor of Pharmacology
Graduate School of Pharmaceutical Sciences
Duquesne University, Pittsburgh, PA
(Committee Member)

Wilson S. Meng, Ph.D.
Associate Professor of Pharmaceutics
Graduate School of Pharmaceutical Sciences
Duquesne University, Pittsburgh, PA
(Committee Member)

Dr. Christopher Surratt
Professor of Pharmacology
Graduate School of Pharmaceutical Sciences
Duquesne University, Pittsburgh, PA
(Committee Member)

Dr. Kerry Empey
Assistant Professor
Graduate School of Pharmaceutical Sciences
University of Pittsburgh, Pittsburgh, PA
(Committee Member)

James K. Drennen, III, Ph.D.
Associate Dean and Associate Professor
of Pharmaceutics
Duquesne University Graduate School of
Pharmaceutical Sciences

J. Douglas Bricker, Ph.D.
Dean, Duquesne University School of
Pharmacy and the Graduate School of
Pharmaceutical Sciences

ABSTRACT

THE NEONATAL ANTI-VIRAL RESPONSE FAILS TO CONTROL MEASLES VIRUS

SPREAD IN NEURONS DESPITE INTERFERON-GAMMA EXPRESSION AND A

TH1-LIKE CYTOKINE PROFILE

By

Priya Ganesan

December 2017

Dissertation supervised by Dr. Lauren A. O'Donnell

Neonates are highly susceptible to infections in the central nervous system (CNS) and have a greater risk of viral infections and encephalopathies. Neurotropic viral infections can lead to blindness, hearing loss and neurological deficiencies such as cognitive impairment, epilepsy, and even death in the neonatal and pediatric populations. Viral infections also are hypothesized to indirectly contribute to neurodegenerative and neuropsychiatric diseases such as Schizophrenia and Parkinson's disease later in life due to early neuronal damage or stress. Many diverse viruses are capable of invading the neonatal CNS including Borna Disease Virus, Coxsackievirus (CV), Herpes simplex viruses (HSV), and measles virus. Although, we understand that many viruses can cause CNS disease, the mechanisms of viral pathogenesis in the brain and the character of the neonatal anti-viral immune response are not well understood. However, it is hypothesized that neurological damage results from the combined effect of the virus and the immune response.

Therefore, it is critical to develop immune-mediated strategies to promote viral clearance from the CNS while preventing neuronal damage or loss. This remains a challenge during neonatal CNS infections because of the uniquely immature nature of the neonatal immune system and the sensitivity of developing neurons to inflammation. In order to better understand how the neonatal immune response behaves in the brain, we use neurotropic measles virus (MV) as a model to understand the deficits in the neonatal immunity. Measles is a single-stranded, negative-sense RNA virus that is highly contagious in humans. Typical infection involves inhalation of infected respiratory droplets, infection of dendritic cells and macrophages in the respiratory tract resulting in transient immunosuppression, and a characteristic fever and rash. However, in some cases, MV also causes severe neurological diseases such as Post-infectious encephalomyelitis (PIE), Subacute sclerosing panencephalitis (SSPE), and Measles inclusion body encephalitis (MIBE). Currently, there is no cure for these MV-related neurological conditions, which occur overwhelmingly in newborns and children. Thus, the goal of this project is to define how neonatal immunity responds to MV infection in the unique microenvironment of the brain.

The role of interferon-gamma (IFNγ), a key anti-viral cytokine in controlling adult CNS infections, was explored during a neuronally-restricted MV infection in the neonatal brain. We hypothesized that neonatal mice would be deficient in either IFNγ production or in the infiltration of IFNγ-producing immune cells in the brain. In order to address this question, we utilized the CD46+ mouse model, in which the human CD46+ receptor for MV is expressed only in mature neurons of the CNS. We explored the differences in the neonatal immune response, where the mice succumb to MV infection, and compared that to the CD46+ adults, which successfully control MV and survive. Our findings suggest that IFNγ, which is critical for viral control and survival in

adults, only delays mortality in CD46+ neonates. The neonatal brains also show the infiltration of natural killer cells, neutrophils, infiltrating monocytes and T cells in an IFNγ-independent manner, all of which are capable of contributing to the IFNγ pool. However, neonates and adults differentially express pathogen recognition receptors (*e.g.* Toll-like receptors) and Type I interferons during infection in the CNS, which suggests that the initial recognition of the virus by the immune system may differ in an age-dependent manner. Both neonates and adults expressed IFNγ, CXCL10, IL-1, and IL-1RA, among other cytokines/chemokines. Regardless, CD46+ neonates succumb to infection despite mounting a Th1-like, but apparently defective, inflammatory response. We further explored whether there are age-dependent differences in IFNγ signalling given that both ages of mice expressed this critical cytokine. Both neonatal and adult CD46+ mice express similar levels of IFNγ but only adults show robust induction of the IFNγ-responsive genes CIITA and CXCL9. This suggests that IFNγ signaling may be defective in the induction of IFNγ-responsive genes in neonates compared to adults.

To dissect the role of individual components of the immune system, we utilized CD46+ mice crossed to specific immune knockouts: CD46+/IFNγ-KO mice, which lack IFNγ, and CD46+/RAG2-KO mice, which lack mature B and T cells. We found that neonates lacking IFNγ succumbed more rapidly than wildtype CD46+ mice, while neonates lacking mature B and T cells showed delayed morbidity and mortality. Neonates without IFNγ show high infiltration of neutrophils and inflammatory monocytes but similar numbers of NK cell infiltration compared to CD46+ neonates. CD46+/IFNγ-KO neonatal brains also show high infiltration of CD4 and CD8 T cells at the later stages of MV infection. Additionally, IFNα is significantly upregulated in the absence of IFNγ in the brain post-MV infection. Thus, compensatory cytokines and high immune

cell infiltration may contribute to uncontrolled inflammation and earlier death in CD46+/IFNγ-KO neonates. CD46+ mice deficient in T-cells and B-cells (CD46+/RAG2-KO) show prolonged survival and mount a robust IFNβ response post-MV infection. This suggests that the adaptive immune response may be detrimental during the neonatal period, potentially leading to greater tissue damage. Additionally, CD46+/RAG2-KO neonates alone upregulate unique genes such as bone morphogenetic proteins (BMPs), which may mediate neuroprotection. Thus, these results suggest age-dependent expression of cytokine profiles in the brain and distinct dynamic interplays between lymphocyte populations and cytokines/chemokines in MV-infected neonates.

DEDICATION

To my parents, Savithri and Ganesan Rajamani, and my sister Gowri Ganesan whose continuous

support, sacrifices, love and strength throughout my life made this possible.

ACKNOWLEDGEMENTS

I derive all my inspiration from my strong role models, my Mother, Father, and Gowri who have been supportive throughout my life. I also want to thank my grandparents and my in-laws for giving importance to education and for their encouragement. I would like to acknowledge the sacrifices of my mother, Savithri Ganesan and my father Ganesan Rajamani for their unconditional love, unwavering support, and enthusiasm. Lastly, I thank my husband, Vinod Mahalingam for being my best friend, for unconditional support and love, and for bringing me to Pittsburgh, without which this would not have been possible.

TABLE OF CONTENTS

CHAPTER 3: **Role of IFNγ-producing innate and adaptive immune cells during a
neurotropic measles virus infection**

CHAPTER 4: **Neonates succumb to the infection despite a Type I and II interferon expression in the CNS**

LIST OF FIGURES

LIST OF TABLES

LIST OF ABBREVIATIONS

Abs: Antibodies; ANOVA: Analysis of variance; APC: Allophycocyanin; ATCC: American Type Tissue Collection; BMP: bone morphogenetic protein; CIITA: Class II CMV: Cytomegalovirus; Major Histocompatibility Complex Transactivator; DPI: days post-infection; FITC: Fluorescein isothiocyanate; Iba1: Ionized Calcium-Binding Adapter Molecule 1; IFN: Interferon; IFNα: Interferon-alpha; IFNβ: Interferon-beta; IFNγ: Interferon-gamma; KO: Knockout; MV: Measles virus; MDA5: melanoma differentiation-associated gene 5; MHC: Major histocompatibility complex; NK cell: Natural killer cell; NSE: Neuron-specific enolase; N: Nucleocapsid; N.S: Not significant; PRR: Pattern recognition receptors; PFU: Plaque forming unit; PFA: Paraformaldehyde; PE: Phycoerythrin; RIGI: retinoic acid-induced gene-1; TNF: tumor necrosis factor; TLRs: Toll-like receptors

CHAPTER 1: LITERATURE REVIEW

1. Introduction

1.1 Neonatal infections

Although smallpox and polio have been largely eradicated, various pathogens can cause damage to the fetus *in utero* and in young children.L Pathogens that can infect during pregnancy and during the early neonatal period include the TORCH pathogens (*Toxoplasma gondii,* Rubella virus, Cytomegalovirus (CMV), and Herpes simplex viruses (HSV)), *Treponema pallidum*, Respiratory syncytial virus (RSV), Zika virus and Measles virus (MV) (Adams Waldorf and McAdams, 2013, Marodi, 2006). Many of these infections are common in developing countries (MV, Toxoplasma), whereas some infections remain common worldwide (CMV, HSV). Although, this diverse group of pathogens may have different mechanisms of replication, they each contribute to greater neuropathology and neurological changes in younger hosts.

MV is a highly transmissible virus with an R_0 value of 15, meaning that one infected person will infect 15 other people on average (Griffin et al. , 2008). MV is associated with high infant mortality although, it is vaccine-preventable. In 2014, 267,000 measles cases were reported and 146,000 estimated deaths, mostly in young children worldwide. According to the CDC, there was a 75% decline in measles deaths from 2000-2013 (15.6 million deaths prevented). But in 2017, till June 17th, there have been 117 reported cases of MV infection in the United States (Centers for Disease Control and Prevention, 2017). A two-dose vaccination approach has made significant strides towards global measles control. However, there is resurgence in MV and MV-related deaths due to logistical and financial challenges in sustaining the current mass campaign strategy in developing countries (Shibeshi et al. , 2014). In addition,

parental concerns about vaccine safety in addition to philosophical and religious objections has led to a resurgence of MV as an endemic disease in many industrialized nations, despite a lack of evidence between the MV vaccine and autism (Richard and Masserey Spicher, 2009) (Muscat et al. , 2009).

Table 1

Virus	CNS pathology
Cytomegalovirus	Encephalitis, epilepsy, blindness, deafness
Herpes Simplex Virus	Encephalitis, blindness, herpetic neuralgia
Zika Virus	Microcephaly, agyria
Eastern equine encephalitis virus	Panencephalitis, meningitis, cerebral edema
West Nile Virus	Encephalitis, meningitis, myopathy, paralysis
Human Immunodeficiency virus	Dementia, loss of motor function, encephalitis, myelitis
Borna Disease Virus	Schizophrenia, depression
Measles Virus	Encephalitis (PIE, SSPE, MIBE)
Japanese Encephalitis Virus	Seizures, acute flaccid paralysis
Coxsackie B virus	Epilepsy
Chikungunya virus	Altered consciousness, Seizures, Brain lesions and swelling
Varicella Zoster Virus	Vasculopathy of small and large cerebral vessels

Table 1: Neurotropic Viruses and associated neuropathologies

Neurons are terminally differentiated, long-lived cells. Neurotropic viruses may spread by axonal transport and move from neuron to neuron through interconnected synapses (Ehrengruber et al. , 2002). Certain neurotropic infections can be resolved, but in some cases excessive or chronic inflammation in the CNS can be have disastrous effects. The virus and/or the immune response can irreversibly disrupt the complex architecture of the brain. For example, human infections with variegated squirrel Borna virus-1 show the presence of brain lesions with edema, necrosis, and glial activation, and *in utero* infections with CMV are associated with lissencephaly and enlarged ventricles (Volpe, 2008) (Hoffmann et al. , 2015, Ludlow et al. , 2016). Thus, viral infections can lead to substantial alterations in the structure and subsequent function of the brain.

Viral infections in the CNS also are hypothesized to indirectly contribute to neurodegenerative and neuropsychiatric diseases later in life due to damage from a previous infection (*e.g.* schizophrenia, Parkinson's Disease) (Jang et al. , 2009, Khandaker et al. , 2013, Landreau et al. , 2012). Infection in the CNS is due to a failure in the immune surveillance mechanism and is common in immunocompromised hosts (Ito et al. , 2000, McArthur, 2004, Utley et al. , 1997). Thus, it is apparent that neurotropic viruses cause significant disease in the neonatal brain, but the functionality of the anti-viral immune response in the brain during the neonatal period is poorly understood. Therefore, it is essential to understand mechanisms that contribute to neuropathological and immunopathological alterations post viral entry into the CNS.

1.2 Mechanisms of cell death in the CNS

The resolution of infection varies depending on the tissue that is affected and on the type of invading pathogen (Miller et al. , 2016). We cannot tolerate the loss of non-renewable cells like neurons compared to lysis of renewable cells such as epithelial cells during infections. For example, HSV-1 causes severe immune and virus-mediated cell death of epithelial cells (Braaten et al. , 2005, Jones et al. , 2003, Paludan et al. , 2011). However, the lost cells are readily replaced, as observed by healing of a cold sore. In contrast, Human herpes virus Type 6 infections cause seizures and meningoencephalitis in children, which is characterized by neuronal loss with gliosis and microglial nodules in the temporal cortex (Forest et al. , 2011).

Neuronal loss and neuropathology during CNS infections may occur through direct infection and cytolysis by the virus, or through the inflammatory strategies that cause immune-mediated lysis of the virally-infected cell.   In the CNS, a more favorable immune response in the brain would be non-cytolytic towards infected neurons and maintain neuronal integrity (Miller, Schnell, 2016). But when lytic approaches occur, such as through granzymes and perforins, they carry the risk of irreversible damage and cell death to the infected neurons, which could contribute long-term neurological impairments.   In many adult CNS infection models, the pleiotropic cytokine interferon gamma (IFNγ) is key to suppressing viral spread while sparing the infected neurons through non-cytolytic clearance, thus limiting neuropathology and viral replication (Burdeinick-Kerr et al. , 2007, Hausmann et al. , 2005, Larena et al. , 2013, Patterson et al. , 2002, Stubblefield Park et al. , 2011). However, in neonates, viruses often spread rapidly in brain tissue despite the initiation of an immune response (Hausmann, Pagenstecher, 2005, Kopp et al. , 2014, Manchester et al. , 1999).

Although the anti-viral role of many immune cells and factors have been well studied, how immune cells behave in the brain to mediate non-cytolytic clearance is not as clear. Moreover, the impact of age on the function of the anti-viral response in the brain is largely undefined. In the next section, we review the current literature on immune cell function during viral infection and their roles in the CNS, and highlight any known differences based on the anatomical location of the infection (brain vs. peripheral organs) and age.

1.3   Immune clearance of neuronal infection

1.3.1 Innate immunity

The innate immune response occurs within minutes to hours after infection or injury, such as meningitis, stroke or other brain trauma (Reviewed in (Ransohoff and Brown, 2012). It is characterized by activation of pattern recognition receptors, which are expressed by all cell types in the brain. Activation of microglia (brain-specific macrophages) causes expression of proinflammatory mediators (chemokines and cytokines) followed by infiltration of other innate immune cells such as natural killer cells and neutrophils (Downes and Crack, 2010). The innate immune response is not antigen-specific, and thus it can be mounted quickly against a variety of insults.

1.3.2   Pattern recognition receptors (PRRs)

The innate immune system detects a viral infection by PRRs present either on the cell surface or within intracellular organelles. These PRRs include Toll-like receptors (TLRs), retinoic acid-induceble gene I-like receptor (RLRs), nucleotide oligomerization domain like receptors (NLRs), and cytosolic DNA sensor families. During viral infection, the virus replicates in different

compartments of the cell, where they are detected by the PRRs. These receptors recognize pathogen-associated molecular patterns (PAMPs) such as 5' triphosphate RNA, which is not normally found in host RNA or nucleic acids such as viral DNA or double-stranded RNA (Reviewed in (Thompson and Whitley, 2011).

RNA viruses, such as measles virus, are recognized by the cytoplasmic PRRs, retinoic acid-induced gene-I (RIGI) and MDA5, and the endosomal TLRs. TLR3, RIG-1, and MDA5 recognize double stranded RNA (dsRNA) molecules, which can be a replication intermediate or the functional genome of the virus, depending on the viral life cycle. TLR7/8 and TLR9 recognize viral single-stranded RNA (ssRNA) and DNA. The activation of these receptors lead to the induction of Type 1 interferons (IFNs), which are significant early steps in viral control (Akira et al. , 2006, Takeuchi and Akira, 2009, Yoneyama et al. , 2004, Zalinger et al. , 2015).

A. Toll like receptors (TLRs)

Various forms of viral nucleic acids are detected by TLR3, TLR7, TLR8, and TLR9 and play key roles in the recognition of viral genetic materials in endolysosomal compartments (Reviewed in (Lester and Li, 2014). All TLRs share a similar architecture consisting of extracellular leucine-rich repeats and a cytoplasmic Toll/Interleukin-1 Receptor (TIR) domain. TLRs are type I transmembrane protein that traffic between the plasma membrane and endosomal vesicle and recognize PAMPs in the extracellular environment. TLRs on the plasma membrane recognize hydrophobic lipids and proteins and those in the endosomes detect nucleic acids **(Figure 1).** TLR3, TLR7, TLR8 and TLR9 are endosomal receptors and signal through the adaptor protein myeloid differentiation primary response gene 88 (MyD88) (Kawai and Akira, 2008). TLR3 utilizes the

TIR domain containing adaptor inducing interferon-β (Trif) adaptor molecule. TLR3, in particular, has been shown to be induced by the MV-Edmonston strain in cell lines (Tanabe et al. , 2003). TLR stimulation leads to macrophage activation, followed by cytokine and chemokine production and initiation of adaptive immunity. Macrophage activation is defined by expression of major histocompatibility complex (MHC) class I and II molecules, which is induced by the IFNs that are triggered by TLR activation (Frei et al. , 2010).

PRRs are expressed by immune cells as well as in the CNS (Suh et al. , 2009). Both neurons and microglia express TLRs, RIG-1, and MDA5 and thus, play critical roles in the initiation of innate immunity (Nazmi et al. , 2011). There is evidence that intracellular TLRs in human neurons mediate viral recognition and initiation of the innate immune response during HSV-1 infection. Both IFNα and IFNβ are induced during neuronal HSV-1 infection as a result of TLR engagement (Zhou et al. , 2009). There is conflicting evidence on the functionality and expression of TLRs in neonates. Some studies suggest that newborns exhibit well developed TLR sensor function. Healthy children over the first 5 years of life appear to express stable TLRs and downstream signaling molecules at adult-like levels (Reviewed in (Kollmann et al. , 2012). Other studies indicate that murine neonatal intestinal epithelial cells fail to express TLR3 in response to rotavirus infection through post-natal days 1-10, which overlaps with the time points reflected in our studies (Pott et al. , 2012). Similarly, human cord blood samples do not induce TLR3 in response to poly(I:C) treatment or HSV activation in comparison to adult NK cells (Slavica et al. , 2013). Thus, the age-dependent effects of TLR induction and functionality in the neonatal CNS are not well understood.

B. Retinoic acid-inducible gene I-like receptors (RLRs)

The RLR family is comprised of MDA-5 and RIGI and sense PAMPs in viral RNA. The expression of RLRs are low in resting cells but increase during viral infection and due to IFN exposure (Reviewed in (Loo and Gale, 2011)). MDA5 expression is induced by the virus in cells without the IFN receptor, indicating that RLR expression is controlled by a direct virus-inducible signal (Yount et al. , 2007). Various families of virus such as Paramyxoviridae, Rhabdoviridae, Picornaviridae, and Orthomyxoviridae are recognized by RIGI and MDA5. Viruses such as Dengue virus, West Nile virus, and Reovirus are recognized by both MDA5 and RIGI. Studies suggest that mice lacking RIGI or MDA5 receptors are highly prone to RNA viral infections, highlighting the importance of these proteins in recognizing RNA viruses. (Reviewed in (Loo and Gale, 2011).

RLRs signal through the common adaptor mitochondrial antiviral signaling protein (MAVS) (Kawai and Akira, 2008). RIG1 and MDA5 share several similarities such as i) N-terminal region consisting of tandem caspase activation and recruitment domains (CARD) ii) a central DExD/H box RNA helicase domain with the capacity to hydrolyze ATP and to bind and unwind RNA, and iii) a C-terminal repressor domain (RD) for autoregulation. RIGI is present in the cytoplasm in resting conditions. During a viral infection, RIGI binds to PAMPs and undergoes a conformational change to release CARDs from RD. This conformational change results in formation of dimers in an ATP-dependent manner. The CARDs in the RIGI complex mediate signalling via mitochondrial antiviral signaling protein (MAVS). MDA5 also signals through downstream adaptor protein, MAVS, which in turn induces type I IFNs and host defense gene expression (Reviewed in (Loo and Gale, 2011)). Both TLRs and RLRs lead to activation NF-κB, MAP kinases and IRF3, resulting in production of pro-inflammatory and anti-viral response genes (Akira, Uematsu, 2006).

Figure 1
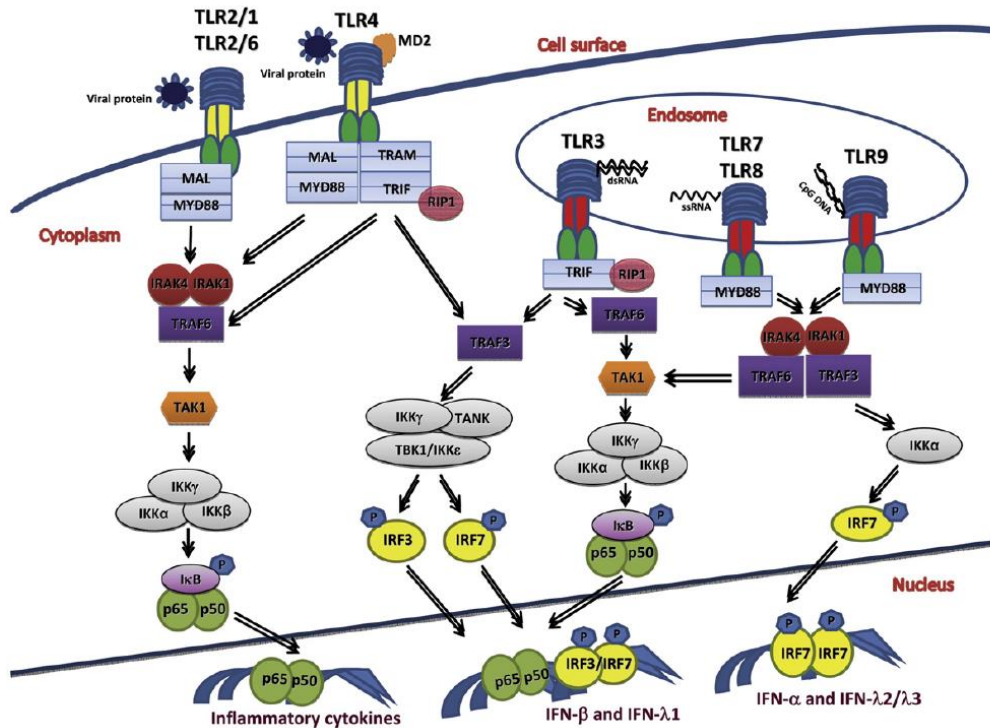
Figure 1. TLR signaling

TLRs recognize viral proteins such as dsRNA, ssRNA and CpG DNA and antiviral immune response is initiated. TLR2 and TLR4 are cell surface receptors and recognize viral proteins. TLR3, TLR7, TLR8, and TLR9 are intracellular receptors present on the endosomes and recognize viral dsRNA, ssRNA and unmethylated CpG DNA. All TLRs recruit MyD88 except TLR3. Both TLR3 and TLR4 recruit adaptor protein TRIF. Both MyD88 and TRIF-dependent signaling complexes activate transcription factors such as NF-KB, IRF3, and IRF7. Inflammatory cytokines and chemokine expression is regulated by NF-KB. Whereas IRF3 and IRF7 mediate the transcription of Type I IFN and type III IFN genes. **(**(Lester and Li, 2014); Reprinted from Toll-Like Receptors in Antiviral Innate Immunity, Volume 426, Issue 6, Sandra N. Lester, Kui Li, Pages 1246-1264, 20 March 2014, with permission from Elsevier**)**

1.3.3 Type I Interferon

After a virus, has initiated infection in a host cell, the early anti-viral response is started by sensing of pathogen associated molecular patterns (PAMPs) by pattern recognition receptors (PRR), which are expressed in all cells. The binding of conserved motifs such as single stranded RNA (ssRNA), double stranded RNA (dsRNA), and glycoproteins induces the production of the type I IFNs: IFNα and IFNβ. Type I IFNs are produced by infected cells and act in a paracrine and autocrine manner through IFNAα/β (IFNAR) receptor. Engagement of IFNα/β with the cognate receptor results and in phosphorylation of tyrosine kinases (Janus kinases) and tyrosine phosphorylation of cytoplasmic signal transducer and activator of transcription (STAT1) and STAT2. Activated heterodimers of STAT1-STAT2 bind to IFN regulatory factor 9 (IRF9) to form Interferon-stimulated gene factor 3 (ISGF3), which translocates to the nucleus and binds to IFN-stimulated response elements within the promoters of IFN-stimulated genes (ISGs). These genes produce proteins that inhibit viral replication and promote virus clearance. ISGs can directly cleave viral nucleic acids, trigger apoptosis or autophagy of the infected cell, and upregulate major histocompatibility complex (MHC) class I expression to mediate CD8 T cell cytotoxicity. Type I IFNs bind to neighbouring uninfected cells and protect them from infection, thereby containing the initial spread of the virus. Type I IFNs also contribute to the recruitment of adaptive immune effectors to infected sites, which further promotes viral clearance (Goodbourn et al. , 2000, Holmgren et al. , 2015). In canonical type I IFN signalling, JAK/STAT pathway is activated leading to transcription of ISGs and IFNβ. During viral spread and secondary infection, IFN-β drives IRF7 gene expression to enable a full type I IFN response (Perry et al. , 2005).

Infected neurons may secrete type I IFNs, which act in an autocrine and paracrine manner on other neurons and brain parenchymal cells (Delhaye et al. , 2006). Studies in Theiler's virus and La Crosse virus models of CNS infection suggest that type I IFN is produced by infected ependymal cells, macrophages and neurons; but only 3% of infected neurons express Type I IFN (Delhaye, Paul, 2006). Other studies with La Crosse virus found that neurons do not express Type I IFN, but glial cells expressed Type I IFNs (Kallfass et al. , 2012). However, hippocampal neurons have been shown to express a higher basal level of interferon beta (IFNβ) than peripheral fibroblasts, suggesting that neurons are capable of expressing Type I IFNs under a variety of circumstances (Cavanaugh et al. , 2015). Whether virally-infected neurons express Type I IFNs may then be dependent upon the type of virus that is infecting the cells and the type of PRRs that detect it.

Figure 2
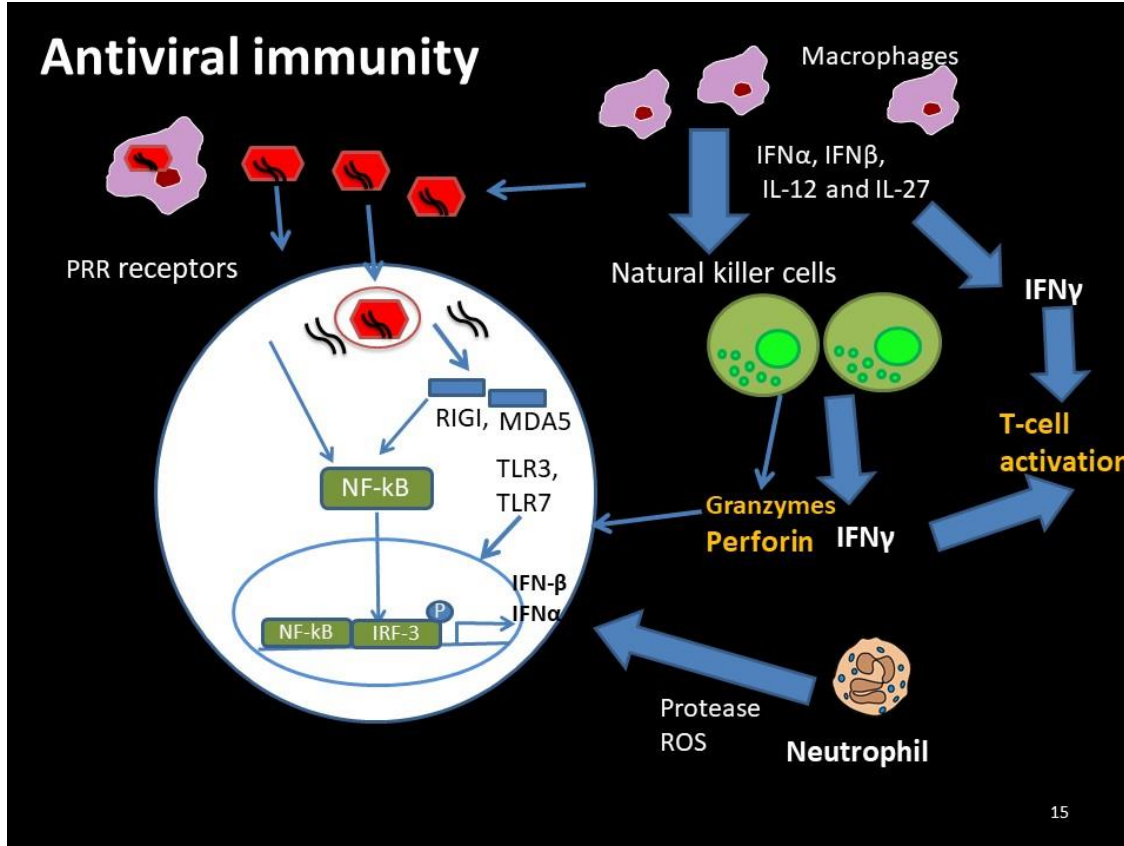
Figure 2. Antiviral innate immunity.

Virus (red) infects the host cell (white circle). The virus is recognized by pattern recognition receptions (PRRs) such as RIGI, MDA5, TLR3 or TLR7. They activate downstream signaling cascades after they recognize the viral molecular patterns and lead to the induction of IFNα and IFNβ. Macrophages are innate cells that recognize a foreign pathogen and can phagocytose the pathogen and release several cytokines. Macrophages release cytokines that activate Natural killer cells (NKs). NK cells release IFNγ which further activates the T-cell response (adaptive immunity). NK cells also act through granzymes and perforin can attack the virally infected cells. Neutrophils, part of innate immunity release protease and reactive oxygen species during a viral infection.

1.3.4 Microglia

Microglia and astrocytes are resident cells of the brain that respond immediately to neuronal injury. Microglia are the resident macrophages of the brain. They are derived from the early yolk sac from macrophage progenitor cells (Ginhoux et al. , 2010, Kierdorf et al. , 2013). They play critical roles during normal brain development, disease, injury, and homeostasis. There is negligible infiltration of peripheral monocytes to the brain parenchyma under physiological conditions and the microglia population is likely sustained by self-renewal (Ajami et al. , 2007). When microglia undergo activation, they transform from ramified phenotype to an amoeboid phenotype with greater motility, migratory, and phagocytic capacities. Activated microglia produce neuroinflammatory mediators and cellular expansion (Atallah et al. , 2014, Lull and Block, 2010). Depending on the type of insult, microglia are polarized to M1 or M2 phenotype. M1 are activated or classical phenotype, produce proinflammatory cytokines such as TNF, IL-6. IL-1β and reactive oxygen species and nitric oxide. M2 microglia are anti-inflammatory and play a role in tissue repair. *In vitro* studies indicate that M1 microglia are neurotoxic. (Fernandes et al. , 2014). The age dependent differences in microglial phenotype during a neonatal CNS infection are not well understood.

1.3.5 Neutrophils

Neutrophils are part of the first line of defense and migrate from the bone marrow in response to chemokines that mediate the inflammatory response. These cells respond to PAMPs via TLRs and NLRs and are stimulated by cytokines such as TNFα and IFNγ. Activated neutrophils upregulate expression of CD15 and CD11b, adhesion molecules that help them bind to the endothelium and migrate into infected tissue (Mantovani et al. , 2011). Neutrophils produce large amounts of

reactive oxygen species (ROS) and release proteases that are stored in specific granules after activation. During viral infections, IFNs modulate the neutrophil response to the chemoattractant, CXCL1, and induce adaptive immunity (Munir et al. , 2011). Additionally, neutrophils are the dominant immune cell in the brains of mice deficient of IFNγ (Abromson-Leeman et al. , 2004, Wensky et al. , 2005), suggesting that IFNγ modulates neutrophil migration.

Depending on the severity of infection, neutrophils may contribute to an unfavorable response. In multiple sclerosis models, neutrophils are among the earliest cells that infiltrate into the CNS. Depletion of neutrophils are associated with reduction in the severity of the disease in MS models (Carlson et al. , 2008). Studies in a neurotropic JHM strain of mouse hepatitis virus (JHMV) indicate that neutrophils and inflammatory monocytes are the first leukocytes to enter the brain post-infection (Zhou et al. , 2003). If neutrophils are eliminated, JHMV-infected mice preserve BBB integrity and show reduced infiltration of other immune cells. Thus, these studies suggest that infiltrating neutrophils may contribute to neuropathology in the CNS.

Neonatal innate immune cells such as neutrophils and monocytes show decreased chemotaxis, phagocytosis, and microbicidal properties compared to adult cells (Mariscalco et al. , 1998). The number of polymorphonuclear leukocytes (PMNs)/granulocytes in neonates are higher than the numbers found in adults (Manroe et al., 1979). Neonatal neutrophils have similar amounts of myeloperoxidase and defensins, but lower amounts of lactoferrin and elastase. This suggests that neonatal neutrophils may have quantitative and qualitative deficits that predispose newborns to infections.

1.3.6 Natural killer (NK) cells

NK cells can respond to pathogens by mediating cytotoxicity and producing cytokines (Vivier et al. , 2008). These lymphocytes are critical players in innate immunity during viral infections and affect the outcome of adaptive immunity. Several viruses escape cytotoxic T-cells (CD8+) by decreasing MHC I expression in the infected cell. This prevents the host cell from presenting viral proteins to virus specific cytotoxic T-cells, but it makes the infected cell prone to NK cell defenses. NK cell activation is blocked by inhibitory receptors that bind to MHC I. These receptors are called the Killer Cell Immunoglobulin-like receptor (KIR) family. Therefore, cells with low MHC I expression, such as due to virus-dependent downregulation, are susceptible to attack by NK cells. Cytokines such as Interleukin 12 (IL-12) and IL-18 mediate IFNγ production from NK cells during viral infections (Biron et al. , 1999). NK cells produce cytokines such as tumour necrosis factor (TNF) and IFNγ and various chemokines during an inflammatory response. NK cells mediate their anti-viral functions by lysis of infected cells, promoting recruitment of other non-specific innate cells such as neutrophils and macrophages, and modulate the T-cell and B-cell response (adaptive immunity) (Ljunggren and Malmberg, 2007).

NK cells mediate protection in several neurotropic virus models such as HSV, Theiler's murine encephalomyelitis virus, mouse hepatitis virus (MHV). For example, children with herpes encephalitis show deficiencies in NK cell function. There is also evidence of NK cells being neurotoxic as well as neuroprotective (Reviewed in (Poli et al. , 2013)). NK cells are known to not just promote the T-cell response but also to limit the immune response by killing APCs and lymphoid cells. In neonates, there are higher numbers of circulating NK cells in the periphery than in adults, but the neonatal NK cells have limited cytotoxic function (Lee and Lin, 2013). However,

the role of NK cells in the neonatal brain and how they infiltrate into the CNS are not well understood.

1.4   Adaptive immunity

The main cells involved in adaptive immunity are antigen-specific lymphocytes, including the CD4 and CD8 T cells and B-cells. When a virus infects a host cell, it utilizes the protein machinery of the host cell to synthesize viral proteins. During this process, the viral proteins are degraded into peptides that will bind to major histocompatibility complex (MHC) class I molecules. The MHC I/peptide complex will be presented on the surface of the infected cells and CD8+ T cells specific to the peptide will identify the complex. The CD8 T cells then induce apoptosis of virally-infected cells through its cytotoxic molecules **(Figure 3)** (Rosendahl Huber et al. , 2014). However, in some circumstances, the CD8 T cells may be triggered to release cytokines that do not kill the infected cell but rather help to initiate an anti-viral program. IFNγ, belonging to Type II IFN family, is mainly produced by mature CD4 T helper–1 (Th1) cells, but also by CD8 T cells and NK cells. IFNγ is a key cytokine for mediating non-cytolytic clearance, allowing the infected cells to intiate an anti-viral program without cell death or lysis.

T cells induce an effective adaptive immune response, particularly an effective induction of MHC proteins. Type I IFNs contribute to the Th1 skew of naïve T-cells (Hibbert et al. , 2003), promote CD8 T-cell activity, and thus, promotes the B-cell response by antibody production (Curtsinger et al. , 2005, Nishikomori et al. , 2002). Depending upon the type and dose of antigen, T cells often skew towards a Th1, Th2, or a Th17 phenotype **(Figure 3)**. Thus, Th1 cells aid in the clonal expansion of CD8+ T-cells, specifically through IFNγ. CD4+ cells can also skew towards a Th2 phenotype and produce cytokines such as IL-4, IL-5, and IL-21. Th17 cells are a subset of

17

CD4+ T cells which produce IL-17 (Reviewed in (Libbey and Fujinami, 2014). In Theiler's murine encephalomyelitis virus (TMEV) infection, Th17 cells promotes viral pathogenesis by inhibiting apoptosis of virally infected cells and decreasing the cytotoxic function of CD8+ T-cell (Hou et al. , 2009). The other arm of adaptive immunity is the humoral immune response which consists of antibodies (Abs) specific to virus mediated by B-cells. Activated CD4 T cells will stimulate B cells that present a matching MHC II/peptide complex to lead to Ab production. These Abs neutralize extracellular viruses before they can enter a host cell (Rosendahl Huber, van Beek, 2014).

Studies suggest that infiltrating lymphocytes are the main source of critical cytokines in the brain. In parenchymal cells, IFNγ induces MHC class I (MHC-I) and MHC-II expression, particularly in microglia (Merrill et al. , 1992, Renno et al. , 1995). T-cells may play either a pathogenic role or a protective role in neurotropic infections. For example, in Borna virus infection, infiltrating CD8 T-cells in the absence of IFNγ cause hippocampal neuronal death and neurological disease in young and old mice. In the presence of IFNγ, virus was cleared from the neurons, suggesting that IFNγ is neuroprotective factor and limits neuronal loss during the antiviral immune response in the brain. (Hausmann, Pagenstecher, 2005). CNS MHV infection is controlled by CD4+ and CD8+ T-cells. They decrease the viral load through IFNγ and cytolytic activity and lead to viral control and protection (Bergmann et al. , 2004, Parra et al. , 1999, Stohlman et al. , 1998).

In respiratory syncytial virus (RSV) infection, CD8 T-cells and IFNγ are critical for viral control in adults (Olson et al. , 2008, Olson and Varga, 2007). Whereas, infants with RSV exhibit a defective CD8 T-cell response, reduced IFNγ production, and an aberrant Th2 skewed response (Harker et al. , 2010, Larranaga et al. , 2009). Evidence from other peripheral infections shows that

the neonatal immune response induces a distinct cytokine profile when compared to an adult response against the same pathogen (reviewed in (Adkins et al. , 2004). Neonatal T cells often skew towards Th2-like response (including production of IL-4, IL-5, and IL-13) as opposed to a Th1 response, characterized by the production of IFNγ and TNF (Zaghouani et al. , 2009). Thus, in neonates, viruses often spread rapidly in brain tissue despite the initiation of an immune response (Hausmann, Pagenstecher, 2005, Kopp, Ranaivo, 2014, Manchester, Eto, 1999). During a CNS infection, one could hypothesize that a Th1 response would be preferred in order to ensure adequate IFNγ expression and control viral replication in developing neurons while minimizing neuronal loss. However, IFNγ also has been shown to play both neurotoxic and neuroprotective roles for developing neurons, making the influence of IFNγ in controlling neonatal infections in the brain less clear (Mizuno et al. , 2008, O'Donnell et al. , 2015).

Figure 3.
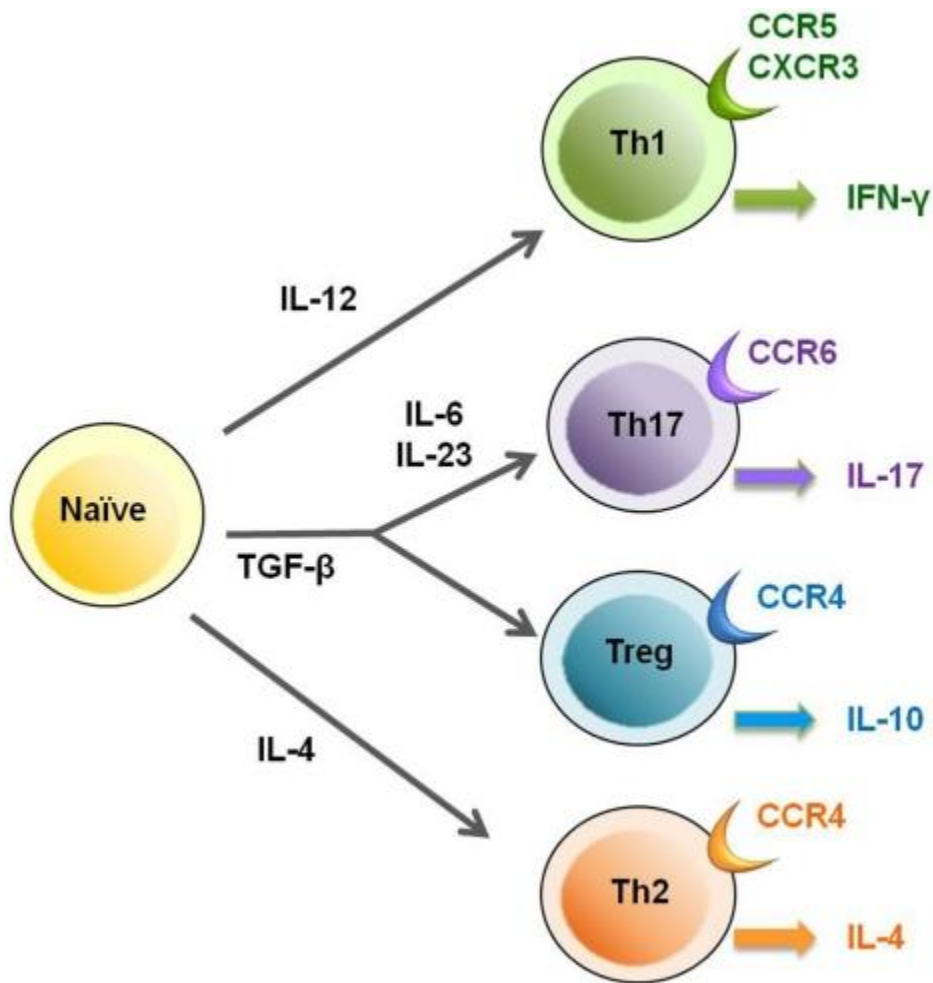
Figure 3. T-cell subsets. Peptides from pathogens are processed and presented by MHC to naïve T-cells in the draining lymph node. CD4 T-cell depending on the type of pathogen and cytokines may skew towards either a Th1, Th2 or a Th17 phenotype. Th1 cells drive clonal expansion of CD8 T-cell through IFNγ. Th2 cells drive B-cell expansion via IL-4. Th17 cells secrete IL-17 and T regulatory (Treg) cells secrete IL-10. **(Used with permission (Araya et al. , 2011)**

A. Interferon gamma (IFNγ)

Both innate immune cells such as NK cells and adaptive immune cells such as activated T-cells produce IFNγ during neuronal infections. IFNγ helps to enhance the NK cell and macrophage response, upregulate MHC II expression on macrophages, and activates CD8+ T-cells. (Biron, Nguyen, 1999, Heise and Virgin, 1995). Murine CMV and HSV infections are severe in mice without IFNγ or its receptor (Novelli and Casanova, 2004). This cytokine signals through Interferon gamma receptor (IFNγR), a multimeric complex composed of two chains, the cell-surface α-chain and a transmembrane β-chain. The α-chain of IFNγR binds IFNγ with high affinity, triggering its dimerization with the β-chain of IFNγR, and induction of a signaling cascade that results in that activation of Janus kinase (JAK) and signal transducer and activator of transcription (STAT) pathway. JAK-1 associates with the IFNγR α-chain while JAK-2 associates with β-chain. Activation of JAK 1 and 2 leads to the phosphorylation and activation of (STAT)-1α. STAT1 homodimers translocate to the nucleus and binds to gamma-activated sequences (GAS), a specific DNA response element present in more than 200 IFNγ-responsive genes (Popko, et al., 1997). This promotes transcription and translation of antiviral proteins against infections or to induce apoptosis of infected cells (Goodbourn, Didcock, 2000).

Figure 4.
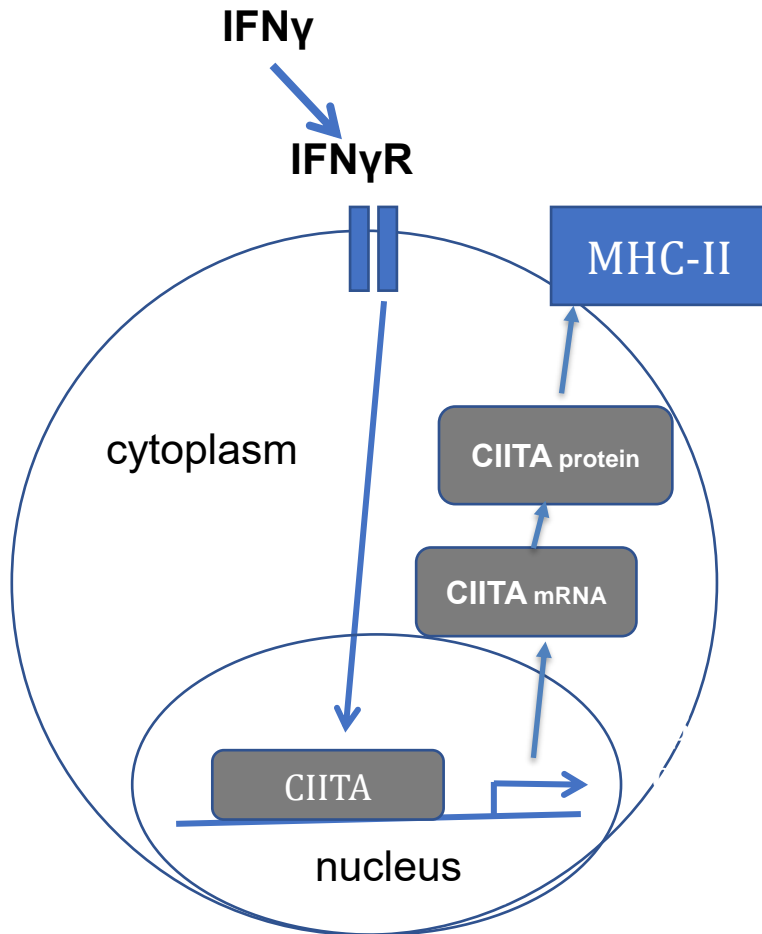
Figure 4. IFNγ signalling

IFNγ binding to the receptor results in the formation of dimers and activation of (JAK-STAT) pathways. IFNγ mediated CIITA activation, which is a master regulator of Class II MHC expression. CIITA is a co-activator whose expression is regulated at a transcriptional level. Class II MHC molecules play a critical role in the immune response in antigen presentation of CD4^{+} T cells, resulting in their activation and differentiation.

B. CIITA (Class II Major Histocompatibility Complex Transactivator

CIITA, a critical regulator of MHC II induction, is an IFNγ-responsive gene (Reith et al. , 2005). MHC II is expressed constitutively on antigen presenting cells (APCs) and its expression is IFNγ-inducible in macrophages, microglia, and endothelial cells (O'Keefe et al. , 2002, Reith, LeibundGut-Landmann, 2005) (Cullell-Young et al. , 2001). CIITA is the master regulator of class II gene activation and its expression is regulated at a transcriptional level. Studies suggest that neonatal macrophages are defective in antigen presentation due to its inability to stimulate MHCII expression after IFNγ treatment. This impairment is at the transcriptional level due to low expression of downstream CIITA (Lee et al. , 2001). Such impairments may also occur in the neonatal CNS during infection. In this dissertation, we explore the role of IFNγ and CIITA transcription to understand their role in the pathogenesis of a neurotropic measles virus in neonates. The next section provides an overview of MV pathogenesis in the periphery and the CNS.

1.5 MV pathogenesis

Measles is a negative-sense, double-stranded RNA virus. MV is a member of genus *Morbillivirus* belonging to the family Paramyxoviridae (Malvoisin and Wild, 1993). It leads to a highly contagious disease. Before the introduction of measles vaccine it was one of the most devastating infections that caused millions of infant deaths worldwide (Moss and Griffin, 2012). MV is believed to have been established 5000-10000 years ago, when populations reached sufficient size in Middle Eastern river valley civilization to sustain virus transmission. Phylogenetic analysis reveals a recent divergence from rinderpest virus that infects cattle in the 11th or 12th century. MV attenuated and killed vaccines were introduced in 1960s after successful isolation of the virus from tissue culture (Black, 1966). There is no latent or persistent MV

23

infection. There is no animal reservoir that maintains virus transmission (Moss and Griffin, 2012). Thus, the eradication of MV is favored by the monotypic nature of the virus.

1.6 MV spread

MV is efficiently transmitted via the respiratory route by aerosol or respiratory droplets. MV initiates infection in the respiratory tract where immature pulmonary (DCs) dendritic cells and alveolar macrophages are the initial cellular target. MV is transmitted to the regional lymph node (LNs) by migrating infected immune cells. Thus, virus replication and spread occurs from the lymph nodes and the immune response is initiated (Ludlow et al. , 2013, Mesman et al. , 2012). The incubation time is about 10 days for the onset of fever and 14 days for the onset of rash. The symptoms include cough, coryza, fever and white spots in the mouth called Koplik's spots. It is then followed by maculopapular rash that starts in the face and neck and spreads to the rest of the body (Coughlin et al. , 2013, O'Donnell and Rall, 2010). The initial hypothesis was that MV pathogenesis starts in the respiratory epithelial cells followed by proliferation of MV in the lymphatic tissue eventually leading to monocyte-mediated viremia. But the SLAM receptor used by wildtype strains of virus was not expressed in any of these targets, suggesting the existence of alternative MV receptors that were yet to be discovered (de Swart et al. , 2007).

CD46, CD150 (signaling lymphocyte activation molecule - SLAM) and nectin-4 are the known cellular receptors for MV. CD46 is a complement regulatory molecule which is expressed on all nucleated cells in human beings. Activated T and B lymphocytes and antigen presenting cells express the SLAM receptor. SLAM is favored by the wildtype MV strains. CD46 receptors are favored by vaccine strains, although both wildtype and vaccine strains are capable of using

either receptor to varying levels of efficiency (Navaratnarajah et al. , 2009). There are other putative MV receptors called CD147/EMMPRIN (extracellular matrix metalloproteinase inducer) on epithelial cells (Moss and Griffin, 2012). C-type lecithin DC-specific intercellular adhesion molecule 3-grabbing non-integrin (DC-SIGN) plays a role in MV infection of dendritic cells (DC). It appears to act as attachment receptor for DC. The epithelial cell receptor, Nectin-4, is a recently identified receptor for MV (Noyce and Richardson, 2012). This receptor binds to proteins involved in viral attachment with high affinity. MV entry and non-cytopathic spread in primary epithelial cells is through Nectin-4 (Muhlebach et al. , 2011).

Several studies have tracked the movement of the virus through infected animals. Rhesus macaques were infected with a strain of MV encoding genes for enhanced green fluorescent proteins (EGFP). Examination of organs in MV-EGFP infected macaques revealed that lymphoid tissues were the primary sites of replication (de Vries et al. , 2010, Lemon et al. , 2011). Viral replication was seen primarily in T-cells, B-cells, and DCs first followed by replication in epithelial cells during the later stages of infection. Similar studies were performed using hSLAM transgenic mice, which were infected intranasally with wild-type MV expressing GFP. In this study, they observed MV replication in alveolar macrophages and dendritic cells in lungs prior to spread to lymphatic organs (Ferreira et al. , 2010). Lung epithelial cells were not infected. After the initial replication, the virus migrates to other organs such as skin, kidneys, gastrointestinal tract and liver. The virus also replicates in epithelial cells, endothelial cells, lymphocytes, monocytes and macrophages. In the upper respiratory tract, lymphocytes are not present in large numbers but DCs are abundant. DCs express CD150 and DC-SIGN and are found at the site of infection (de Vries et al. , 2012). DCs are the predominant antigen presenting cells (APC) to the T cells, acting

as a bridge between the innate and the adaptive immune system. Studies *in vitro* indicate that infection of DCs with MV leads to syncytia and infectious virus formation. Both interstitial DC (iDC) and myeloid DC are infected with MV and more than 40-90% of infected cell express MV H envelope glycoprotein (Fugier-Vivier et al. , 1997, Grosjean et al. , 1997, Murabayashi et al. , 2002). Thus, infected DCs lead to a highly productive infection. The host lymph node acts as a factory for virus production after escaping the respiratory tract. From the lymph nodes, MV causes a systemic infection.

Infection of wildtype MV in mice expressing human SLAM on DCs led to downregulation of CD80, CD86, CD40 and MHC class 1 and 2. Thus, allogeneic T-cell stimulation and the mitogen-dependent T-cell proliferation is inhibited. At the later stages of infection, an increase in IFN-β transcripts was observed in MV-infected iDCs (Hahm et al. , 2004). The expression of the co-stimulatory molecule may be reduced in mDCs in the secondary lymphoid organs. Therefore, DCs attain a poor functional maturation status. MV-infected mDCs also produce IFNs, which ultimately increases expression of maturation markers. Infected DCs lead to aberrant T-cell function leading to reduced IFNγ production and inhibition of a Th1 response (Duhen et al. , 2010, Shingai et al. , 2007).

1.7 Viral Replication

MV encodes for eight proteins including replication factors such as RNA-dependent RNA polymerase (L) and phosphoprotein (P) and structural proteins such as nucleoprotein (N), matrix (M), hemagglutinin (H), fusion (F), V, and C protein **(Figure 5)**. The viral H and F proteins are envelope glycoproteins that are critical for attachment and membrane fusion. MV-H attaches to

the cellular receptor of the host cell providing a platform for MV-F to perform fusion activity. (Rima and Duprex, 2009) The P gene encodes for three proteins: the P protein when the mRNA is unedited and V and C proteins from alternate opening reading frames (Moss and Griffin, 2006).

After attachment of the virus to the host cell, the virus envelope fuses with the host plasma membrane and viral RNA and proteins are released into the host cytoplasm. The viral genome is complexed with N, P, and L which are the components of the viral ribonucleoprotein (RNP). This complex is formed in the cytoplasm in infected cells. The RNA-dependent RNA polymerase (RdRp) complex contains the L and P protein. It acts as viral transcriptase and replicase (Rima and Duprex, 2009). For infectivity, every virion must contain a nucleocapsid/L/P complex. After the cell fusion into the host, the negative strand RNA genome is inserted into the host cytoplasm where it as acts as a template for both transcription and replication (Horikami and Moyer, 1991).

Transcription uses a negative-strand RNP complex to generate positive-strand mRNAs, but during replication there is a switch from negative-strand RNP to positive-strand RNP by RdRp, using its replicase function (de Swart, Ludlow, 2007). Viral proteins bind to the original negative strand RNA to stop the signals of polymerase from stopping and restarting. Therefore, full length positive strand can be generated which can be copied to create new negative strand RNA viral genomes. The presence of a strong promoter at the 3'end of positive-strand RNP allows several copies of RNP to be produced. Due to such replication mechanism, there exist both positive-strand RNP and negative-strand RNP at the ratio of 0.43:1 in the infected cell (Rima and Duprex, 2009). MV does not have any global effects on host protein translation. MV tends to establish noncytolytic and persistent infections that leads to balanced synthesis of viral

and host mRNAs and translation. The new virions bud from the host cells and acquires H and F

from the plasma membrane. This is the classical mechanism of virus spread to the neighboring

cells **(Figure 5)**.

Figure 5

a

Fusion (F)
Haemagglutinin (H)
Nucleocapsid (N)
Large protein (L)
Matrix (M)
Phosphoprotein (P)

RNA

Lipid bilayer

b

N	P/C/V	M	F	H	L
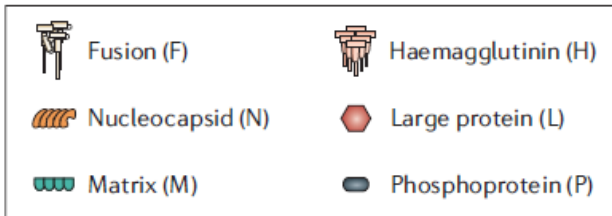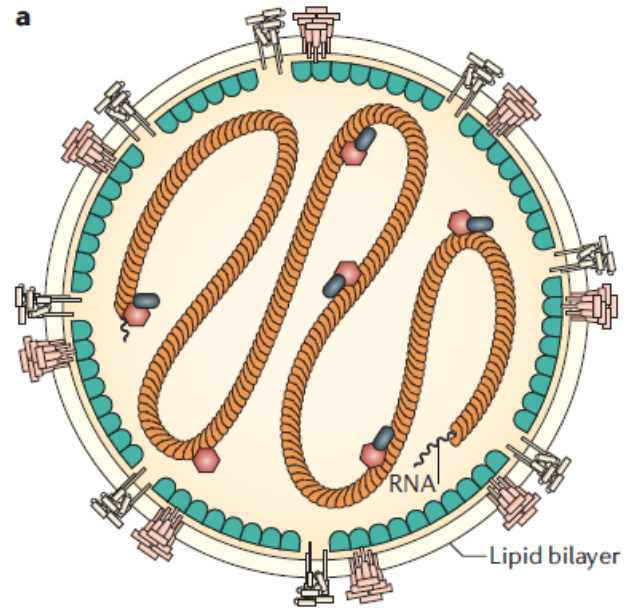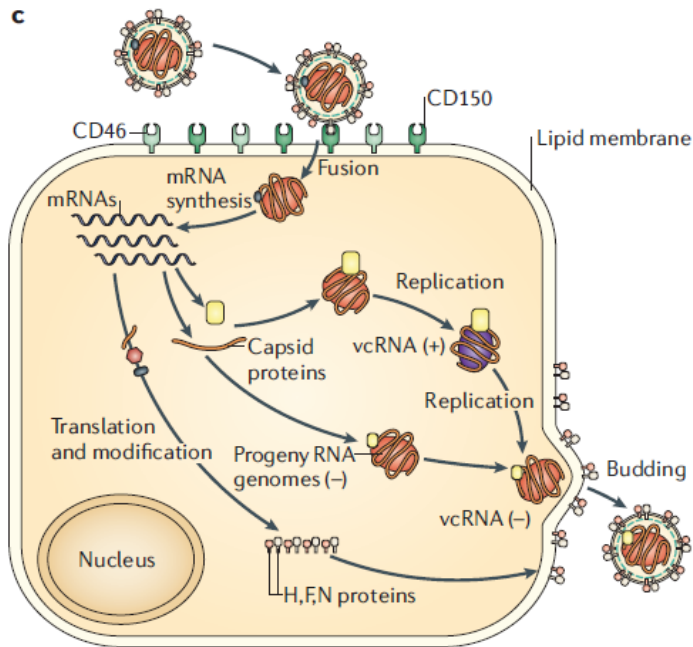
Figure 5. Measles virion and replication

A. Envelope proteins (H and F) are anchored on the lipid envelope of the virion. N, L and P form the RNP complex, which is the basic unit of infectivity. B. MV genome consists of 16,000 nucleotides. The genome codes for 8 protein: V, C, P, N, M, F, H, and L. V and C are non-structural proteins encoding P. C. MV enters the host through H and F by binding and attaching to the host cell membrane. After entry transcription, translation and viral replication occurs. The newly synthesized viral particle buds out of the cell and infects the neighboring cell to start this process again. Therefore, it was proposed that there are "two initiation site one at 3' end that helps in synthesis of positive strand replicative RNA and the other one at the start of N gene for mRNA synthesis (Horikami and Moyer, 1991). Thus, six short positive RNA strands are generated and translated by the ribosomes to generate MV proteins. Along with RNP, there are host proteins, actin and tubulin,

that play a vital role in transcription. There are gene end sequences after every gene that helps the transcription process to terminate. RNP follow follows this particular start and stop mechanism of gene transcription that can give rise to a gradient of gene expression. Due to this mechanism, the proximal genes (N and P/V/C) are expressed more repeatedly as that of distal genes that is H and L. (Coughlin, Bellini, 2013) **(Used with permission (Moss WJ, Griffin DE. 2006. Global measles elimination. Nature reviews. Microbiology 4:900-908))**

1.8 Evasion of host response

As MV does not possess a segmented RNA genome, it is unable to undergo antigenic shifts in an animal or bird reservoir to generate new sequences. MV also does not mutate extensively to avoid neutralizing antibodies. The MV-F protein helps in viral entry by sticking the viral envelope to the external membrane of target cells. This leads to formation of a giant cell with multiple nuclei to be formed allowing MV to spread internally from cell to cell. Cytotoxic T-cells (CD8 T-cells) play a critical role in eliminating the infected giant cells. MV evades the host defenses temporarily by causing transient immunosuppression of the host. Infection with MV confers lifelong immunity after an immune response (Reviewed in (Mina et al. , 2015)). Thus, susceptibility to opportunistic infections of respiratory and gastrointestinal tract is increased. The common characteristics of immunosuppression includes lymphopenia and imbalance of cytokines towards a prolonged Th2 response, which reduces cellular immunity to secondary infections and T-cell non-responsiveness. Lymphopenia affects B-cells, monocytes, neutrophils, CD4+ and CD8+ T-cells (Malvoisin and Wild, 1993). There also is a loss of delayed hypersensitivity response to recall antigens, suggesting that memory immune responses may also be impaired. (Tamashiro et al. 1987).

Several mechanisms have been postulated to explain immunosuppression. MV infected DCs cause an upregulation of various cytokines, IL-1β, IL-6, IL-11, IL-12 and IL-15 (Griffin, 2010). The reduction of IL-12 is one of the proposed mechanisms of immunosuppression. However, when monkeys were vaccinated with IL-12-expressing virus, it did not change the lymphoproliferative effects of PBMCs *ex vivo*. This suggested that IL-12 alone cannot compensate for the reduced proliferation of lymphocytes and other mechanism seem be

essential. There may be compromised expression of chemokine receptor CCR7 in MV-infected DCs. CCR7 is upregulated in mDCs, which allows cells to home to secondary lymphoid organs. *In vivo* studies indicate a lower expression of CCR7 in PBMCs in infected children, which might lead to impaired CCR7-dependent chemotaxis. Thus, further studies are required to understand the role of CCR7 expression in chemotaxis of DCs during MV infection.

MV-infected DCs abrogate the expansion of T-cells. Functions of DCs such as T-cell conjugation and activation are impaired post MV-infection. Vaccine and wildtype MV-infected DCs are unable to stimulate T-cells in *in vitro* co-culture. The crosstalk between MV-infected DCs and T-cells is compromised, which leads to insufficient T-cell stimulation. Griffin and colleagues have shown that there is a reduction in interleukin-12 (IL-12) after MV infection of APCs, which skews the CD4+ T-cell response to a Th2 profile. Several mechanisms other than loss of mature lymphocytes have been proposed. The hematopoietic stem cells (HSC) that express SLAM remains unaffected by infection, but unknown components are released from infected stroma cells that target HSC differentiation. Thymocytes expressing CD150 may be depleted during infection. Thymic epithelial cells may release chemicals that may induce apoptosis. Thus, when T cells enter secondary lymphatic tissues, they are activated normally but might behave differently in the periphery.

1.9 Measles in the central nervous system

MV replicates in the lymphoid tissue and spreads to the other organs. CNS invasion may occur through the blood stream, transmigration of infected leukocytes across the blood brain barrier, migration through the choroid plexus or infection of microvascular endothelial

cells and basolateral release of virus. Infected nerves of the olfactory bulb also can transport the virus to the CNS (Reviewed in (Griffin, 2010)). Regardless of the mechanism of CNS entry, MV routinely infects neurons in the CNS, and it may involve other neural cell types such as oligodendrocytes and astrocytes. In neurons, MV assumes a distinct viral life cycle from the periphery; the virus does not produce extracellular particles but moves between neurons through transfer at the neuronal synapse. Thus, extracellular virus is not found in CSF or in brain tissue. Makhortova *et al* have demonstrated the role of neurokinin-1 (NK-1) in transynaptic spread of the virus by serving as a receptor for MV-F protein. But still, the molecular pathways involved in viral entry neurons is not well understood. (Markhortova 2007).

1.9.1 CNS complications associated with MV infection

A. Subacute sclerosing panencephalitis (SSPE) is a progressive, slow, and fatal disease that develops from 1 to 15 years after a MV infection (Dubois-Dalcq et al 1974). SSPE occurs in approximately 1/100,000 cases of acute measles infection and clinical symptoms appear months to years after the primary infection. The disease is characterized by progressive dementia, starting with subtle cognitive loss early on and progressing to cognitive dysfunction, motor loss, seizures, organ failure and death. Human SSPE specimens and MV animal models show MV infection in the neurons and involvement of gray and white matter. SSPE brains show the presence of cellular inclusion bodies, inflammation, glial activation, blood brain barrier (BBB) integrity loss and neuronal loss. (Johnson 1994, Rall 2003). SSPE patients have elevated MV-specific antibodies in the blood and cerebrospinal fluid (Dubois-Dalcq et al). MV does not bud from the infected neurons either *in vivo* or *in vitro*. Unlike fibroblasts and epithelial cells,

there is no formation of syncytia in MV-infected primary neurons. It is suggested that the viral spread is contact-dependent and trans-synaptic in nature. Infected brains show extensive presence of MV RNA and protein in SSPE and measles inclusion body encephalitis (MIBE) (Katz 1995; Payne et al 1969).

Molecular epidemiological studies reveal that primary MV infection of patients with SSPE occurs under the age of two, although the symptoms of SSPE may not occur until years later. The immune response is immature during the neonatal period and the residual maternal antibodies may either be absent or insufficient to neutralize the virus. SPPE is characterized by intrathecal synthesis of MV-specific antibodies, which suggests that an antibody response is ultimately mounted in the brain even if the antibodies are ineffective at controlling the virus. There are also differences in MV replication and spread in the human CNS. The viral transmission in the neuron is less cytopathic and productive compared to non-neuronal cells. Studies in rat hippocampal slices found that the spread of rMV-EGFP occurs in a retrograde direction with the MV F, H, M and P proteins localized to the dendrite in the infected neuron (Ehrengruber, Ehler, 2002, Schneider-Schaulies et al. , 2003). Electron microscopy was used to show the presence of MV nucleocapsids at the presynaptic membrane of infected primary neurons. This suggested that the spread is in an anterograde direction or from the axon of the infected neuron (Lawrence et al 2000).

B. Post-infectious encephalomyelitis (PIE) is more frequent than SSPE, affecting 1 in 1000 infected individuals. PIE symptoms occur 5 to 14 days after the characteristic MV rash. (Johnson 1998). PIE and MIBE are is thought to be an autoimmune reaction characterized by

perivascular inflammation and demyelination and does not involve viral entry into the CNS. Symptoms of the PIE patients include seizures, deafness, ataxia, and movement disorders. The mortality rate is high and survivors are prone to suffer from frequent neurologic symptoms. Adults have a worse prognosis than young children (Schneider-Schaulies, Meulen, 2003) (Baba et al. , 2006) (Perry and Halsey, 2004). PIE is not unique to MV, and can occur after other bacterial and viral infections. This suggests PIE is not driven by specific damage by MV in the brain but by an inappropriate immune response in CNS tissue.

C. Measles inclusion body encephalitis (MIBE)

This disease occurs in immunocompromised individuals within 1 year of MV infection or vaccination. Young immunocompromised patients with conditions such as lymphoblastic leukemia, HIV, and autoimmune diseases are affected by MIBE. The clinical symptoms include seizures, partial epilepsy, and ataxia. These patients show the presence of MV specific antibodies (IgM and IgG) in the cerebrospinal fluid (Mustafa et al. , 1993). Biopsies of MIBE patient's brains reveal neuronal loss, astrocytic, and microglial proliferation, focal necrosis, perivascular inflammation, and intranuclear or intracytoplasmic inclusion bodies, which are the pathological hallmark of the disease. There is no treatment for MIBE and it has a 76% mortality rate (Fisher et al. , 2015, Mustafa, Weitman, 1993).

1.10 CD46+ Model

Genetically engineered mice are a powerful model to dissect the immune cell types and effector functions that contribute to encephalitis or to successful resolution of the infection without pathogenesis (Bergmann et al. , 2006, Brooks et al. , 2010, Burdeinick-Kerr et al. , 2009)

(Manchester and Rall, 2001). Wildtype mice are not susceptible to MV because the murine isoforms of the viral entry receptors (CD46, SLAM, nectin-4) do not support MV entry. Transgenic mice have been engineered for MV susceptibility through the CNS neuron-specific expression of the human isoform of CD46 (NSE-CD46), which acts as a receptor for the Edmonston B strain of MV. Transgenic CD46+ mouse, which expresses the human isoform of the measles virus receptor CD46 under the control of the neuron-specific enolase promoter (NSE) (Rall et al. , 1997), is used as a model to study MV pathogenesis in the brain. In this model, the human CD46 expression and viral infection are restricted to mature CNS neurons. Previous studies observed that CD46+ adult mice control and clear MV in a T-cell and IFNγ-dependent manner. There is no evidence of loss of neurons or damage, suggesting a non-cytolytic mechanism of viral clearance. CD46+ adults show no signs or symptoms of illness and show viral clearance by 15 days post infection (dpi). However the neonatal CD46+ mice succumb to the infection with severe neurological signs (Patterson, Lawrence, 2002) (O'Donnell et al. , 2012). The mechanisms behind this failure of the neonatal immune response in the brain are unknown.

In the current study, our goal was to understand the shortcomings of the neonatal immune response in the brain and study the neuropathology post infection. Specifically, this work will help to develop effective therapeutic strategies for viral infections in the neonatal CNS, which are currently lacking, and provide a better understanding of neonatal susceptibility to viral infections in the brain.

CHAPTER 2

2. MATERIALS AND METHODS

2.1. Animals and ethics statement

Mice were maintained and treated in accordance with the Institutional Animal Care and Use Committee of Duquesne University and the *NIH Guide for the Care and Use of Laboratory Animals*. CD46+, CD46+/IFNγ knockout (KO), and CD46+/Recombination activating gene 2 (RAG-2) KO mice (A gift from Dr. Glenn Rall; Fox Chase Cancer Center, Philadelphia, PA) were maintained on a 12:12 light/dark cycle under controlled temperature conditions (20 ± 2 °C) with free access to food and water. Upon arrival, mice are acclimatized prior to use.

Breeding pair cages were established for the CD46+, CD46+/IFNγ KO and CD46+/RAG2 KO mice in order to generate neonatal pups for infections. All mice at p21 were sexed and equal numbers were used for adult experiments.

2.2 Genotyping CD46+ mice

In order to detect the CD46+ transgene, P21 mice were anesthetized, tail clipped, and numbered by an ear punch at weaning. The tails were stored at -20°C until extraction. DNA was extracted from the tails using 1 mg of proteinase K (Fisher - BP-1700-50) in 500ul of Sodium Chloride-Tris-EDTA (STE) buffer for each tail. The tails are kept overnight at 60°C on a dry heat bath. The DNA was extracted with 1X-Phenol:Chloroform:Isoamyl alcohol (25:24:1), vortexed at high speed, and spun on high (13.2 RPM) in an Eppendorf centrifuge for 3 mins. The top aqueous layer was removed and mixed with 500ul of chloroform: isoamyl alcohol. The vortexing and spinning step is repeated. The aqueous layer was removed with a p200 pipette tip and added into 1 ml of 100% ethanol. The DNA precipitates out and the centrifugation step

is repeated. Then the DNA was air-dried after removing the ethanol for 10 mins. The pellet was resuspended pelleted in sterile Tris-EDTA (TE) buffer and stored at 4°C.

2.3 Measles virus infections

Mice were infected with Measles virus (MV)-Edmonston obtained from the ATCC (American Type Culture Collection; Cat. No: VR-24). The virus was passaged twice in Vero fibroblasts to create a passage 3 (P3) stock for infections. The vero cells were plated on a 6-well plate. After 24 hours, the stock virus was diluted and different concentration of 10^{-1}, 10^{-2}, 10^{-3}, 10^{-4} and 10^{-5} virus was added on the vero cells. The cells are incubated with the virus for 1 hour. 1% agarose was heated in a microwave and then placed in a 56 C waterbath. The DMEM is placed in a 37 C water bath. After 1 hour, 1:1 ratio of DMEM and agarose are mixed. Each well is overlayed with 4ml of the mixture.

Before infection, the inoculum was freshly diluted to 10,000 plaque forming units (PFU)/10 µl with phosphate-buffered saline (PBS) prior to injection. On postnatal day 2 (P2), pups were intracerebrally injected with virus, using a 27½ gauge needle, along the cerebral midline. The uninfected control group was injected in the same location with an equal volume of PBS (10 µl). Pups were monitored daily for symptoms of illness (seizures, tremors and dehydration) and survival, up to 35 days post-infection. Mice were euthanized if seizures developed. Adult mice (3-4 months of age) were anesthesized with isoflurane and injected with 30 µl (30,000 PFU) of MV along the cerebral midline. Infected mice were monitored for signs of illness daily throughout the course of infection.

2.4 Body weight and brain weight measurement

Both infected and control mice were weighed using digital balance and weights are recorded in grams. The neonates were also assessed for measures of health and sickness. Edema was recorded when observed at the later stages of infection.

2.5 Polymerase chain reaction (PCR)

To detect the CD46+ gene, PCR was performed using 10x PCR buffer, MgCL2, Taq polymerase (Fisher FEREP0402) and dNTP (FERR0192), CD46+ forward (*CGGTCGCTACCATTACCAGT)* and reverse primer (*CCCCCTGAACCTGAAACATA).* The PCR mixture along with 1ul of DNA was run on the thermocycler in RNAase free PCR tubes. The primers are diluted in TE buffer and aliquots are stored at -20 C. For each PCR mixture the following volumes were used.

Reagent	Volume
10x PCR buffer (KCL)	5 uL
25mM Magnesium chloride	3 ul
40mM dNTP mix	1 ul
Taq polymerase	0.5 ul
CD46+ forward primer (10 uM)	5 ul
CD46+ reverse primer (10 uM)	5 ul
Nuclease free water	29.5 ul
DNA template	1 ul
Total	50ul Final volume/sample

For each PCR, both a positive control (CD46+ tail) and a negative control (PCR mixture without DNA) are run on the thermocycler. The thermocycler is set to (94 C 5 mins, 52 C 1min, 72 C 1min) x 25 cycles, 72 C for 5 mins. The CD46+ gene is a 250bp

DNA Electrophoresis

A 1.5% agarose gel was made in Tris/Borate/EDTA (TBE) buffer. The gel was poured in the electrophoresis apparatus and allowed to solidfy. The 10ul of PCR product was diluted with 6X DNA Loading dye. The samples were loaded on the gel and run at 50V for 2 hours. The gel was then incubated with SYBR™ Green I Nucleic Acid Gel Stain, 10,000X concentrate in DMSO (S7585, Thermofisher) for 1 hrs at 20C and imaged in the UV box (Red Personal Gel Imager, Proteinsimple). The figure for the imaged gel is in (Figure 6). For each run, both a tail from a CD46+ mice - positive control (+) and negative control were run along with Generuler 100bp ladder (SM0241). The CD46+ product is 200bp **(Figure 6)**.

Figure 6.
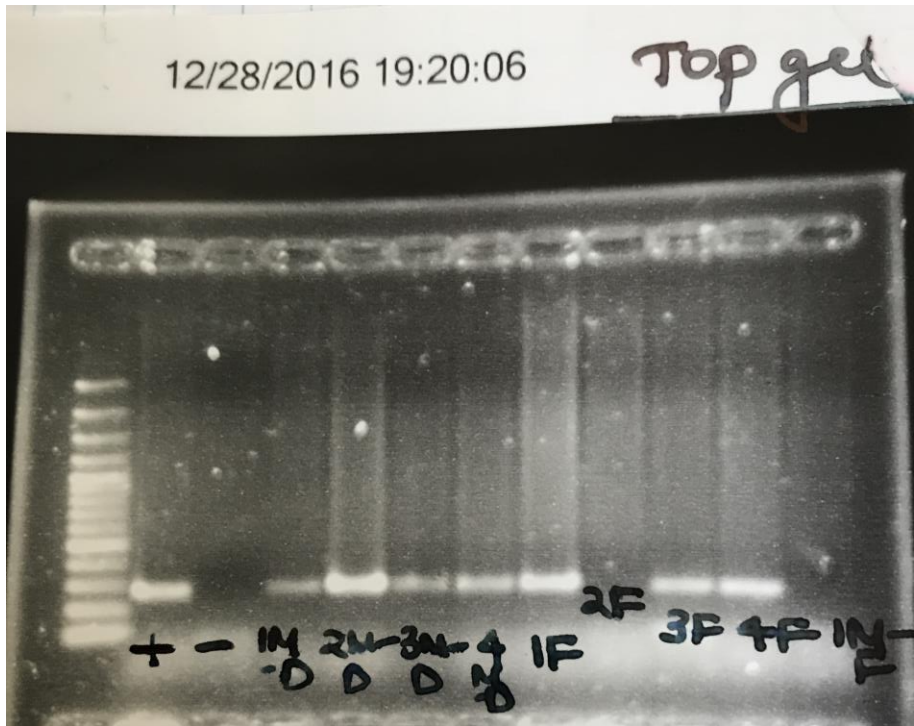
Figure 6. DNA electrophoresis gel imaged by UV box.

A 1.5% agarose gel was run with tail DNA samples from CD46+ mice. The first column is the 100bp generuler ladder, followed by the positive and negative control. The adjacent wells include the PCR product from RAG2-KO tails to confirm the presence of CD46+ in those animals (For example 1M-D, 2M-D).

2.6 Quantitative Reverse transcription polymerase chain reaction (qRT-PCR)

Quantitative RT-PCR for measles virus nucleocapsid (N) was performed as described previously (O'Donnell, Conway, 2012). Mouse brains were snap frozen in liquid nitrogen and stored at -80°C. RNA was isolated by TRIzol, according to the manufacturer's instructions (Sigma-Aldrich). Contaminating DNA was removed from RNA preparations using DNase I treatment (Invitrogen). Purified RNA was quantified using a Nanodrop instrument. RNA was reverse transcribed using Moloney murine leukemia virus reverse transcriptase (Ambion) and a mixture of anchored oligo-dT and random decamers. For each sample, two reverse transcriptase reactions were performed with inputs of 100 and 20 ng. An aliquot of the cDNA was used for 59-nuclease assays using TaqMan chemistry. A TaqMan set specific for the N gene of MV (GenBank sequence AB046218) was used for detecting viral nucleocapsid RNA. Sequences were as follows: forward, 59-CGCAGGACAGTCGAAGGTC-39; reverse, 59-TTCCGAGATTCCTGCCATG- 39; probe, 59-6Fam-TGACGCCCTGCTTAGGCTGCAA-BHQ1-39. Assays were used in combination with Universal Master mix and run on a 7900 HT sequence detection system (Applied Biosystems). Cycling conditions were 95°C, 15 min, followed by 40 (twostep) cycles (95°C, 15 s; 60°C, 60 s). The assay for MV-N was validated with a 4-fold five-points dilution curve of cDNA. The slope was 23.54, corresponding to a PCR efficiency of 95%. For each sample, the values are averaged and SD of data are derived from two independent PCRs. Relative quantification to the control was done using the comparative cycle threshold method**.**

For qRT-PCR analysis of the pathogen recognition receptors and interferons, we reverse transcribed 1ug of RNA using QuantiTect Reverse Transcription Kit (20531, Qiagen) to

produce cDNA, then amplified using primers from Integrated DNA Technologies (Coralville, IA). We determined whether MV altered the mRNA expression of TLR3, TLR7, MDA5, RIGI, Type I and Type II IFN and CIITA relative to Glyceraldehyde 3-phosphate dehydrogenase (GAPDH). GAPDH is a loading control. The sense and antisense primer sequences are listed **(Table 1)** (McCarthy et al. , 2015, Zalinger, Elliott, 2015). Real time PCR was performed using Bullseye EvaGreen qPCR Mastermix (MIDSCI) on an StepOne Plus qPCR detection system (Thermo Fisher Scientific) using a MicroAmp Fast optical reaction plate (4346906, Applied Biosystems). mRNA was quantified as ΔCT (threshold cycle) values relative to GAPDH. ΔCT values of the infected samples were expressed as fold changes over ΔCT values of control samples. All statistical tests were performed using SPSS software. Significance of the F statistic was defined as $p \leq 0.05$. The sense and antisense primer sequences are listed below (McCarthy, Procario, 2015, Zalinger, Elliott, 2015).

2.7. Cytokine and chemokine gene expression (PCR array)

RNA was isolated from adult and neonate mouse brains using the Qiagen RNeasy Midi Kit (75124, Qiagen, Valencia, CA) as per the manufacturers information. The brains were homogenised in a Qiazol lysis buffer. The extracted RNA was assessed by UV spectrophotometry to measure concentration and purity on a Nanodrop (ND-1000, Thermo Scientific). Cytokine and chemokine gene expression was assessed using the mouse cytokine and chemokine RT2 Profiler PCR Arrays (PAMM-150Z, Qiagen) by the manufacturer. The expression of 84 inflammatory genes and 5 housekeeping genes were assessed. Data analysis was done using the SABiosciences RT2 Profiler Web-Based PCR Array Data Analysis software, which automatically performs the Delta Ct (ΔΔCt) fold-change calculations from the uploaded

44

raw threshold cycle data. The fold changes were calculated after normalizing to their housekeeping genes. This is followed by normalising all groups to uninfected CD46+ p9 control when adults are compared to neonates and when neonatal comparisons are made. For the baseline differences, all the genes were normalised to CD46+ p9 uninfected controls (Table 3 and Table 4). For each condition, infected neonatal brains (n = 16) and for uninfected n = 8 were used for the PCR array.

Table 2 - Primer sequences

Gene	Abbreviation	Sequence
Measles	MV-F	CGCAGGACAGTCGAAGGTC
	MV-R	TTCCGAGATTCCTGCCATG-
CIITA	CIITA-F	GGAGGAGATCGAACTCAGCTC
	CIITA-R	GTTCCGCAATGTTGGCATAGG
GAPDH	GAPDH- f	ACCACAGTCCATGCCATCAC
	GAPDH- r	TCCACCACCCTGTTCTGTA
IFNα	mIFN-a4-F3	CCCACAGCCCAGAGAGTGACC
	mIFN-a4-R3	GGCCCTCTTGTTCCCGAGGT
IFNβ	mIFN-B-F4	TCCGCCCTGTAGGTGAGGTTGAT
	mIFN-B-R4	GTTCCTGCTGTGCTTCTCCACCA
IFNγ	IFNG-F	AAAGAGATAATCTGGCTCTGC
	IFNG-R	GCTCTGAGACAATGAACGCT
MDA5	MDA5-F	GCTGCTAAAGACGGAAATCG
	MDA5-R	CTTGTCGCTGTCATTGAGGA
RIGI	RIGI-F	GCGTCTCAGTGCAGCACATCATT
	RIGI-R	GGGTCCCGTGACTCTCCAAGTTT
TLR3	TLR3-F	AGCTTTGCTGGGAACTTTCA
	TLR3-R	GAAAGATCG AGCTGGGTGAG
TLR7	TLR7-F	CCACAGGCTCACCCATACTT
	TLR7-R	CAAGGCATGTCCTAG GTGGT

2.8. Flow cytometric analysis of brain homogenates

At specific days post-infection (dpi), mice were deeply anesthetized with isoflurane. Once the mice were unresponsive, the brain and spleen were removed and pressed through a 70 micron nylon mesh cell strainer in PBS. The dissociated tissue was run over a 30/70% discontinuous percoll gradient at 1500 rpm for 20 min at 4°C (Eppendorf 5810 R). Mononuclear cells were collected from the interface, washed with PBS, treated with 0.84% ammonium chloride to remove contaminating red blood cells (RBCs), and washed again in PBS. Primary antibodies (Abs) were applied in a solution of 1% fetal bovine serum/PBS for multi-color flow cytometry. The following Abs (BD Biosciences) were used to identify T cells: APC CD8a (561093), FITC CD19 (557398), PE CD4 (553048), PerCP-CY^{TM} 5.5 CD3 Molecular complex (560527). To identify NK cells, APC NK1.1 (55067), PE CD49b (553858), PerCP-CY^{TM} 5.5 CD3 Molecular complex (560527) and FITC CD19 (557398) were used. All antibodies were added at a concentration of 600ng/ml.

To identify neutrophils and inflammatory monocytes, PerCP CD45 (557235), CD11b APC (eBioscience 17-0112-81) and Ly6G FITC (551460) were used at 1:50 dilution. Infiltrating neutrophils were identified as CD45(hi)CD11b(+)Ly-6G(+) and F4/80-. Inflammatory monocyte are classified as CD45(hi)CD11b(+)Ly-6G(-) F4/80+. Cells were incubated with Ab for 1h at 4°C and then washed with 1% FBS/PBS, pelleted, stained cells were resuspended and analyzed in a BD Accuri CFlow flow cytometer (BD Biosciences). For each sample, 1x10^5 events were run, with gates to exclude debris and doublet cells. Single antibody stains were used for color compensation and isotype controls were used for gating (O'Donnell, Conway, 2012).

Table 3A. Antibodies for T-cell and B-cell flow cytometry

T-cell panel		
Catalog number	**Antibody**	**Concentration**
BD 560527	PerCP-CYTM 5.5 CD3 Molecular complex	600ng/150ul
BD 561093	APC CD8a	600ng/150ul
BD 557398	FITC CD19	600ng/150ul
BD 553048	PE CD4	600ng/150ul

Table 3B. Antibodies for NK cell flow cytometry

NK cell panel		
Catalog number	**Antibody**	**Concentration**
BD 560527	PerCP-CYTM 5.5 CD3 Molecular complex	600ng/150ul
BD 55067	APC NK1.1	600ng/150ul
BD 553858	PE CD49b	600ng/150ul
BD 553048	PE CD4	600ng/150ul

Table 3C. Antibodies for neutrophil flow cytometry

Neutrophil panel		
Catalog number	**Antibody**	**Concentration**
eBioscience 557235	PerCP CD45	1:50
eBioscience 17-0112-81	CD11b APC	1:50
eBioscience 551460	Ly6G FITC	1:50
eBioscience 553048	F4/80	1:50

2.9. Immunohistochemistry of mouse brain tissue

Neonates and adult mice were anesthetized and perfused with ice-cold 4% Paraformaldehyde/PBS (PFA/PBS). Brains from MV-infected and mock-infected neonates and adults were collected and cut along the midline into two halves. The brains were post-fixed with 4% PFA/PBS for 48 hours and cryoprotected with 30% sucrose solution till the brains sank to the bottom of the tube at 4°C. Then the brains were immersed in tissue embedding compound (TFM-5, TBS), frozen in a dry ice-isopentane bath, and stored at -80°C. Sagittal cryosections (16 µM) were cut on a cryostat (Microm HM-550, GMI). Sections were post fixed with 4% PFA/PFA and blocked with 5% goat and donkey serum. Standard immunohistochemistry was performed to detect mouse anti-measles hemagglutinin (Millipore MAB8905; 1:200), mouse measles matrix protein (Millipore MAB8910; 1:200), and rabbit anti-ionized calcium-binding adapter molecule 1 (Iba1) (Wako 019-19741; 2µg/ml) for microglia overnight at 4°C with combination of primary antibodies. Sections were washed (3x in PBS) and incubated with Alexa fluor 488 donkey anti rabbit IgG (Molecular Probes A21206; 1:500), Alexa fluor 555 goat anti-mouse IgG (Molecular Probes A21424; 1:500) secondary antibodies, and Hoechst 33343 stain (Thermofisher; 1 µg/ml) for 1 hour at room temperature in the dark. Immunoreaction controls were carried by omission of primary antibodies. Sections were imaged using an EVOS epifluorescence microscope at 200x magnification. No primary antibody and isotype controls were performed. For all the histological analyses, at least five sections per brain were examined and at least four mice per experimental group were assessed. The stich images were captured using Olympus epifluorescence.

3. TUNEL staining

Brains from control and MV-infected mice were collected after perfusion. Sagittal brain sections were fixed with 3.7 % formaldehyde and subjected to terminal deoxynucleotidyl transferase dUTP nick end labeling (TUNEL; (TdT-FragEL DNA fragmentation detection kit; Millipore) using diaminobenzidine as a substrate. For counting of TUNEL-positive cells, four non-overlapping fields ($\times$20) were chosen by a blinded examiner moving dorsally to ventrally across the slice. TUNEL-positive cells were counted on an Olympus BX41 Laboratory Microscope (Olympus Corporation). Three sagittal slices were counted from each brain, with three mice assayed per condition. The average number of TUNEL-positive cells per $\times$20 field $\pm$ standard error was determined.

3.1 IFNα ELISA

Whole brains were lysed in RIPA buffer with 500ul of PMSF, 1% protease inhibitor cocktail and 10% NP-40. After sonication, the samples were centrifuges at 27,000g for 20 mins and stored at -20 C. The protein concentration was determined by Pierce BCA Protein Assay Kit (Life Technologies). The standards provided in the IFNα kit (PBL lifesciences) were run. The brain homogenates (150ug of protein) and standards were diluted with 1% casein/sample buffer.

3.2 Intracellular IFNγ staining/ T cell culture.

Spleens from 5 MV-infected and uninfected CD46+ adults were isolated and mechanically dissociated with plunger and forceps. The petri dish was rinsed and the homogenate was transferred to a conical flask. Percoll discontinuous gradient was used to isolate the lymphocytes. The cells from the interphase were resuspended in 50ml of RPMI media and

Interleukin 2. The cells were then plated in a T-75 flask and allowed to settle in the incubator for 1 hr. The cells were viewed under the microscope to check if they had settled. Once the cell attached, the media containing the floating T-cells were removed and transferred to a new T-75. The cells were then incubated until the APC counts were finished.

T-cells and APCs were counted and plated in the following ratios: 1:4, 1:10, 1:25, and 1:50. The experimental groups that were included in the analysis were: 1. Uninfected APC: Uninfected T-cells and 2. Infected APC: Ionomycin + infected T-cells. After incubation, sterile PBS w/o Ca^{+2}/Mg^{+2} was added followed by 2.5% trypsin. The trypsin was incubated at 37 C in the incubator for five minutes. Once the cells started to float, RPMI media was added and the cells were then resuspended. Macrophages/APCs were plated separately. The cells were spun at 1500rpm at or 23 C for 5 mins at a high brake. The cells were resuspended in a smaller volume of 100ul for T-cells. In a 96 well plate, 2×10^6 Tcells/well were plated in a 96 well plate for both infected and uninfected group. 10U/ml of IL-2 was added to each well.

Brefeldin A and Golgi Stop (Monesin) (2ul/well Brefeldin and 1.3ul/well Golgi Stop) were added to each well. After 3 hours, the cells were washed and resuspended in FACS buffer. A mixture of CD3, CD4 and CD8 Ab were made in FACS buffer. The cells were incubated in the dark for 1 hr and washed and resuspended. The cells were then run on the flow cytometer as for T cell flow cytometry.

3.3 Western Blot

Neonatal brain tissue was harvested at 3, 7 and 10 days post-infection (dpi) for western blot analysis. Mice were perfused with 10mM NaF in ice-cold PBS in order to inhibit endogenous

phosphatases. The brains were dissected for the cerebellum, hippocampus, neocortex, and thalamus and lysed in cell Lysis Buffer with Protease inhibitors (Cell Signaling; 20 µl/mg of tissue). The lysate was stored at -80°C until further use. The protein concentration of each lysate was measured using Pierce BCA Protein Assay Kit (Life Technologies). For each sample harvested, 20 µg of lysate was subjected to western blot analysis. The membranes were treated with primary antibody solutions overnight at 4°C on a rocker. The primary antibodies used included goat anti-mouse CXCL10 (1ug/ml; RAF466NA, R&D Systems) and mouse anti-mouse interferon gamma (1:100, Santa Cruz Biotechnology). The membranes were washed thrice and incubated in secondary antibody solutions for 60 mins at room temperature. The membranes were imaged on the Odyssey infrared imaging system (Licor Biosciences). Individual bands on blots were quantified by Image Studio. Multiple antibodies IFNα (ab191903, Abcam) and IFNβ (sc-17569, Santacruz; NBP177288E, Novus; ab85803, Abcam) was used, but these resulted in non-specific bands (data not shown)

3.4. Statistical Analysis

Statistical analysis for the Kaplan-Meier plot was performed by log rank test to compare survival across different genotypes. A two-way ANOVA was performed to compare body weight, brain weight, viral load, NK cell infiltration, T-cell infiltration, neutrophil, and qRT-PCR data with Bonferroni post hoc test ($p<0.05$ considered as significant). For the cytokine array, p values were calculated based on a student's t-test to compare the control and treatment groups. Three-way ANOVA was done to compare the differences between the Type I IFN and MDA5 gene expression **(Figure 21)**. Differences were deemed significant when *p* values were less than 0.05. Statistical analysis was performed using GraphPad Prism software 6 (GraphPad

Software, Inc., La Jolla, CA) and SPSS. Outliers were identified using the Grubb's method and

the alpha level was set to 0.05 using Graphpad Prism.

CHAPTER 3

Role of IFNγ-producing innate and adaptive immune cells during a neurotropic measles virus infection

3.1 Hypothesis

Inadequate infiltration of IFNγ-producing immune cells in the CNS may contribute to mortality and neuropathology in the CD46+ neonates.

3.2 Rationale

Neurotropic virus infections continue to impose major disease and economic burdens on society. When these infections are in the neonates or children, they are associated with neurological sequelae and higher morbidity and mortality worldwide (Das and Basu, 2011). Additionally, there are qualitative and quantitative deficiencies in immune cells during the neonatal period (Zaghouani, Hoeman, 2009). Therefore, there are great challenges in treating these patients as age and immature host immunity are key factors. Moreover, the pathogenesis of neurotropic viruses in the neonatal brains are not well understood.

Viral infections in non-replicating neurons lead to lasting neurological consequences, if a cytolytic immune strategy is employed to clear or control the virus (O'Donnell, Conway, 2012). The severity of neurotropic virus pathogenicity may be dictated by the delicate balance between achieving viral clearance and removing virally-infected cells: effective immunity must control the infection while minimizing cytotoxic T lymphocyte (CTL)-mediated lysis of this chiefly nonrenewable cell population. Interferon-gamma (IFNγ) is a potent anti-viral cytokine

that is critical for non-cytolytic clearance of multiple neurotropic viral infections and clearance of measles virus (MV) from the adult CNS. Thus, the role of IFNγ in the neonatal CNS is explored in this study. It is known that the adult immune response can protect the mice from disease, but neonates developed unrestricted neuronal infection and fatal CNS disease (Lawrence et al. , 1999) (Patterson, Lawrence, 2002). Therefore, we explored whether neonates can mount an immune response during a viral CNS infection. The goal of this project was to understand the shortcomings of the neonatal immunity during a viral CNS infection.

The immune system has two main arms: a generic innate response followed by a pathogen-specific adaptive response. The innate immune system cells constitute neutrophils, antigen presenting cells (APCs) such as macrophages, and natural killer cells (NK cells). We studied innate immune cells, such as NK cells, because they can produce pro-inflammatory cytokines such as TNFα and IFNγ and various chemokines during an inflammatory response. These innate cells also are capable of direct lysis of infected cells, recruitment of other non-specific innate cells like neutrophils and macrophages, and modulation of T-cell and B-cell responses (Ljunggren and Malmberg, 2007). Thus, if NK cell infiltration is low it may affect several arms of the anti-viral immune response.

Adult CD46+/RAG2-KO mice, which lack adaptive immunity, show extensive MV-mediated neuropathology and high mortality post infection. This suggests that innate immune response is unable to mediate MV control in an adult CNS (Patterson, Lawrence, 2002). However, the role of the innate and adaptive immune response in the neonatal CNS are not well understood. For example, studies suggest that neonatal neutrophils have quantitative and

qualitative defects (Melvan et al. , 2010). The neutrophil storage pools and neutrophil progenitor production is reduced compared to adults. Neonatal neutrophils also show reduced expression of TLR4 but similar levels of TLR2 compared to adults (Melvan, Bagby, 2010). Additionally, there are defects in downstream signalling of MyD88 and p38 pathways **(Figure 2)** (Al-Hertani et al. , 2007). Thus, multiple lines of evidence suggest that the neonatal innate immune response may demonstrate deficits or impairments in cellular responses and number. To determine whether innate immunity in the brain is similarly impaired, we explored whether the neonates are capable of mounting an innate post a neurotropic infection in the brain.

We used transgenic CD46+ mice to study neuron-restricted measles virus infection in the brain. Immunocompetent CD46+ adult mice initiate a protective adaptive immune response with infiltration of CD4 and CD8 T cells as early as 3 days post-infection (dpi), with peak T cell infiltration between 7-14 dpi. MV infection is resolved typically by 30 dpi without any symptoms or signs of illness and there is 100% survival (Patterson, Lawrence, 2002). Mice without T and B cells (CD46+/RAG2-KO) and mice that lack (CD46+/IFNγ-KO) die with rampant MV spread within a month after infection. Adult CD46+/IFNγ-KO mice do not clear the virus, with ~50% of the mice succumbing to the infection within 21 dpi. The surviving CD46+/IFNγ-KO mice showed long term neurological damage, including ataxia, piloerection, and hunched posture. Therefore, both T cells and IFNγ are critical to the survival of adult CD46+ mice (O'Donnell, Conway, 2012). Thus, we also wanted to define the role of IFNγ and the adaptive immunity in MV-infected neonates.

3.3   Results

3.3.1 IFNγ delays, but does not prevent, mortality in infected neonates

To study the outcome of infection in neonates, 2-day old CD46+ mice were infected with MV and monitored for signs of illness and mortality (**Figure 7**). As a control for the injection procedure, CD46+ neonates were injected with 10μl of PBS intracerebrally and did not show signs of illness over the course of the experiment. MV-infected CD46+ neonates succumbed to the virus by 16 dpi, with 50% mortality by 8 dpi. During the infection, MV-infected neonates showed signs of illness including dehydration, lethargy, and tremors starting at 6 dpi, with seizure activity before death. Previous studies have shown that IFNγ-producing T cells are required for MV clearance in adult CD46+ mice (Lawrence, Vaughn, 1999, O'Donnell, Conway, 2012, Patterson, Lawrence, 2002). To determine if IFNγ contributed to the outcome of infection in neonates, CD46+/IFNγ-KO pups were infected with MV and observed for signs of illness **(Figure 7, closed circles)**. MV-infected CD46+/IFNγ-KO pups succumb to the infection earlier than CD46+ pups, reaching 100% mortality by 10 dpi. We also investigated the role of the adaptive immune system in neonates using recombinase activating gene 2 knockout (CD46+/RAG2-KO) mice that lack mature T and B cells **(Figure 7, open diamonds)**. Surprisingly, CD46+/RAG2-KO neonates survive longer than CD46+ and CD46+/IFNγ-KO neonates. At 35 dpi, 20% of CD46+/RAG2-KO neonates had survived the infection with less signs of illness than the other CD46+ genotypes. These observations suggest that the adaptive immune response may play a detrimental role during neonatal infection, in contrast to the protective role that it plays in the adult brain. These findings also demonstrate that IFNγ delays the outcome of infection but is insufficient to protect the CD46+ neonates from death.

3.3.2 Measles virus RNA is lower in the absence of IFNγ compared to CD46+ neonates

As CD46+/IFNγ-KO neonates succumb to the infection earlier than CD46+ neonates; one possibility is that MV replication is greater in the absence of IFNγ, thereby leading to more rapid death. To determine if survival correlates with the viral load in the brain, expression of measles virus nucleocapsid (N) RNA was determined in brain tissue using qRT-PCR (**Figure 8**). We focused on 4 and 6 days post-infection, as these time points correspond with early T cell infiltration (4 dpi) and with more extensive T cell infiltration (6 dpi). Regardless of immune background, MV RNA increased in all neonates over time, although this increase was only significant in CD46+ pups ($p < 0.001$). Unexpectedly, CD46+ neonates had a higher viral load compared to CD46+/IFNγ-KO ($p < 0.05$) and CD46+/RAG2-KO neonates at 6 dpi ($p < 0.001$, **Figure 8A**). Thus, the level of viral RNA did not correlate with survival in the CD46+ neonates **(Figure 7)**. This result suggests that the virus may not be directly causing death in neonates, but rather the nature of the host immune response may be a better predictor of survival. Regardless of genotype, levels of MV N-transcripts were higher in neonates than in adults (**Figure 8B**), which may reflect both a more successful anti-viral response in adults and/or the ability of the virus to readily spread in young neurons.

Figure 7.
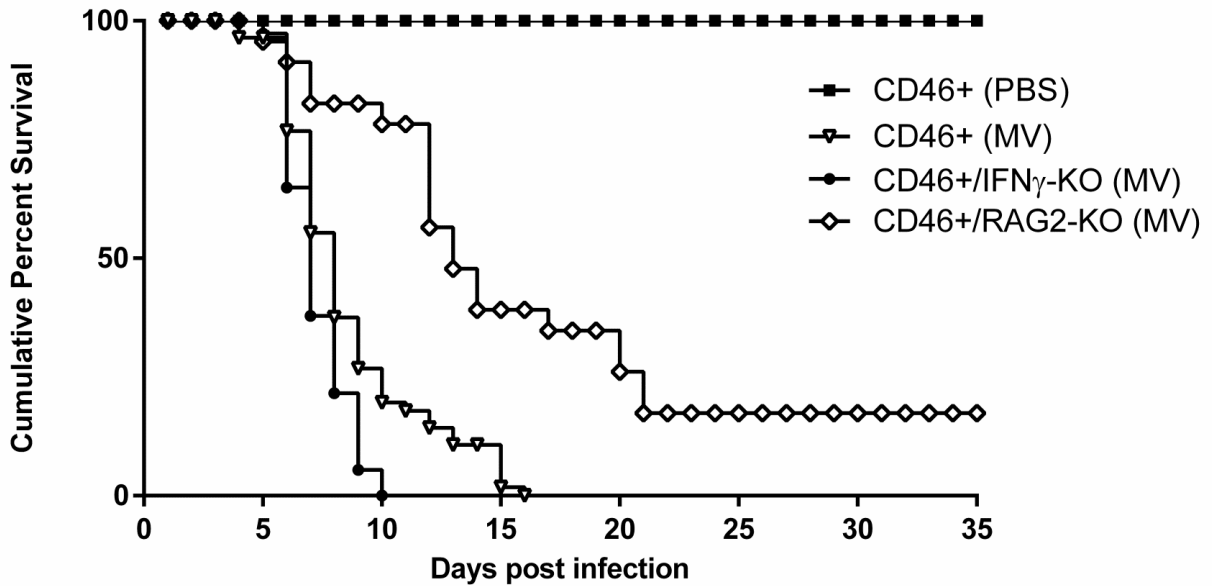
Figure 7. IFNγ delays, but does not prevent, mortality in infected CD46+ neonates.

Kaplan-Meier plot of CD46+ neonates on various knockout backgrounds. CD46+, CD46+/INFγ-KO, and CD46+/RAG2-KO neonates were infected intracranially with measles virus (MV) (10^4 PFU/10μl PBS) at 2 days of age. Mice were monitored for symptoms of illness and death for 35 days post-infection. Statistical analysis was applied by log rank test (p < 0.0001). Results from 4-6 separate litters were pooled (n = 30-50 mice per condition).

Figure 8.

A. Neonates

B. Adults
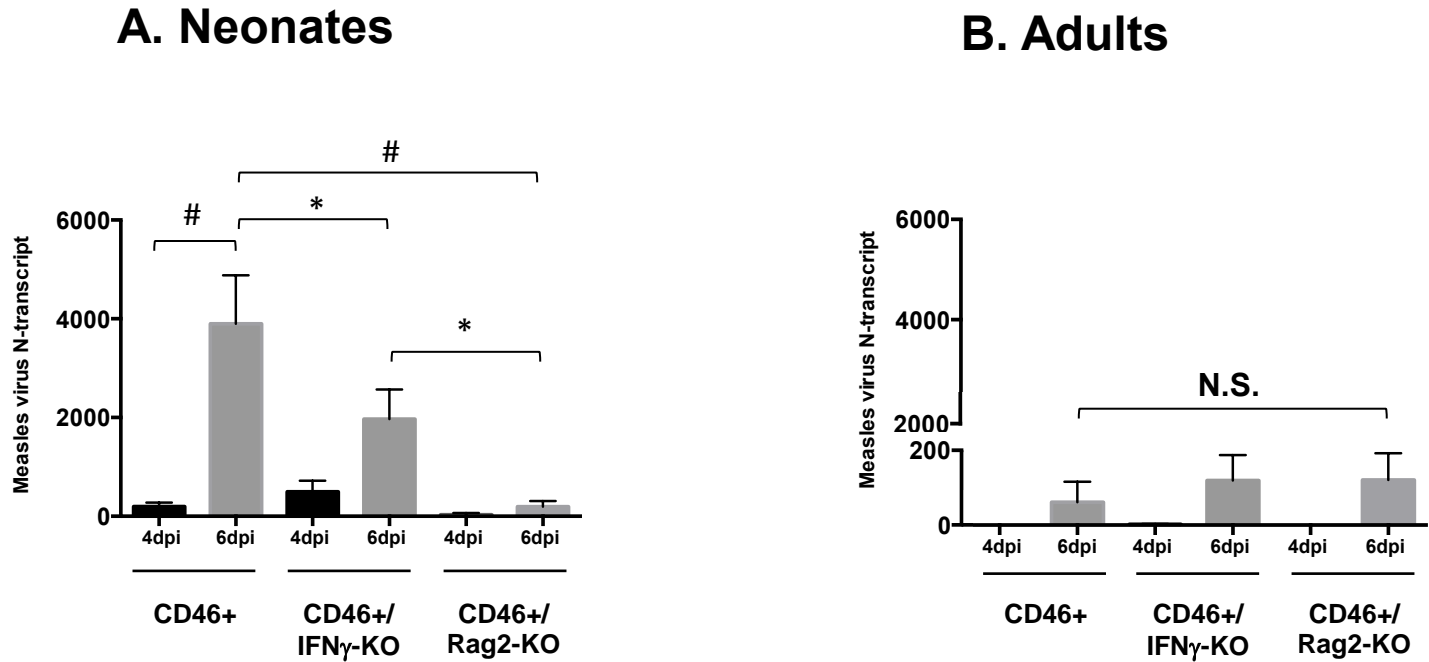
Figure 8. CD46+ neonates have the highest viral load compared to CD46+/INFγ-KO and CD46+/RAG2-KO neonates. Whole brains from neonatal (B) and adult (C) MV-infected mice were collected at 4 and 6 dpi. RNA levels of measles virus nucleocapsid (N) transcript were quantified using qRT-PCR. Bars represent the average of mice from three independent experiments (n=9-14) and error bars represent SD. Statistical analysis was applied by two-way ANOVA (# p<0.001, * p<0.05, NS = not significant) with Bonferroni post hoc test.

3.3.3 Impact of MV-infection on body and brain weights

MV-infected neonates showed clinical neurological symptoms such as ataxia and seizures, as well as signs of weight loss and dehydration. From 7 dpi onwards, the clinical symptoms increase followed by neonates succumbing to the infection. We also observed that some CD46+/IFNγ-KO neonates (~8%) developed hydrocephaly, with relatively smaller brains upon dissection. The enlarged head and skull was filled with fluid upon dissection, but the actual brain was smaller **(Figure 9)**. Thus, we wanted to determine if the loss of body weight correlated with changes in brain weight during infection (**Figure 10**). At the initial stages of infection (2 dpi), there is no difference in the body or brain weight of MV-infected CD46+ neonates (**Figure 10A and 10C**) or MV-infected CD46+/IFNγ-KO (**Figure 10B and 10D**) compared to uninfected controls. As the infection progresses, CD46+ neonates lose body weight at 4 dpi (11.7% loss compared to uninfected controls) followed by a transient increase in body (13.5%) and brain weight (6.2%; $p<0.05$) at 6 dpi. MV-infected CD46+/IFNγ-KO neonates also show an increase in brain weight at 6 dpi (13%), but there is no difference in body weights compared to control. At 10 dpi, MV-infected CD46+ (loss of 10.3% brain weight, 21% body weight) and CD46+/IFNγ-KO (loss of 14.3% brain weight, 29% body weight) neonates show a significant decrease in brain and body weight compared to age-matched controls. Thus, MV-infected pups showed limited growth at the end stages of infection (10 dpi), when neurological symptoms are also the most severe. The finding that brain weights increased at 6 dpi, regardless of IFNγ expression, was surprising, as neurological symptoms are apparent at this time point. However, one possibility is that the temporary increase in brain weight could be due to edema or increased fluid retention in the tissue at that stage of infection, as the brains were not dried to eliminate water weight before measurement. Regardless of the increase in

weight at 6 dpi, the loss of brain and body weights occurred independently of IFNγ, even when

edema was not observed.

Figure 9.

Control

CD46+/IFNγ-KO MV

Figure 9. Hydrocephaly is observed in MV-infected neonates in the absence of IFNγ.

CD46+/IFNγ-KO and CD46+ mice were infected with MV (1x10^4 PFU) at 2 days of age.

Mice were monitored for signs of illness. CD46+ neonates did not demonstrate overt

changes in head size during the infection. In ~8% of CD46+/IFNγ-KO neonates (Figure 8B),

enlarged heads and skulls were observed at the later stages post-infection.   Upon

dissection, edema was observed in the intracranial space, with fluid accumulation in the brain

and reduced brain size. CD46+/IFNγ-KO neonates 8dpi MV skull (Figure 8B) is compared to

age matched uninfected CD46+/IFNγ-KO neonate.

Figure 10.

A. CD46+

B. CD46+/IFNγ-KO

C. CD46+
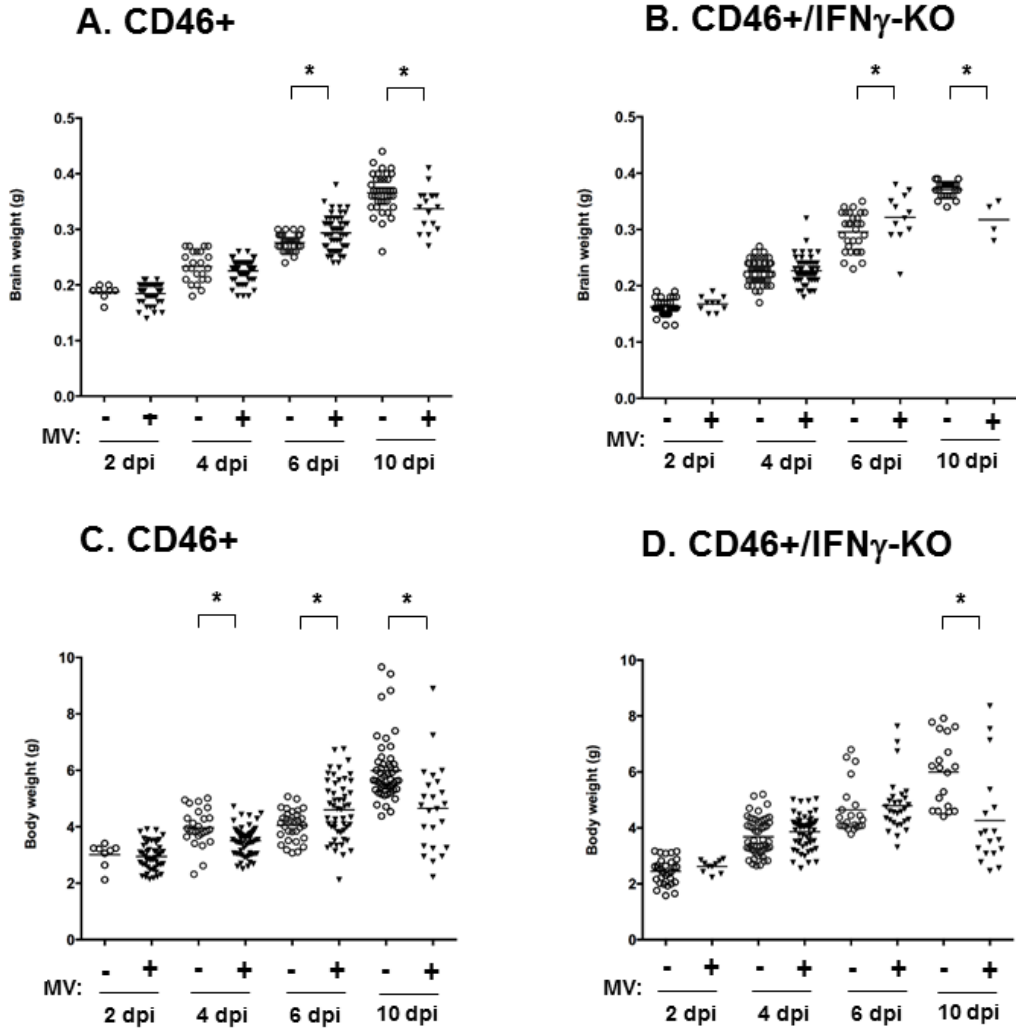
D. CD46+/IFNγ-KO

Figure 10. CD46+ neonates lose body and brain weight at early and late time points post-infection.

The brain weights (A, B) and body weights (C, D) of CD46+ (A, C) and CD46+/IFNγ-KO neonates (B, D) at different time points post-infection were measured. Weights were recorded at the time of harvest for flow cytometry experiments. Mean values are represented by horizontal bars for each condition. Statistical analysis was applied by two-way ANOVA (* $p<0.05$) with Bonferroni post hoc test.

3.3.4. IFNγ expression does not prevent apoptosis during infection.

Previous studies from our laboratory have demonstrated that IFNγ can be neuroprotective against certain insults *in vitro*. Therefore, we wanted to test whether the CD46+/INFγ-KO neonatal brains showed greater apoptosis post infection. Terminal deoxynucleotidyl transferase dUTP nick-end labeling (TUNEL) staining was performed. We found that brain sections are strongly positive in the TUNEL reaction, particularly in the cerebellum. There is a significant increase in the number of TUNEL+ cells in both MV infected CD46+ and CD46+/IFNγ-KO brain sections compared to their age-matched uninfected controls **(Figure 11)**. However, there is no significant difference between CD46+ and CD46+/INFγ-KO, indicating IFNγ may not reduce the number of cells undergoing apoptosis in the neonatal brain.

Figure 11.
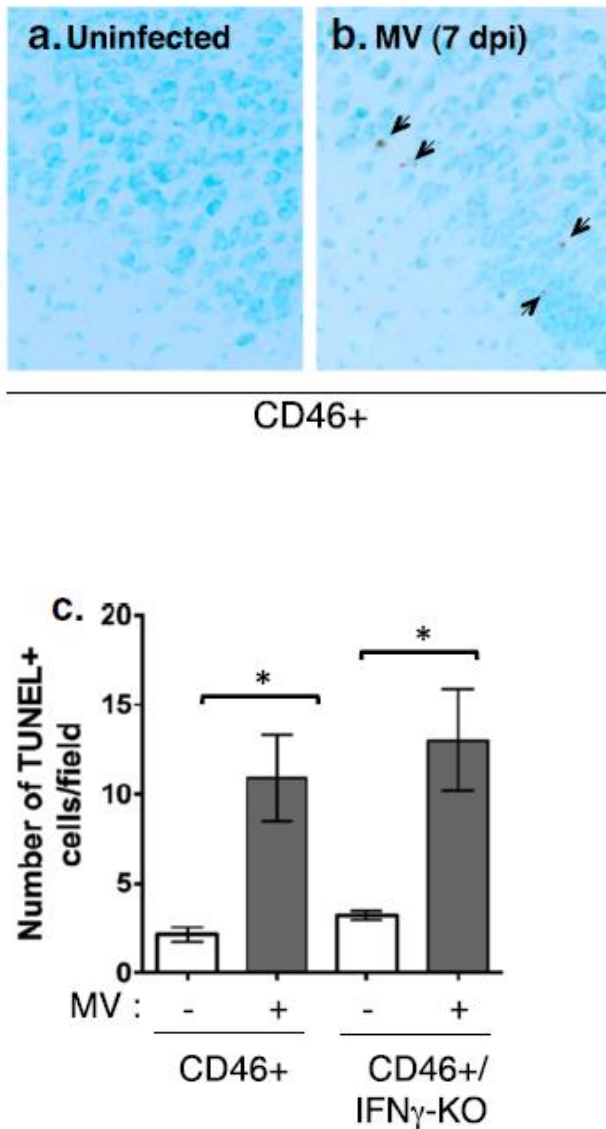
Figure 11: IFNγ does not prevent apoptosis in neonatal brain tissue during infection.

Whole brains CD46+ control neonates (A) and CD46+ MV-infected neonates (B) were

collected at 7 dpi. Sagittal sections from the neocortex were immunostained for apoptotic

cell (brown) and healthy cells (green). Slides from 4-5 mice per condition were examined,

and representative sections with TUNEL+ cells are shown. The number of TUNEL+ cells is

counted from 3 fields per condition.

3.3.5. Microglial activation occurs in the absence of IFNγ during infection

IFNγ stimulates the activation of microglia and induces expression of chemokine genes that are mediators of T-cell recruitment (Rock et al. , 2005). Because microglia is highly sensitive to IFNγ, we examined changes in microglial activation post MV-infection in the neonatal brains. We hypothesized that pups lacking IFNγ would show limited microglial activation during infection. Sagittal brain sections were immunostained for a marker for activated macrophage/microglia (Iba1; green) and for measles virus antigen using antibodies against the matrix and hemagglutinin protein (red, **Figure 12**). In CD46+ (**Figure 12A**), CD46+/IFNγ-KO brains (**Figure 12B**), activated microglia were observed with bright Iba1 staining in the brain parenchyma in comparison to uninfected controls. MV antigen was observed in the prefrontal cortex, thalamus, and cerebellum at 7 dpi regardless of IFNγ expression. At later stages from 7 to 10dpi, there is widespread MV infection throughout the CNS, including involvement of the hippocampus, which is also highly infected in adults (data not shown). Activated microglia was consistently observed in close proximity to MV-infected neurons. In brain regions with MV+ cells, Iba1+ cells showed ameboid morphology with rounder cell bodies and retracted processes, which is indicative of activation during infection, in both CD46+ and CD46+/IFNγ-KO pups. Iba1+ cells in uninfected brains show thin, ramified processes and with less intense Iba1 staining (**Figure 12A and 12B**, top rows) in comparison to MV-infected brains. Thus, microglial activation is observed in the absence of IFNγ, suggesting that other cytokines/chemokines can trigger activation of microglia during infection. We further looked at the distribution of infection in several brain regions such as hippocampus and thalamus **(Figure 13A)**. We also observed greater Iba1 expression in areas of the brain that

also contained higher numbers of MV-infected neurons (**Figure 13B**).   These results suggest

that neuronal infection leads to microglial activation in the surrounding brain tissues in neonates.

Figure 12.
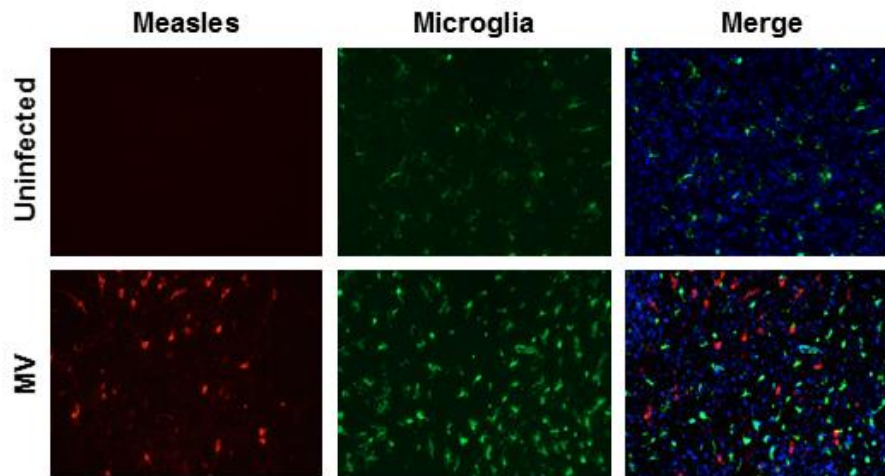
A. CD46+ neonates
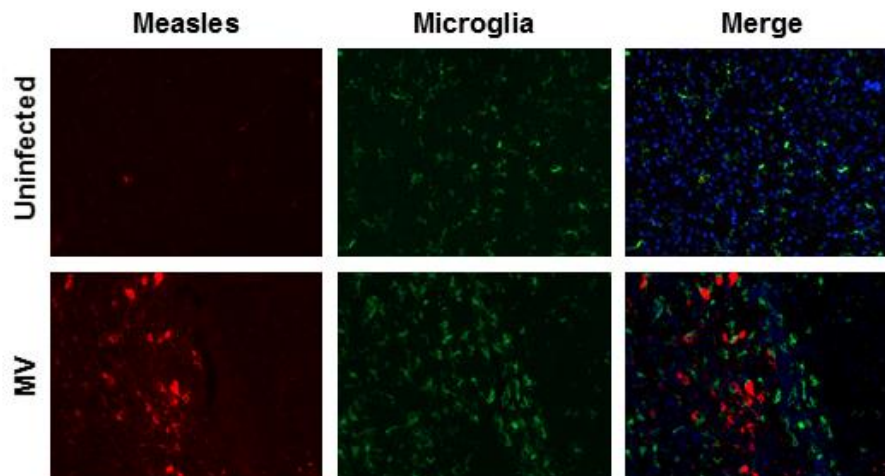
Figure 12. Microglial activation occurs during MV-infection in an IFNγ-independent manner.

Whole brains from MV-infected and uninfected control CD46+ neonates (A) and CD46+/IFNγ-KO neonates (B) were collected at 7 dpi. Sagittal sections from the neocortex were immunostained for measles (Hemagglutinin and matrix; red) and microglia (Iba1; green). Slides from 4-5 mice per condition were examined, and representative sections with MV+ cells are shown.

Figure 13.

A. CD46+ 7dpi MV – Thalamus (20x)

Hoechst   Measles   Microglia   Merge
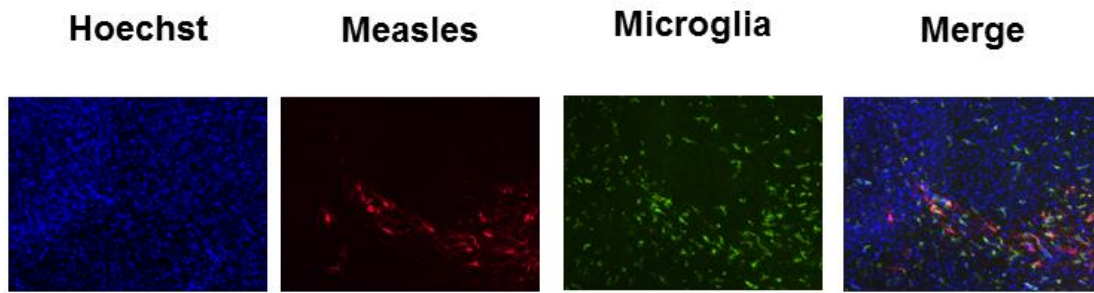
B. CD46+ 7dpi MV – Thalamus (40x)

C. CD46+/IFNγ-KO

Magnification: 10 x

1 mm
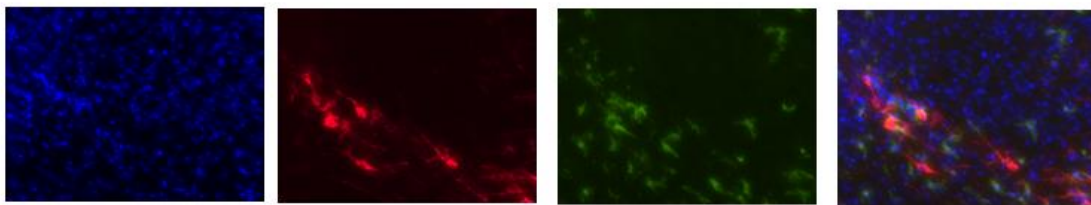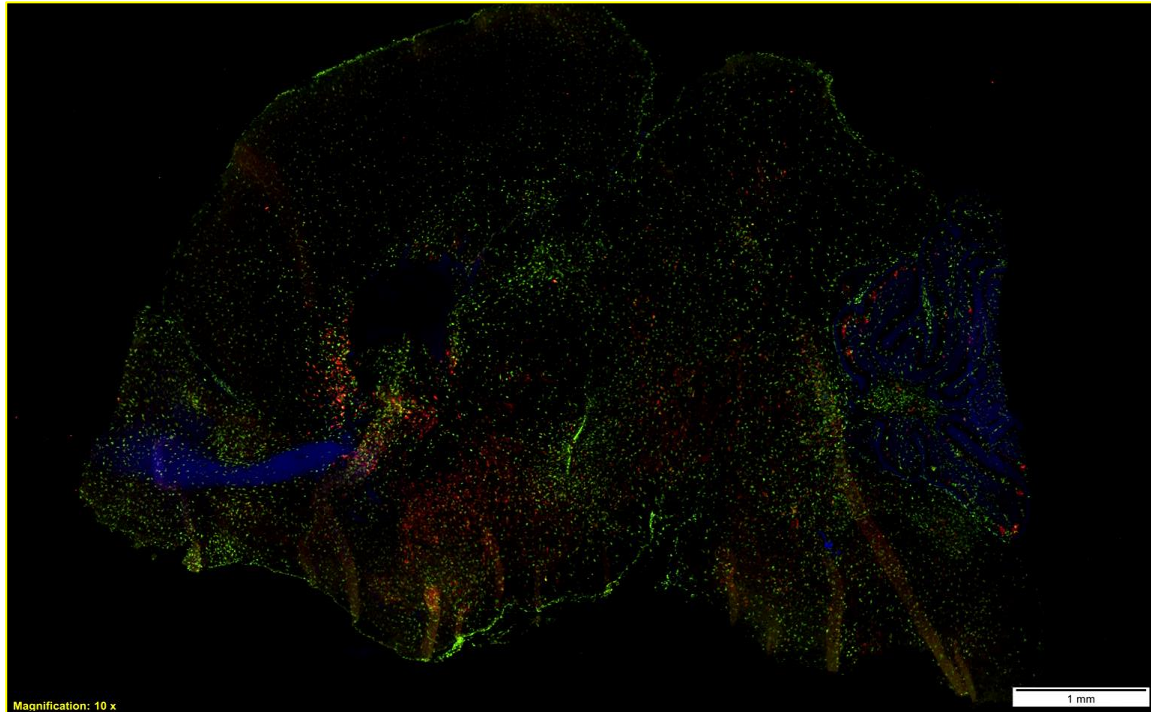
Figure 13. MV infection in the thalamas in both CD46+ and CD46+/IFNγ-KO neonates

Sagittal sections were immunostained for measles (Hemagglutinin and matrix; red), microglia (Iba1; green) and Hoechst 33342 stain (blue) as a nuclear marker. CD46+ 7dpi MV infected thalamus at 20x (A) and 40x (B). Stitched image of CD46+/IFNγ-KO brain at 7dpi MV *(*Scale bar = 200μm) (C). Slides from 4-5 mice per condition were examined, and representative sections with MV+ cells are shown.

3.3.6. IFNγ does not affect natural killer cell infiltration

Natural killer (NK) cells play an important antiviral role by direct lysis of infected cells and/or release of antiviral cytokines such as IFNγ, particularly during early stages of infection before a specific adaptive response is mounted (Biron, Nguyen, 1999, Paolini et al. , 2015). Since NK cells can be major producers of IFNγ, we investigated whether NK cells infiltrate into the brain parenchyma in neonates. As NK cells are part of the innate immune response, we quantified the early stages of infection (2 and 4 dpi) as well as a time point where T cell infiltration was increasing (6 dpi) (**Figure 14**). At 2 and 4 dpi, there is no significant difference in MV-infected pups compared to uninfected controls in both the genotypes. At 6 dpi, there is a significant increase in total NK cell number (NK1.1+, CD49b+, and NK1.1+/CD49b+) in MV-infected neonates compared to uninfected controls in both CD46+ (**Figure 14A**, $p<0.05$) and CD46+/IFNγ-KO (**Figure 14B**, $p<0.001$) genotypes. Collectively, these data show that NK cells arrive in the CNS during infection independently of IFNγ.

Figure 14.

A. CD46+ (NK cells)
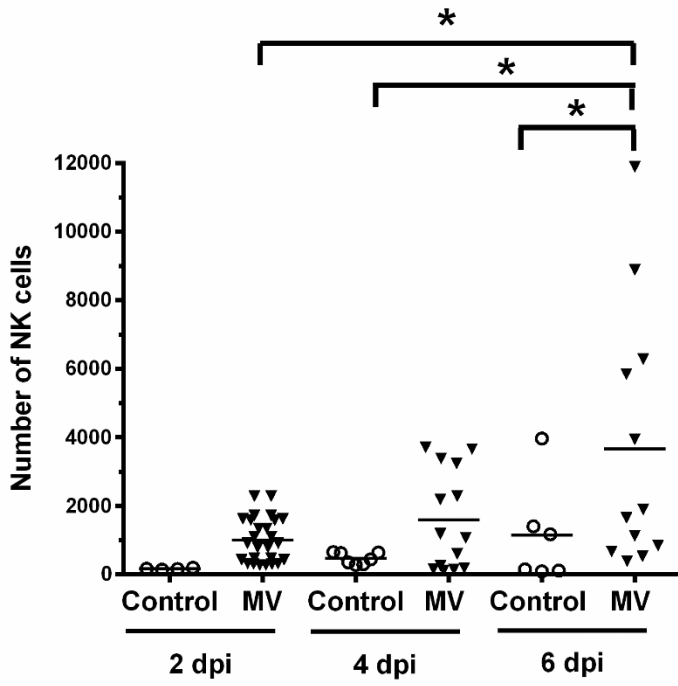
B. CD46+/IFNγ-KO (NK cells)
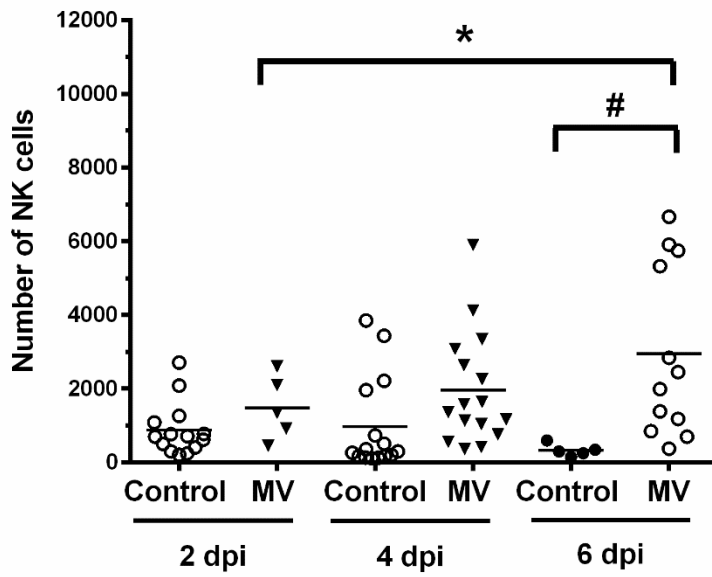
Figure 14. Infiltration of NK cells into the CNS is independent of IFNγ.

Whole brain homogenates from CD46+ (A) and CD46+/IFNγ-KO (B) neonates were analyzed

for total natural killer (NK) cell numbers at 2, 4, and 6 dpi by flow cytometry (CD3-

/NK1.1+/CD49b+). The horizontal line represents the mean number of cells for each

condition. Results from 4-5 different litters were collected, and statistical analysis was applied

by two-way ANOVA (# $p<0.001$, * $p<0.05$) with Bonferroni post hoc test. Whole brain

homogenates from MV-infected CD46+, CD46+/IFNγ-KO, and CD46+/RAG2-KO neonates

(C) were analyzed for neutrophils numbers (CD45^{hi}/CD11b+/Ly6G+) at 4 dpi and 6dpi by flow

cytometry. Results from 3 different litters were collected, and statistical analysis was applied

by one-way ANOVA (* $p<0.05$) with Bonferroni post hoc test.

3.3.7 *IFNγ limits neutrophil and inflammatory monocyte infiltration into the CNS*

We next investigated whether IFNγ affects neutrophil infiltration in the CNS. Neutrophils are recruited early in viral infections, and can contribute to tissue damage through protease and oxidase release during viral clearance (Drescher and Bai, 2013). Activated neutrophils produced ROS that activates innate immunity during HSV infection (Gonzalez-Dosal et al. , 2011). Neutrophils were identified as a population with CD45$^{(hi)}$, CD11b$^+$, Ly-6G$^+$ cell type (Mutnal et al. , 2010). CD11b is a marker found on several cells such as monocytes, granulocytes, macrophage, and natural killer cells. The F4/80 Ag is expressed on tissue resident macrophages such as microglia. Ly6G is exclusively expressed on neutrophils; hence helps distinguish it from monocyte and macrophage population. Thus, a neutrophil is defined as CD45^{hi}CD11b+++F4/80- Ly6G+ cells are neutrophils (Howe et al. , 2012).

In neonates that lack IFNγ, neutrophil infiltration is significantly higher compared to CD46+ neonates at 4 and 6 dpi **(Figure 15A)**. CD46+/RAG2-KO neonates also show progressively elevated levels of neutrophils in the CNS, but it is not significantly different from CD46+ or CD46+/IFNγ-KO neonates at either time point. This suggests that IFNγ may downregulate neutrophil recruitment in the CD46+ neonates during infection, and that excessive neutrophil infiltration may correlate with earlier death in CD46+/IFNγ-KO neonates.

During brain insults, circulating monocytes migrate to the breached BBB and enter the brain. Thus, both the infiltrating monocyte and microglia contribute to the neuroimmune response in the brain (Mildner et al. , 2009, Prinz et al. , 2011). Gene expression profiles indicate that infiltrating monocytes are highly inflammatory in experimental autoimmune

encephalomyelitis (EAE) models compared to microglia. Inflammatory monocytes were defined as cells expressing CD45^{hi}CD11b++F4/80+Ly6G- markers by flow (Howe, Lafrance-Corey, 2012). In neonates without IFNγ, inflammatory monocyte numbers are highest at 6dpi compared to CD46+ and CD46+/RAG2-KO neonates **(Figure 15B)**. From 4 to 6dpi, there is a significant influx of inflammatory monocyte in CD46+/IFNγ-KO neonates post infection. In CD46+/RAG2-KO, there is an increase in infiltrating monocytes as the infection progresses from 4 to 6dpi. This suggests that both neutrophils and monocytes respond to the infection at 6dpi. In other CNS infection models, these cells were seen 12 hours post infection.

Figure 15.

A. Neutrophils
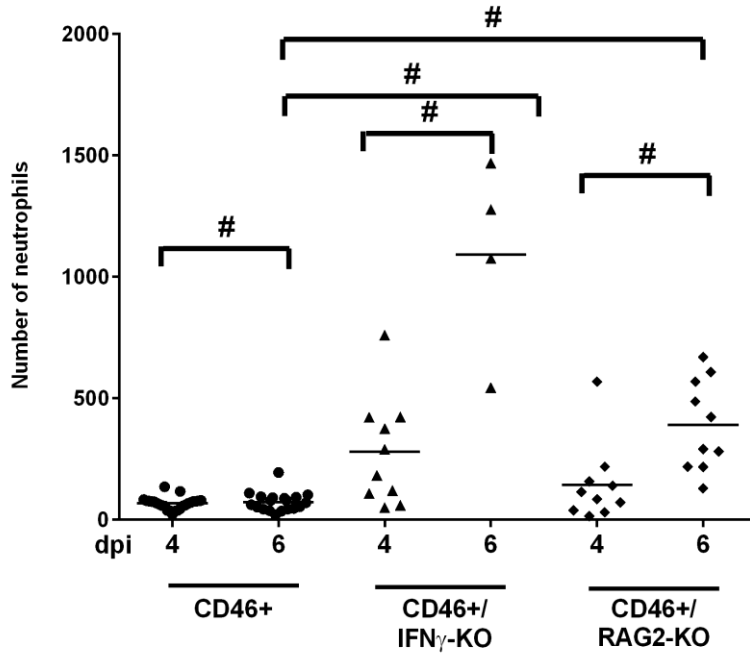
B. Inflammatory monocyte
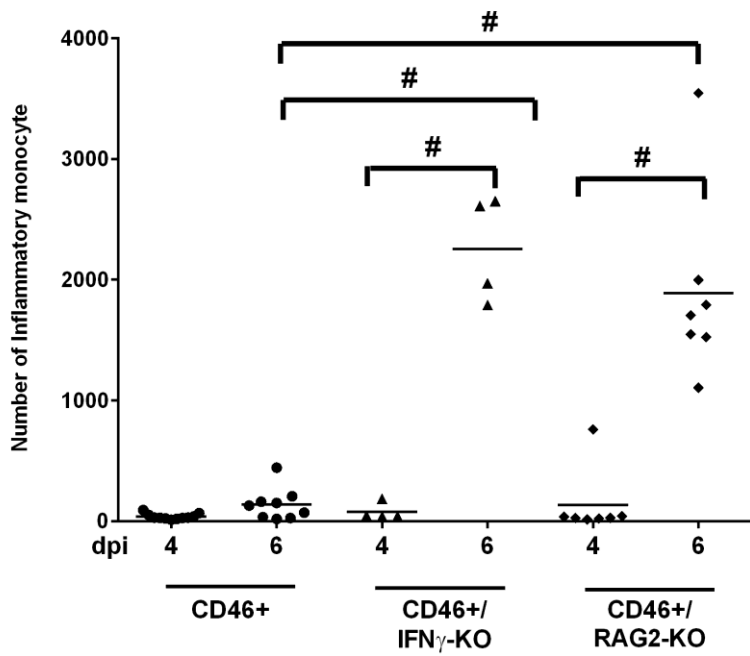
Figure 15. Infiltration of neutrophils and inflammatory monocytes cells into the CNS is independent of IFNγ.

Whole brain homogenates from CD46+ (A) and CD46+/IFNγ-KO (B) neonates were analyzed for neutrophils cell numbers at 2 and 4 dpi by flow cytometry (CD45^{hi}/CD11b+/Ly6G+/F4/80) and inflammatory monocytes (CD45+/CD11b+/Ly6G-/F4/80+). The horizontal line represents the mean number of cells for each condition. Results from 4-5 different litters were collected, and statistical analysis was applied by two-way ANOVA (# $p<0.001$, * $p<0.05$) with Bonferroni post hoc test.

3.3.8 *Higher infiltration of neonatal T cells in the absence of IFNγ at later stages of infection*

We observed the presence of NK cell, neutrophils, and inflammatory monocytes in an IFNg independent manner in the neonatal CNS. We wanted to understand if CD4 and CD8+ T-cells, which are critical for MV control in the adults (O'Donnell, Conway, 2012) infiltrate into the neonatal CNS. Using flow cytometry of whole brain homogenates, the numbers of CD4 and CD8 T cells in the neonatal brain were quantified at 4, 7, and 10 dpi, which corresponds to time points where T cells are first observed by immunohistochemistry (4 dpi) and time points that parallel peak infiltration of T cells in adults (7 and 10 dpi). At 4 dpi, there is no difference in the number of CD4 or CD8 T cells in the infected CD46+ neonates compared to uninfected controls (**Figure 16A and 16B**). There is higher infiltration of CD4 T cells in the absence of IFNγ early in infection at 4 dpi (**Figure 16A**). Similarly, at 7 dpi, significant CD4 T cell infiltration was observed only in the absence of IFNγ (**Figure 16C**), whereas CD8 T cell infiltration was induced in MV-infected neonates regardless of IFNγ expression (**Figure 16D**). At later stages of infection (10 dpi), significant infiltration of CD4 (**Figure 16E**) and CD8 T cells (**Figure 16F**) was observed only in the CD46+/IFNγ-KO pups in comparison to uninfected controls. CD46+ pups did not show a significant increase in CD4 or CD8 T cells at 10 dpi, although a trend toward increasing CD8 T cell number was observed (p=0.082). Comparing across genotypes, CD46+/IFNγ-KO neonates have significantly higher infiltration of CD4 T cells (p<0.001) and CD8 T cells (p<0.05) compared to CD46+ neonates at 10 dpi. Thus, these results suggest that IFNγ may have a suppressive/anti-inflammatory effect on T-cell infiltration at later time points in infection.

We also monitored the changes in T-cells over time **(Figure 17)**. In CD46+/IFNγ-KO neonates, there is significant decrease in CD4+ T-cell influx from 4 to 7dpi. This is followed by a significant influx of CD4+ T-cells from 4 to 10dpi and from 7 to 10dpi in CD46+/IFNγ-KO neonates **(Figure 17A)**. In CD46+ neonates, there is a slight increase in CD4+ and CD8+ T-cells over time but it is not significant **(A and B)**. When compared across genotypes, CD46+/IFNγ-KO neonates have higher infiltration of CD4+ T-cells at 4dpi and 10dpi compared to age matched infected CD46+ neonates. Infiltration of CD8+ T-cells is the highest in CD46+/IFNγ-KO compared to infected CD46+ neonates at 10dpi **(Figure 17B).** As the infection progresses, CD46+/IFNγ-KO neonates show a significant influx of CD8+ T-cells from 4 to 10dpi and from 7 to 10dpi. This may be due to a breakdown of blood brain barrier in CD46+/IFNγ-KO neonates at the later stages of infection. There is no change in CD8+ T-cell infiltration during early stages of infection from 4 to 7dpi in CD46+/IFNγ-KO brains. In the CD46+ neonatal CNS, there is increase in CD4 and CD8 T-cells as the infection progresses from 7 to 10dpi. This may contribute to high viral load seen in the CD46+ neonatal brains **(Figure 8)**.

Figure 16.

Figure 17.
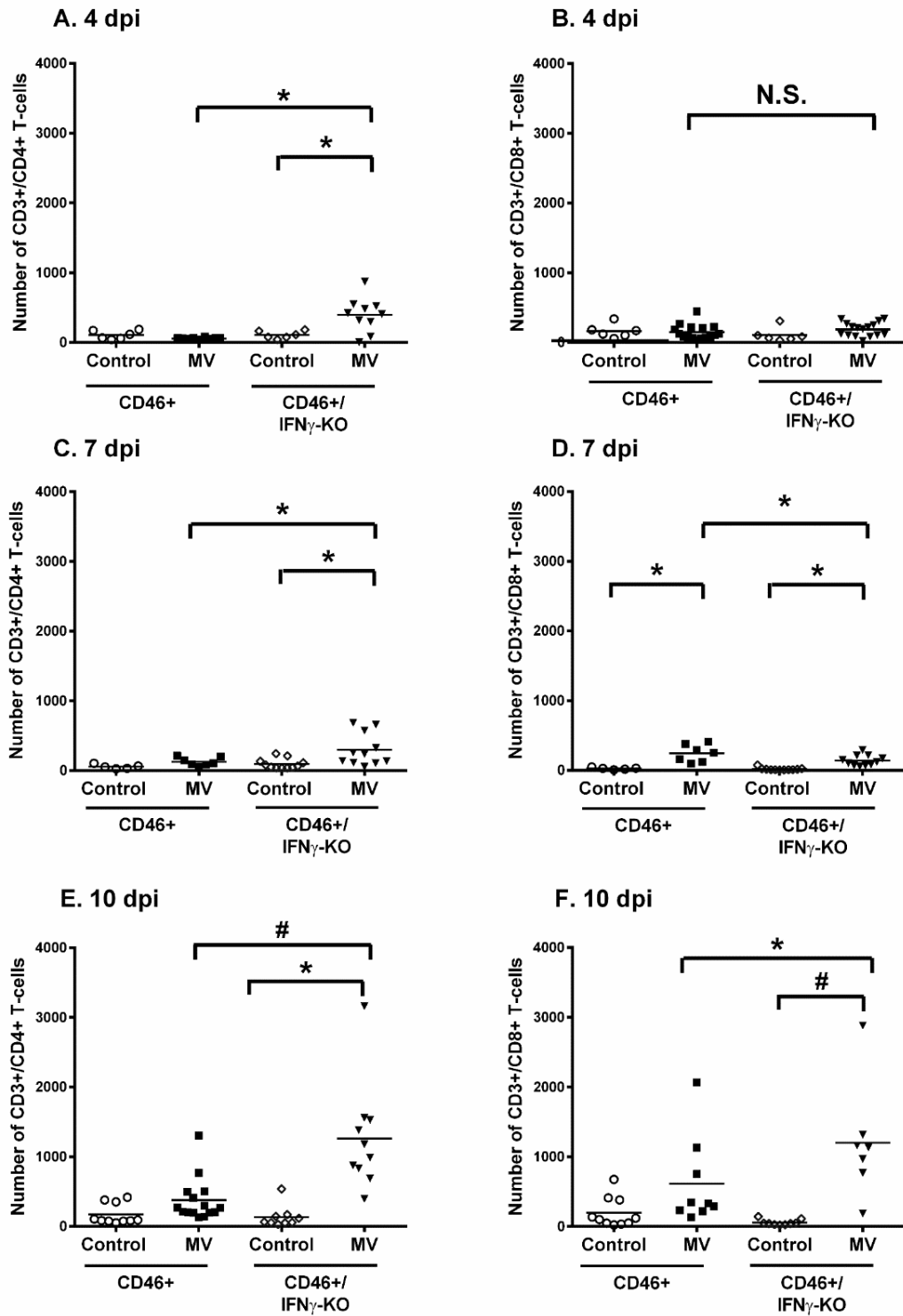
A. CD4+ T-cell
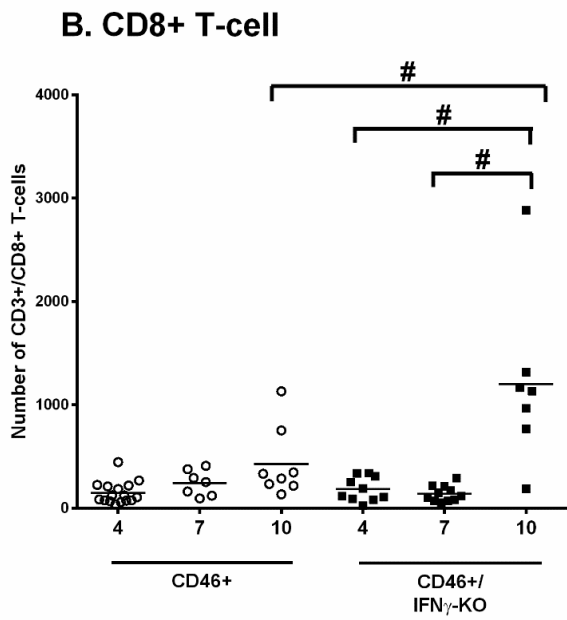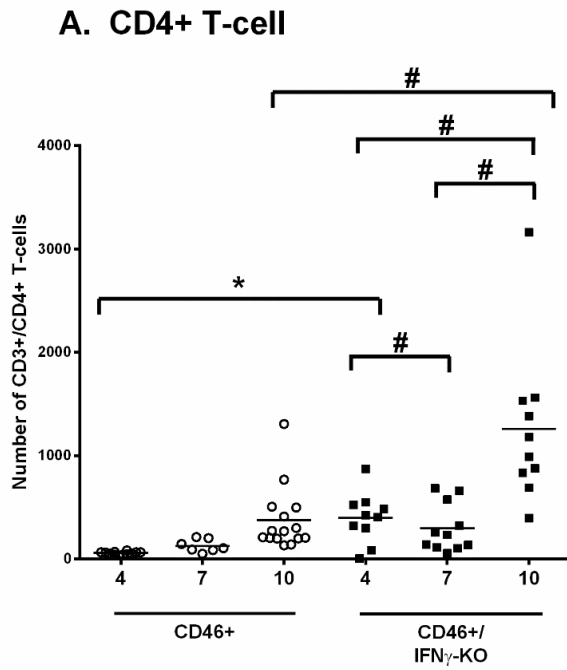
B. CD8+ T-cell

Figure 16. Neonates show higher T cell infiltration at later stages of infection in the absence of IFNγ.

Flow cytometry was performed on whole brain homogenates for CD4 T cells (CD3+/CD4+/CD19-) or CD8 T cells (CD3+/CD8+/CD19-). CD4 T-cells (left column; A, C, E) and CD8 T cells (right column; B, D, E) were quantified in uninfected and MV-infected CD46+ and CD46+/IFNγ-KO neonates at 4 (A, B), 7 (C, D), and 10 dpi (E, F). The black line represents the mean number of cells for each group. Results represent pups from 4-5 different litters. Statistical analysis was applied by two-way ANOVA (* p<0.05, # p<0.001) with Bonferroni post hoc test.

Figure 17. Higher infiltration of CD4 (4 and 10dpi) and CD8+ T-cells (10dpi) in the absence of IFNγ at 10dpi. Flow cytometry was performed on whole brain homogenates for CD4 T cells (CD3+/CD4+/CD19-) or CD8 T cells (CD3+/CD8+/CD19-). CD4 T-cells (A) and CD8 T cells (B) were monitored as the infection progresses. The black line represents the mean number of cells for each group. Results represent pups from 4-5 different litters. Statistical analysis was applied by two-way ANOVA (* p<0.05, # p<0.001) with Bonferroni post hoc test.

3.3.9 Greater CD4 T cell infiltration in adults compared to neonates regardless of IFNγ

expression

We next determined whether there were age-dependent differences in the number of T-cells infiltrating into the brain (**Figure 18**). CD46+ and CD46+/IFNγ-KO adults have a significantly higher number of CD4 T cells compared to neonates of both genotypes in infected whole brain tissue (**Figure 18A**, $p<0.05$). CD8 T cells in CD46+/IFNγ-KO adults are significantly higher compared to MV-infected neonates (**Figure 18B**, $p<0.05$). However, in the CD46+ genotype, there is no difference in the number of CD8+ T cells between adults and neonates. Additionally, in contrast to the neonates, there is no difference in the T cell numbers between CD46+ and CD46+/IFNγ-KO adults.

We also determine the ratio of CD4:CD8+ T-cell in adult and neonatal CNS. CD46+ adults (5.9:1), CD46+/IFNγ-KO adults (2.6:1), and CD46+/IFNγ-KO neonates (2.9:1), skew towards CD4+ T-cells. Whereas CD46+ neonates (0.5:1) have a ratio that is skewed towards CD8 T-cells. Of note, only CD46+ adult mice can control MV in the CNS (O'Donnell, Conway, 2012). This suggests that CD46+ neonates may lack adequate CD4+ T cell helper function, which may contribute to the relatively high viral load and poor pathological outcome.

Figure 18.
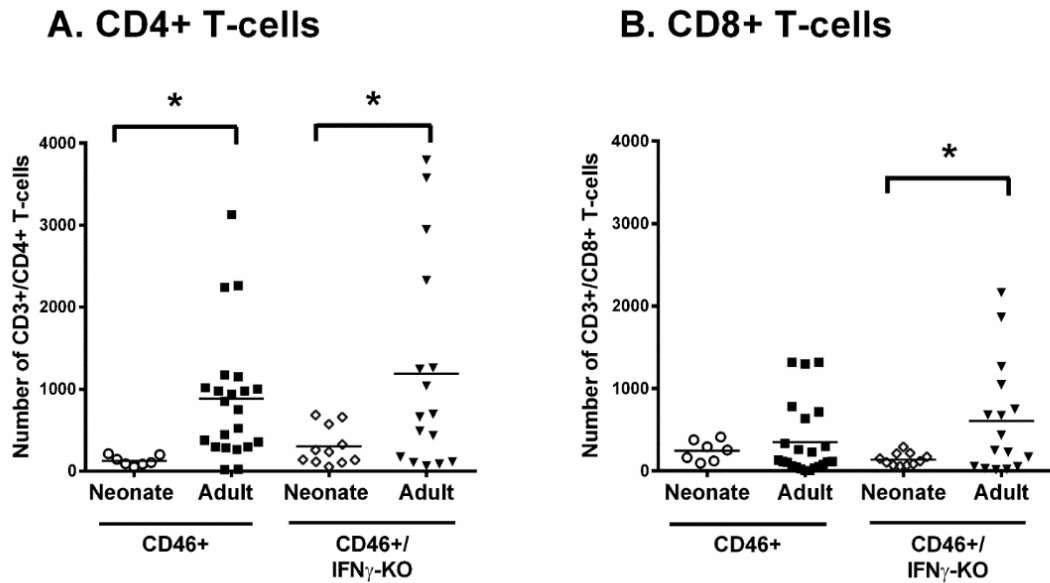
Figure 18. CD4 T cell infiltration in the CNS is greater in MV-infected adults than in neonates.

Whole brain homogenates from neonatal and adult CD46+ (A) and CD46+/IFNγ-KO (B) mice were analyzed for infiltrating T cells at 7 dpi. Flow cytometry was performed for CD4 T cells (CD3+/CD4+/CD19) or CD8 T cells (CD3+/CD8+/CD19-). Mice from 4-5 different litters were compared for each condition. Statistical analysis was applied by two-way ANOVA (* $p < 0.05$) with Bonferroni post hoc test.

3.3.10. B-cell infiltration at later stages is IFNγ independent

B-cells play a protective role during RNA virus infection such as Sindbis virus, Semliki Forest virus, rabies virus, and neurotropic coronaviruses (Fragkoudis et al. , 2008, Griffin et al. , 1997, Hooper et al. , 2009, Levine et al. , 1991). Studies in murine CMV models observe the infiltration of B-cells that produce mCMV specific antibodies (Ab) (Mutnal et al. , 2012). In adult CD46+ mice, B-cells are not required for survival or control of the virus (Solomos et al. , 2016). In neonates, there is a significant increase in B-cell numbers from 7 to 10 dpi in the absence of IFNγ **(Figure 19).** But in CD46+ neonates, there is no differences in B-cell infiltration as the infection progresses. When compared across genotypes, CD46+/IFNγ-KO neonates show significantly higher influx of B-cells compared to age matched CD46+ neonates at 10 dpi. Thus, this suggest that there may be a blood-brain-barrier breakdown in the absence of IFNγ at the later stages of infection, which allows for entry of B-cells into the CNS.

Figure 19.
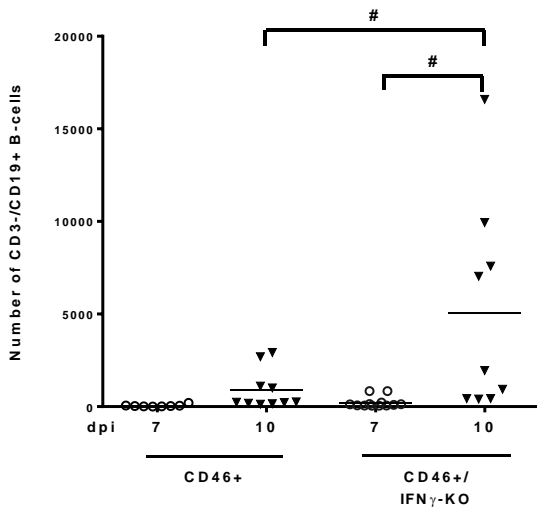
Figure 19. B-cell infiltration is IFNγ independent at later stages of infection.

Flow cytometry was performed on whole brain homogenates for B cells (CD3-/CD19+). B-cells were quantified in MV-infected CD46+ and CD46+/IFNγ-KO neonates at 7 and 10dpi. Black line represents the mean number of cells for each group. Results represent pups from 4-5 different litters. Statistical analysis was applied by two-way ANOVA (* p<0.05, #p<0.001) with Bonferroni post hoc test.

3.4   Discussion

The goal was to define the course of pathology and immune cell infiltration in the neonatal brain during a viral infection. In the current study, CD46+ pups lacking IFNγ succumb earlier to the infection despite greater infiltration of neutrophils and T cells than in wildtype pups, which highlights the pleiotropic nature of this cytokine in influencing both leukocytes. We demonstrated that the neonates mount an innate immune response with microglial activation, NK cell, neutrophil and inflammatory infiltration in the brain. In CD46+/RAG2-KO mice, the neonatal innate response is capable of delaying mortality and disease. But despite this, neonates of all genotypes succumb to the infection. Our findings are consistent with the observation that neonatal immune responses are often ineffective at controlling viruses and other pathogens (reviewed in (Rouse and Sehrawat, 2010).

We characterized the role of the Th1 cytokine IFNγ during a neonatal immune response in the brain because IFNγ is indispensable for neuronal clearance of many different viruses (Burdeinick-Kerr, Wind, 2007, Chesler et al. , 2004, Komatsu et al. , 1996, Larena, Regner, 2013, Patterson, Lawrence, 2002). However, it is important to note that IFNγ also plays both pro- and anti-inflammatory roles in a variety of pathological conditions (Muhl and Pfeilschifter, 2003), in addition to roles in host defense. We reasoned that IFNγ may be protective in the developing CNS during an infection, where neurogenesis and synaptic refinement are active. We have previously shown that IFNγ protects neural stem cells, but not newly-differentiated neurons, in MV-infected CD46+ neonates (Fantetti et al. , 2016). Although IFNγ maintains the neural stem cell pool during infection, it does not preserve neurogenesis, demonstrating that IFNγ can prevent neural stem loss but cannot prevent loss of

function. In the current study, CD46+ pups lacking IFNγ succumb earlier than wildtype pups, which highlights the pleiotropic nature of this cytokine in influencing both lymphocyte and neural cell activity**.** This finding also is consistent with models of experimental autoimmune encephalitis, where IFNγ-knockout mice demonstrate more severe inflammation in the brain (Willenborg et al. , 1999). Studies in IFNγ receptor deficient mice infected with sindbis virus show greater infiltration of CD3+ T cells and perforin+ cells and more intense inflammation in the CNS compared to wildtype mice (Lee et al. , 2013). Thus, further studies will determine if CD46+/IFNγ-KO neonates express a more pro-inflammatory cytokine profile in the brain, which would parallel the increased T cell infiltration at late stages of infection **(Chapter 4)**.

The innate immune cells are the first responders of host defense against pathogens and are mediated by phagocytes such as macrophages and dendritic cells. Innate immunity may also contribute to early viral control, even if it is not responsible for the ultimate resolution of infection in the brain. There were no differences in microglial morphology or intensity of Iba1 staining in the presence and absence of IFNγ. This result was surprising because microglial cells are exquisitely sensitive to IFNγ. Therefore, this suggests that compensatory cytokines may be activating the microglia in CD46+/IFNγ-KO. Resident microglia (CD45+[(int)] and CD11b(+)) do not express MHC class II in resting state. Microglia, become activated either in response to virus or IFNγ and upregulate MHC II (Hamo et al. , 2007). Studies in murine CMV suggest that upregulation of MHC II on microglia and high CXCL2 expression may lead to high infiltration of neutrophils. Thus, MHC II is a marker of microglial activation and in some cases may indicate an exaggerated neuroinflammatory process in the brain (Mutnal, Cheeran, 2010). Thus, further studies to address the differences

in MHC II expression may provide insights on microglial activation and how genetic deficiencies impact this.

Natural killer cells can be significant producers of IFNγ during viral infections ((Biron, Nguyen, 1999)). We observed that there are no differences in NK cell infiltration **(Figure 14)** between CD46+ and CD46+/IFNγ-KO pups. Because NK cell cytotoxicity is highly dependent upon the type of cytokine stimulation, it is conceivable that the inflammatory milieu in CD46+/IFNγ-KO pups encourages greater cytotoxic activity in NK cells (Lauwerys et al. , 2000), which may contribute to greater pathology. Another possibility is that the cytokine milieu in neonates does not activate the microglia in a manner that is favorable for viral clearance or antigen presentation. Additionally, children with herpes encephalitis show deficiencies in NK cell function. There is also evidence of NK cells being neurotoxic as well as neuroprotective (Reviewed in (Poli, Kmiecik, 2013)). Thus, further studies to explore the functional differences in neonatal NK cells to adult NK cells may explain the differences in age dependent outcome of infection.

Neutrophils in circulation respond to proinflammatory, chemotactic signals and migrate to injured and infected tissue. Neutrophils play a role in extracellular bacterial infections and several viral infections. Studies indicate that in the absence of anti-inflammatory cytokines such as IL-10, high numbers of neutrophil enter the brain and cause neuropathology (Jeong et al. , 2009, Mutnal, Cheeran, 2010). Thus, in the absence of IFNγ, infiltration of excessive neutrophils and inflammatory monocytes may contribute to edema and neuropathology. There is evidence that neutrophils have destructive potential through

neurotoxic effects through the release of proteolytic enzymes (Allen et al. , 2012, Stowe et al. , 2009). Neutrophil activation during viral infections also leads to tissue damage (Drescher and Bai, 2013, Stout-Delgado et al. , 2009). C57Bl/6 mice infected with influenza A virus require IFNγ to modulate neutrophil activity in the lung and prevent tissue pathology (Stifter et al. , 2016). Thus, the heightened numbers of neutrophils, along with a lack of modulation of neutrophilic activity by IFNγ, may play a role in neuropathology in the CD46+/IFNγ-KO neonates. It will be interesting to study the differences in neutrophils in the adult CNS and compared it to neonates. This may help understand the inherent age dependent functionality of neutrophils in the brain.

From these results, we can conclude that the neonatal immune response is capable of inducing infiltration of innate immune cells in the CNS, but may struggle with the extensive viral load that is produced in developing neurons. Neurotropic viruses spread readily in less mature or newly-differentiated neurons, which may pose a greater challenge for viral control and clearance in the developing brain (van den Pol et al. , 2002). This notion is supported by the observation that MV-infected neonates exhibit more widespread expression of viral antigen in multiple brain regions prior to T cell infiltration, which suggests that the virus spreads readily in neonatal brain tissue. Thus, further studies will look at the difference in infiltration of T-cells which were critical for clearance in the adult CNS.

Neonates had the highest levels of neutrophil **(Figure 15)** and T cell infiltration (**Figure 16**) in the absence of IFNγ, and succumbed to the infection sooner than other genotypes. This finding contrasts with CD46+/RAG2-KO neonates, which lack mature T cells and show

delayed mortality. Although we do not yet understand whether such a T cell response could contribute to neuropathology, these findings suggest that the lack of adaptive immune response may be beneficial to survival in the infected neonates. Other models of viral CNS infections, including some strains of west nile virus and dengue virus, show that the CD8 T cell response induces immunopathology while also providing protection against the virus (An et al. , 2004, King et al. , 2007). Cytotoxic T cells also play a more pathogenic role during infections with Murray Valley encephalitis virus, where mice lacking granule exocytosis showed prolonged survival (Licon Luna et al. , 2002). Of note, while providing evidence for a detrimental role for T cell activity during a CNS infection, these studies were performed on adult mice, which contrasts with findings in the adult CD46+ model where viral control is not associated with immunopathology. An outstanding question is whether age-dependent function of T-cell will dictate whether an anti-viral response will result in immunopathology.

Adult CD46+ mice depend upon CD4 T cells in concert with CD8 T cells or B cells in order to survive a CNS infection with MV (Solomos, O'Regan, 2016, Tishon et al. , 2006). The deletion of CD4 T cells alone results in death of adult CD46+ mice, whereas depletion of CD8 T cells is associated with less viral control but no changes in survival (Solomos, O'Regan, 2016). Studies in other transgenic model suggest that CD4, CD8 or B-cells cannot control acute MV infection alone. A combination of either CD4 T cell and B cells or CD4 and CD8 Tcell are essential to control measles virus infection in the CNS (Tishon, Lewicki, 2006). Within the adult brain, the CD4:CD8 T cell ratio revealed a greater proportion of CD4 T cells (5.9:1; **Figure 18).** In C57/Bl6 mice, which are the background strain of the CD46+ model, the CD4:CD8 ratios are relatively low in the spleen, as we also observed in splenocytes from the

CD46+ adult mice (1.7:1; data not shown) (Myrick et al. , 2002). During many viral infections, the CD4:CD8 ratio reverses to greater proportion of CD8 T cells, where the CD8 T cells become necessary for viral clearance either through cytolytic or non-cytolytic mechanisms (Callan et al. , 1996, Tripp et al. , 1995). The high CD4:CD8 ratio in the adult CD46+ brains, where viral clearance is successful, may suggest that a greater proportion of CD4 help is required to respond to neuronal infections non-cytolytically. These observations in MV-infected adult mice contrast with our findings in CD46+ pups, where the CD4:CD8 ratio skewed toward greater CD8 T cells (**Figure 16**). One possibility is that the low proportion of CD4 T cells does not provide sufficient stimulation to the CD8 T cells to contribute to a non-cytolytic response. Support for this idea is found in a model of neurotropic mouse hepatitis virus infection, where depletion of CD4 T cells impaired the anti-viral function and survival of infiltrating CD8 T cells (Phares et al. , 2012). Thus, it is possible that the lack of adequate number of CD4 T cells in neonates may lead to inefficient activation of effector CD8 T-cells and loss of viral clearance.

In contrast, CD46+/IFNγ-KO neonates, which had the highest level of T cell infiltration (**Figure 16C and 16D**), succumbed to the infection sooner than the other genotypes. These findings support the notion that a lack of a neonatal adaptive immune response may be protective in the brain. Other models of viral CNS infections, including some strains of west nile virus and dengue virus, show that the CD8 T cell response induces immunopathology while also providing protection against the virus (An, Zhou, 2004, King, Getts, 2007). Cytotoxic T cells also play a more pathogenic role during infections with Murray Valley encephalitis virus, where mice lacking granule exocytosis showed prolonged survival (Licon Luna, Lee, 2002). Of note, while providing evidence for a detrimental role for T cell activity during a CNS

infection, these studies were performed on adult mice, which contrasts with findings in the adult CD46+ model where viral control is not associated with immunopathology. An outstanding question is whether there are age-dependent changes in T cell activity that dictate whether an anti-viral response will result in immunopathology.

A second possibility is that the expression of IFNγ limits T cell infiltration into the brain, thereby limiting cytotoxicity. Previous studies in respiratory syncytial virus (RSV)-infected neonates demonstrate that IFNγ expression in the lung leads to reduced recruitment of CD4 and CD8 T cells (Eichinger et al. , 2015). Thus, a lack of IFNγ expression may allow for greater recruitment of immune cells into the CNS in CD46+/IFNγ-KO neonates, thereby contributing to greater immunopathology. T cells also play a more pathogenic role during infections with Murray Valley encephalitis virus, where mice lacking granule exocytosis showed prolonged survival (Licon Luna, Lee, 2002). Of note, while providing evidence for a detrimental role for T cell activity during a CNS infection, these studies were performed on adult mice, which contrasts with findings in the adult CD46+ model where viral control is not associated with immunopathology. CD4 T cells were shown to play a major role in protection from MV infection. However, in our system, CD4 T cells do not act independently to control MV infection as reported earlier for MV and for murine gammaherpesvirus (Finke and Liebert, 1994) (Sparks-Thissen et al., 2005). Instead, CD4 T cells in conjunction with B cells or with CD8 T cells are required to abort acute MV infection in the vast majority of MV infected mice. These results indicate that control of MV may be dependent on multiple lymphocyte subsets and not on a single lymphocyte subset. Although, we observed high T-cell and B-cell infiltration

in the absence of IFNγ, these neonates succumb early to infection **(Figure 7)**, suggesting that there are likely functional differences in these lymphocytes that are not present in adults.

From these results, we observe that neonatal immune response is capable of inducing elements of a successful adult response in the brain, including robust infiltration of T-cells, B-cells and NK-cells, but may struggle with the extensive viral load that is produced in the developing neurons. Neurotropic viruses spread readily in less mature or newly-differentiated neurons, which may pose a greater challenge for viral control and clearance in the developing brain (van den Pol, Reuter, 2002). This notion is supported by the observation that MV-infected neonates exhibit more widespread expression of viral antigen in multiple brain regions prior to T cell infiltration, which suggests that the virus spreads readily in neonatal brain tissue (Figure 8). The combination of aggressive viral spread may overwhelm the neonatal CNS.

CHAPTER 4
Neonates succumb to the infection despite a Type I and II interferon expression in the CNS

4.1 Hypothesis: Neonatal immune response will be deficient in the expression of anti-viral cytokines during both early and late responses to a CNS infection.

4.2 Rationale

Neonatal immune response to peripheral infections results in induction of distinct cytokine profile when compared to an adult response against the same pathogen (reviewed in (Adkins, Leclerc, 2004)). Depending upon the type and dose of antigen, neonatal T cells often skew towards a Th2-like response (including production of IL-4, IL-5, and IL-13) as opposed to a Th1 response, characterized by the production of IFNγ and TNF (Zaghouani, Hoeman, 2009). During a CNS infection, one could hypothesize that a Th1 response would be preferred in order to ensure adequate IFNγ expression and control viral replication in developing neurons while minimizing neuronal loss. However, IFNγ also has been shown to play both neurotoxic and neuroprotective roles for developing neurons, making the influence of IFNγ in controlling neonatal infections in the brain less clear (Mizuno, Zhang, 2008, O'Donnell, Henkins, 2015).

Additionally, Type I IFNs (IFNα and IFNβ) also regulate various arms of the immune response against infections and have autocrine and/or paracrine effects. They promote the expression of IFN-stimulated genes (ISGs) during an anti-viral immune response, which can protect both infected and uninfected cells from viral replication (Borden et al. , 2007, Schoggins et al. , 2011). When neurons are infected, they quickly initiate a protective type I IFN response. IFNβ is an immediate early IFN that is produced by neurons and glia (Erlandsson et al. , 1998).

97

The production of IFNβ over IFNα may be neuroprotective as IFNα contributes to greater neurotoxicity. The type I IFN response slows virus spread and constrains virus replication before the induction of a virus-specific adaptive immune response. Studies in CD46+ MV-infected adults suggest that type I IFNs are dispensable for viral clearance in CNS neurons (Cavanaugh, Holmgren, 2015). Rather, viral clearance in the adult CD46+, CNS is mediated by CD4+ T-cells and IFNγ production (Solomos, O'Regan, 2016). Age-dependent effects of Type I and Type II IFNs in the brain post neurotropic infection are not well understood. Thus, we explored the differences in the cytokine and chemokine response in the neonatal brain to identify the shortcomings or deficits compared to an adult CNS.

Studies have suggested that neonates have a predominant Th2 response during peripheral infections (Adkins, Leclerc, 2004) (Lambert et al. , 2014), which is an aberrant response during viral infections. But in context to the neonatal brain and neutrotropic infections, this response has not been studied. Thus, the initial hypothesis was that neonates may express a Th2-biased cytokine response in the CNS and this may contribute to ineffective viral clearance. Based on the results from the PCR array, our data suggests that a both neonates and adults exhibit a Th1 phenotype in the brain at 7dpi. Despite this, the CD46+ neonates succumb to the infection **(Figure 7)**. Therefore, we examined factors beyond the Th1/Th2 bias and focussed on early innate, Type I IFN response and its surrogate markers as well as downstream signalling of IFNγ. As the virus is high at 4 dpi **(Figure 8)**, prior to robust NK and T-cell accumulation, the role of early IFNs and the potential deficits in downstream IFNs signaling may explain the lack of viral control in neonates.

4.3 Results

4.3.1 MV-infected neonates upregulate Th1 cytokine and chemokine genes in the CNS

To address the age dependent differences in chemokine/cytokine production, we examined the

mRNA expression of 84 cytokine and chemokines genes in the MV-infected adult and neonatal

brains using a qRT-PCR array. Table 1 lists genes that were significantly upregulated by ≥2

fold in the MV-infected neonates and adults compared to their age-matched, uninfected controls.

Classical Th2 cytokines such as IL-4, IL-5, and IL-13 were not upregulated in either MV-

infected neonates and in the adult CNS. Rather, many Th1-associated cytokines were

upregulated in comparison to uninfected controls at both ages (p< 0.05; **Table 4**, top panel).

Among the Th1-associated factors, IFNγ (11-fold in neonates, 8-fold in adults), IL-1β (3-fold

in adults and neonates) and chemokine (C-X-C motif) ligand 10 (Cxcl10; 85-fold in neonates,

44-fold in adults) were upregulated during MV infection at both ages. The anti-inflammatory

cytokine interleukin-1 receptor antagonist (IL1rn) is also upregulated in neonates (17.84-fold)

and adults (14.4-fold) post-infection, as well as the expression of several other chemokines

genes (Ccl12, Ccl3, Ccl4, Ccl5, Cxcl11 and Cxcl13). Both adults and neonates do not

upregulate IFNα2 post MV infection. These data suggest that the expression of many

inflammatory genes is age-independent in the brain.

Table 4.

Genes	Description	CD46+ Neonate		CD46+ Adult	
		Fold change	p value	Fold change	p value
Cxcl10	Chemokine (C-X-C motif) ligand 10	84.62	0.011	44.43	0.049
IL1rn	Interleukin 1 receptor antagonist	17.84	0.016	14.4	0.025
Ccl5	Chemokine (C-C motif) ligand 5	15.18	0.007	10.84	0.016
IFNγ	Interferon gamma	11.08	0.027	8.1	0.021
Ccl4	Chemokine (C-C motif) ligand 4	10.54	0.012	5.03	0.026
Ccl12	Chemokine (C-C motif) ligand 12	5.69	0.032	15.91	0.011
Cxcl13	Chemokine (C-X-C motif) ligand 13	3.89	0.029	19.18	0.033
Ccl3	Chemokine (C-C motif) ligand 3	3.73	0.021	3.22	0.0003
IL1β	Interleukin 1 beta	3.27	0.027	3.04	0.014
Ccl2	Chemokine (C-C motif) ligand 2	15.33	0.042		
Ccl7	Chemokine (C-C motif) ligand 7	9.31	0.017		
Tnf	Tumor necrosis factor	8.38	0.016		
IL12b	Interleukin 12B	7.87	0.02		
Osm	Oncostatin M	4.44	0.009		
Xcl1	Chemokine (C motif) ligand 1	3.84	0.03		
IL27	Interleukin 27	3.4	0.031		
Cxcl11	Chemokine (C-X-C motif) ligand 11	2.58	0.025		
IL10	Interleukin 10	2.36	0.03		
Cxcl9	Chemokine (C-X-C motif) ligand 9			17.67	0.02
Ccl11	Chemokine (C-C motif) ligand 11			2.67	0.002
IL1α	Interleukin 1 alpha			2.67	0.021
Cxcl16	Chemokine (C-X-C motif) ligand 16			2.43	0.01
Ccl22	Chemokine (C-C motif) ligand 22			2.27	0.039
Tnfsf10	TNF (ligand) superfamily, member 10			2.26	0.038
Fasl	Fas ligand (TNF superfamily, member 6)			2.14	0.015
IL7	Interleukin 7			2.18	0.046

Table 4. Gene expression of pro- and anti-inflammatory cytokines in MV-infected neonatal and adult brains.

Gene expression of cytokines and chemokines in measles virus-infected neonatal and adult brains. Brain tissue from uninfected and MV-infected CD46+ neonates and adults were collected for RNA extraction at 7 dpi. qRT-PCR array analysis was performed using the RT^2 Profiler™ PCR Array. Changes in the gene expression that were more than two-fold relative to the uninfected controls are shown. For infected mouse brains (n = 16) and for uninfected (n=8) were used for adults and neonates. All data were normalized against levels of housekeeping genes within the same sample. *$p < 0.05$ by students t-test.

Additionally, neonates and adults also upregulate unique subsets of genes in an age-dependent manner during infection (**Table 4**, middle and bottom panel). The expression of tumor necrosis factor (TNF) is significantly increased in MV-infected neonates, but not in adults. Interleukin 10 (IL-10), a global suppressor of the immune response (Moore et al. , 2001), was the only Th2-related cytokine to be upregulated in MV-infected neonates. CCL2, which is associated with reduced microglial/macrophage activation in adult infection with mouse hepatitis virus (MHV), is elevated only in infected neonates (Trujillo et al. , 2013). MV-infected adults also expressed unique inflammatory genes that were not activated in the neonates. Adult mice show increased expression of the IFNγ-inducible gene CXCL9 (17.67-fold) (Brice et al. , 2001), which suggests that IFNγ-responsive gene expression may be partially dependent on age. Of note, gene expression in uninfected neonates and adults revealed modest baseline differences in the absence of infection (**Table 7**). For example, adult mice expressed higher baseline levels of IL-12a (3.98-fold), IL-17a (2.13-fold), and IL-2 (2.13-fold) in the brain than uninfected neonates.   Of these cytokines, IL-12a was the only factor to be upregulated by the neonates upon infection (7.87-fold versus uninfected neonates, Table 1). Together, this data suggests that the majority of cytokines/chemokines that are induced upon infection are distinct from factors that show an age-dependent difference in uninfected controls.

We also wanted to address the differences in survival between the immunocompetent and immunocompromised neonates. In order to define any variation in the cytokine profiles in infected neonates, we examined the cytokine expression in CD46+, CD46+/IFNγ-KO and CD46+/RAG2-KO neonatal brains (**Table 5**). CD46+/IFNγ-KO and CD46+/RAG2-KO

neonates expressed unique subsets of genes that were not upregulated in the immunocompetent CD46+ mice. CD46+/IFNγ-KO neonates upregulated CXCL1 in the brain, which can act as a neutrophil chemoattractant and may partially explain the greater neutrophil infiltration observed in these mice (**Figure 15A**) (Bozic et al. , 1995). Surprisingly, CD46+/IFNγ-KO neonates also upregulated CXCL9, which is classified as an IFNγ-inducible gene, suggesting that IFNγ-independent pathways may also regulate CXCL9 expression in the CNS. The CD46+/RAG2-KO neonates, which demonstrated less mortality during infection, activated a number of genes that were not observed in the other neonates (**Table 5, bottom panel**). Various cytokines (IL-5, IL-7, IL-15, and bone morphogenic proteins (BMP) 2, 4, 6, and 7) and chemokines (CCL11, CCL17, CCL19, CCL22, CXCL16) were induced only in CD46+/RAG2-KO brains upon infection.   However, comparison of the baseline gene expression between uninfected neonates demonstrates that CD46+/RAG2-KOs have lower basal expression of some of the factors that are upregulated during infection (*e.g.* the BMPs, CCL11, and CCL17; (**Table 6**) in comparison to the uninfected CD46+ neonates. Thus, although the CD46+/RAG2-KO neonates express many unique genes upon infection, a subset of these genes are expressed endogenously at low basal levels.

As seen in the CD46+ neonates and adults, there was overlap in the expression of some Th1-related factors in the neonatal mice. CXCL10 showed the greatest induction in all infected neonates: CD46+ (84.6-fold), CD46+/IFNγ-KO (291.4-fold) and CD46+/RAG2-KO neonates (771.1-fold). IFNγ is upregulated in the CD46+ (11.1-fold) and CD46+/RAG2-KO neonates (15.0-fold), suggesting that innate immune cells are contributing to IFNγ production the absence of T cells. With the exception of IL-10, genes that were activated in the CD46+

neonates but not in the CD46+ adults **(Table 4, middle panel)** also were expressed in

CD46+/IFNγ-KO and CD46+/RAG2-KO neonates. For example, TNF is upregulated in CD46+

(8.4-fold), CD46+/IFNγ-KO (17.9-fold) and CD46+/RAG2-KO (72.1-fold) neonates, but there

is no upregulation in the adults. In addition, genes that were only expressed in the CD46+

adults when compared to CD46+ neonates (*e.g.* CXCL9, CCL11; **Table 4, bottom panel)** were

all expressed in the CD46+/RAG2-KO neonates upon infection. Thus, the CD46+/RAG2-KO

neonates express a cytokine profile that includes factors that are controlled in an age-dependent

manner in the immunocompetent CD46+ mice.

In addition to understanding the genes that are upregulated post infection, we wanted

to understand the baseline differences in cytokine expression due to genetic deficiencies.

Thus, in **Table 6**, basal gene expression in uninfected CD46+/IFNγ-KO and CD46+/RAG2-

KO neonates are compared to uninfected CD46+ neonates. As expected, IFNγ and IFNγ

inducible CXCL11 is downregulated in CD46+/IFNγ-KO neonates. In CD46+/RAG2-KO

neonates show downregulated Bmp 2, 4, 6, and 7 expression compared to CD46+ uninfected

neonates. There were no baseline differences in IFNα and chemokines like CXCL10 and

CCL2 among all the neonates **(Table 6)**.

Table 5.

Gene	Description	CD46+ neonate		CD46+/IFNγ-KO neonate		CD46+/RAG2-KO neonate	
		Fold change	p value	Fold change	p value	Fold change	p value
Cxcl10	Chemokine (C-X-C motif) ligand 10	84.62	0.011	291.38	0.001	771.13	0.023
IL1rn	Interleukin 1 receptor antagonist	17.84	0.016	68.96	0.003	214.9	0.0008
Ccl5	Chemokine (C-C motif) ligand 5	15.18	0.007	33.49	0.013	132.97	0.013
IFNγ	Interferon gamma	11.08	0.027	-	-	15.02	0.023
Ccl4	Chemokine (C-C motif) ligand 4	10.54	0.012	32.55	0.007	153.19	0.0001
Ccl12	Chemokine (C-C motif) ligand 12	5.69	0.032	-	-	272.95	0.001
Cxcl13	Chemokine (C-X-C motif) ligand 13	3.89	0.029	14.11	0.016	41.24	0.006
Ccl3	Chemokine (C-C motif) ligand 3	3.73	0.021	8.35	0.003	31.05	0.0001
IL1β	Interleukin 1 beta	3.27	0.027	5.9	0.003	9.85	0.005
Ccl2	Chemokine (C-C motif) ligand 2	15.33	0.042	35.89	0.018	493.99	0.001
Ccl7	Chemokine (C-C motif) ligand 7	9.31	0.017	16.46	0.024	164.18	0.024
Tnf	Tumor necrosis factor	8.36	0.016	17.9	0.007	72.05	0.009
IL12b	Interleukin 12B	7.87	0.02	15.28	0.008	199.93	0.03
Osm	Oncostatin M	4.44	0.009	5.58	0.024	11.29	0.023
Xcl1	Chemokine (C motif) ligand 1	3.84	0.03	13.98	0.009	21.72	0.047
IL27	Interleukin 27	3.4	0.031	6.49	0.001	14.55	0.005
Cxcl11	Chemokine (C-X-C motif) ligand 11	2.58	0.025	5.23	0.007	17	0.018
IL10	Interleukin 10	2.36	0.03	-	-	-	-
Cxcl9	Chemokine (C-X-C motif) ligand 9			9.08	0.004	71.63	0.008
IL1α	Interleukin 1 alpha			3.56	0.0003	3.66	0.021
IL6	Interleukin 6			4.77	0.009	16.85	0.004
B2m	Beta 2 microglobulin			4.49	0.002	11.86	0.024
Cxcl1	Chemokine (C-X-C) ligand 1			2.26	0.036	-	-
Ccl11	Chemokine (C-C motif) ligand 11					11.17	0.012
Cxcl16	Chemokine (C-X-C motif) ligand 16					7.23	0.0001
CSF1	Colony stimulating factor 1					6.92	0.0001
IL15	Interleukin 15					6.12	0.0009
Ccl22	Chemokine (C-C motif) ligand 22					6.18	0.012
Ccl19	Chemokine (C-C motif) ligand 19					5.75	0.0001
Tnfsf10	TNF (ligand) superfamily, member 10					5.55	0.0002
IL5	Interleukin 5					3.68	0.03
Ccl17	Chemokine (C-C motif) ligand 17					3.56	0.04
CNTF	Ciliary neurotrophic factor					3.31	0.008
IL3	Interleukin 3					3.09	0.04
Tnfsf13b	TNF (ligand) superfamily, member 13b					2.43	0.045
IL7	Interleukin 7					2.34	0.046
Bmp7	Bone morphogenetic protein 7					3.9	0.02
Bmp6	Bone morphogenetic protein 6					3.4	0.004
Bmp4	Bone morphogenetic protein 4					3	0.024
Bmp2	Bone morphogenetic protein 2					2.85	0.036
Mstn	Myostatin					2.52	0.029

Table 5: Gene expression of cytokines and chemokine in measles virus-infected CD46+, CD46+/IFNγ-KO and CD46+/RAG2-KO neonates. Brain tissue was collected from uninfected and infected neonates and RNA was extracted at 7 dpi. qRT-PCR array analysis was performed using the RT^2 Profiler™ PCR Array. For each infected neonatal group (n=16) was used in the array. Changes in the gene expression that were more than two-fold relative to the uninfected controls are shown. All data were normalized against levels of housekeeping genes within the same sample. *p< 0.05 by students t-test.

Table 6.

Gene expression	CD46+/IFNγ-KO		CD46+/RAG2-KO	
	Fold change	p value	Fold change	p value
Ccl11	-2.95	0.006	-5.14	0.004
Ccl17	-2.32	0.001	-6.22	0.0001
Ccl20	-3.01	0.005	-10.76	0.001
Cxcl11	-3.14	0.034		
IFNγ	-2.41	0.049		
Il11	-2.06	0.017		
Il1a	-2.74	0.001		
Il5	-2.28	0.049		
Il7	-2.05	0.009		
Lta	-3.36	0.003		
Il17f			2.27	0.002
Ccl19			-8.66	0
Il15			-5.61	0.0001
Bmp7			-5.33	0.0002
Bmp2			-4.75	0.003
Bmp4			-4.02	0.001
Bmp6			-4.12	0.0001
Cd70			-3.33	0.009
Cntf			-3.24	0.01
Csf1			-3.26	0.01
Csf3			-3.25	0.007
Mstn			-3.18	0.004
Il12a			-2.71	0.02
Lta			-2.51	0.028
Il16			-2.25	0.016
Mif			-2.07	0.002

Table 6: Baseline mRNA expression of cytokines/chemokines in uninfected neonatal brains. Brain tissue from uninfected CD46+, CD46+/IFNγ-KO, and CD46+/RAG2-KO neonates was collected for RNA extraction. qRT-PCR array analysis was performed using the RT2 profiler PCR Array. Changes in gene expression that were more than two-fold higher (blue) or more than two-fold less (red) relative to the uninfected CD46+ neonates are shown. All data were normalized against levels of housekeeping genes within the same samples. Genes with P values less than 0.05 are shown (student t-test).

In **Table 7**, the baseline differences in cytokine expression between adult CNS and neonatal CNS are compared. The adult CNS shows downregulated Bmp4, CCL20 and Tnfsf11 expression. There are no differences in any Type I or Type II IFN expression between adults and neonates.

Table 7:

Gene expression	Fold change	p value
Csf3	5.69	0.001
Il12a	3.98	0.00003
Tnfsf13b	2.71	0.00003
Cx3cl1	2.55	0.00001
Ccl22	2.24	0.04
Cd40lg	2.27	0.042
Cd70	2.24	0.001
Cntf	2.22	0.001
Csf1	2.24	0.001
Il16	2.39	0.00001
Thpo	2.3	0.0001
Il17a	2.13	0.004
Il2	2.13	0.004
Bmp4	-2.54	0.001
Ccl20	-4.92	0.002
Il23a	-2.38	0.001
Mstn	-7.34	0.001
Tnfsf11	-3.34	0.043
Pf4	-2.38	0.010

Table 7: Baseline mRNA expression of cytokines/chemokines in uninfected neonatal and adult brains. Brain tissue from uninfected CD46+ neonates and adults was collected for RNA extraction. qRT-PCR array analysis was performed using the RT2 profiler PCR Array. Changes in uninfected adult gene expression that were more than two-fold higher (blue) or more than two-fold less (red) relative to the uninfected CD46+ neonates are shown. All data were normalized against levels of housekeeping genes within the same samples. Genes with P values less than 0.05 are shown (student t-test).

4.3.2 CD46+ neonates and adults differentially express PRRs and Type 1 interferons during infection

Our previous data suggests that adult mice may depend on the Type I interferons early in infection, whereas IFNγ is required for later control and resolution of the infection (O'Donnell, et al. 2012). Furthermore, evidence from the Rall laboratory shows that embryonic hippomcampal neurons from the CD46+ mice express relatively high endogenous levels of IFNα/β compared to other cell types, although the Type I interferons were dispensable for survival *in vivo* (Cavanaugh, Holmgren, 2015). The data in **Table 4** and **Table 5** suggests that neonates succumb to the infection despite a Th1 cytokine response. However, we had not explored the Type I IFNs, which are typically expressed at earlier time points in infection, because they were dispensable for ultimate viral control in adults. In a canonical infection model, IFNβ is produced after recognition of viral PAMPs by PRRs. IFNβ binds to IFNαR leading to IRF7 gene expression to enable a full type I IFN response. *In vivo* studies in Theiler's virus and La Crosse brain infection led to production of type I IFN response by ependymal cells, neurons, and macrophages (Delhaye, Paul, 2006). Thus, we wanted to explore whether age-related differences in the type I IFN response could contribute to loss of viral control in neonates.

Our array data suggested that IFNα2 was not expressed at significant levels in either neonatal or adult mice brains during infection (data not shown). We also wanted to determine if our gene expression data correlated with protein expression. This was to ensure that the mRNA translated into protein and that mRNA degradation does not occur. Thus, we attempted to analyze protein levels of IFNα/ IFNβ through multiple methods. We attempted to

measure 14 of the IFNα isoforms through an ELISA at 3 and 7 dpi. However, we could not

detect any difference in IFNα protein expression between uninfected and MV-infected

neonates and adults (**Figure 20**). This suggests that IFNα expression at early stages of

infection may be low or the background signal for the ELISA may be too high to detect subtle

changes. We also attempted to address protein levels by western blot analyses of hippocampal

brain tissue at 3, 7, and 10 dpi using a variety of antibodies for IFNα and IFNβ.

Unfortunately, we were unable to detect differences in IFNα/β proteins at any time point

using western blot analysis. This data suggests that basal expression of IFNα may not change

dramatically during early stages of infection (Cavanaugh, Holmgren, 2015).

As an alternative approach, we instead measured IFNα/β mRNA levels by qRT-PCR

in the RNA samples, as we have this technique to be more sensitive in our hands (**Figure 21**).

We found that the neonatal mice expressed IFNα4 and IFNβ during infection at 7 dpi,

whereas the adult mice did not show an appreciable increase in expression (**Figure 21**).

These data correlate with our previously published observations on STAT2 activation in

neonates, in which hippocampal tissue from CD46+ and CD46+/IFNγ-KO neonates show

STAT2 phosphorylation at the same time point (Fantetti, Gray, 2016). We looked at 3 dpi

and 7 dpi to understand if there any differences in early type I IFN induction. Early in

infection (3 dpi), we did not observe significant expression of IFNα4 or IFNβ in the adults or

neonates of any CD46+ genotype (**Figure 21A, 21B).** As the infection progressed (7 dpi),

CD46+/IFNγ-KO neonates upregulated IFNα4 (29-fold) to a greater extent in comparison to

CD46+ (7.5-fold) and CD46+/RAG2-KO (5.7-fold) neonates post-infection, whereas CD46+

adults did not increase the expression of IFNα4 significantly (**Figure 21A, 21B**). In contrast,

CD46+/RAG2-KO neonates demonstrated greater upregulation of IFNβ in comparison to other neonates (1644.8-fold; **Figure 21C**). Although IFNβ also was upregulated in the CD46+ neonates (122-fold) at 7 dpi, CD46+ adults did not show significant upregulation of IFNβ at either time point **(Figure 21D)**. Thus, IFNβ upregulation in CD46+/RAG2-KO neonates may contribute to their early viral control and greater survival. We also analyzed levels of the IFN-responsive gene (ISG), Melanoma Differentiation-Associated protein 5 (MDA5), which is a PRR, as a surrogate for Type I IFN signaling. MDA5 was not induced significantly in infected CD46+ neonates or adults at either time point (**Figure 21E, 21F**). At 7 dpi, only the CD46+/IFNγ-KO neonates significantly upregulated MDA5, which may correlate with the elevated IFNα4 observed at this time point.

Figure 20.
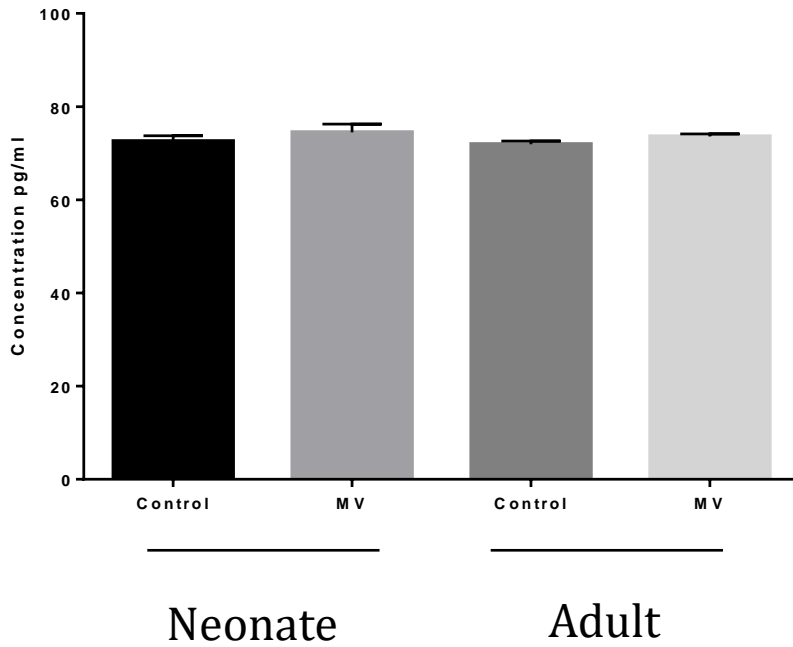
Figure 20. IFNα protein expression in adult and neonatal CNS post infection at 3dpi.

Brain tissue was isolated from infected and uninfected neonate and adult brains and protein

was extracted at 3 dpi. Protein concentration was measured by protein assay and equal

protein was loaded into each well of the ELISA to detect total IFNα (14 isoforms). One-way

ANOVA was used to determine statistical significance.

Figure 21.

Neonates
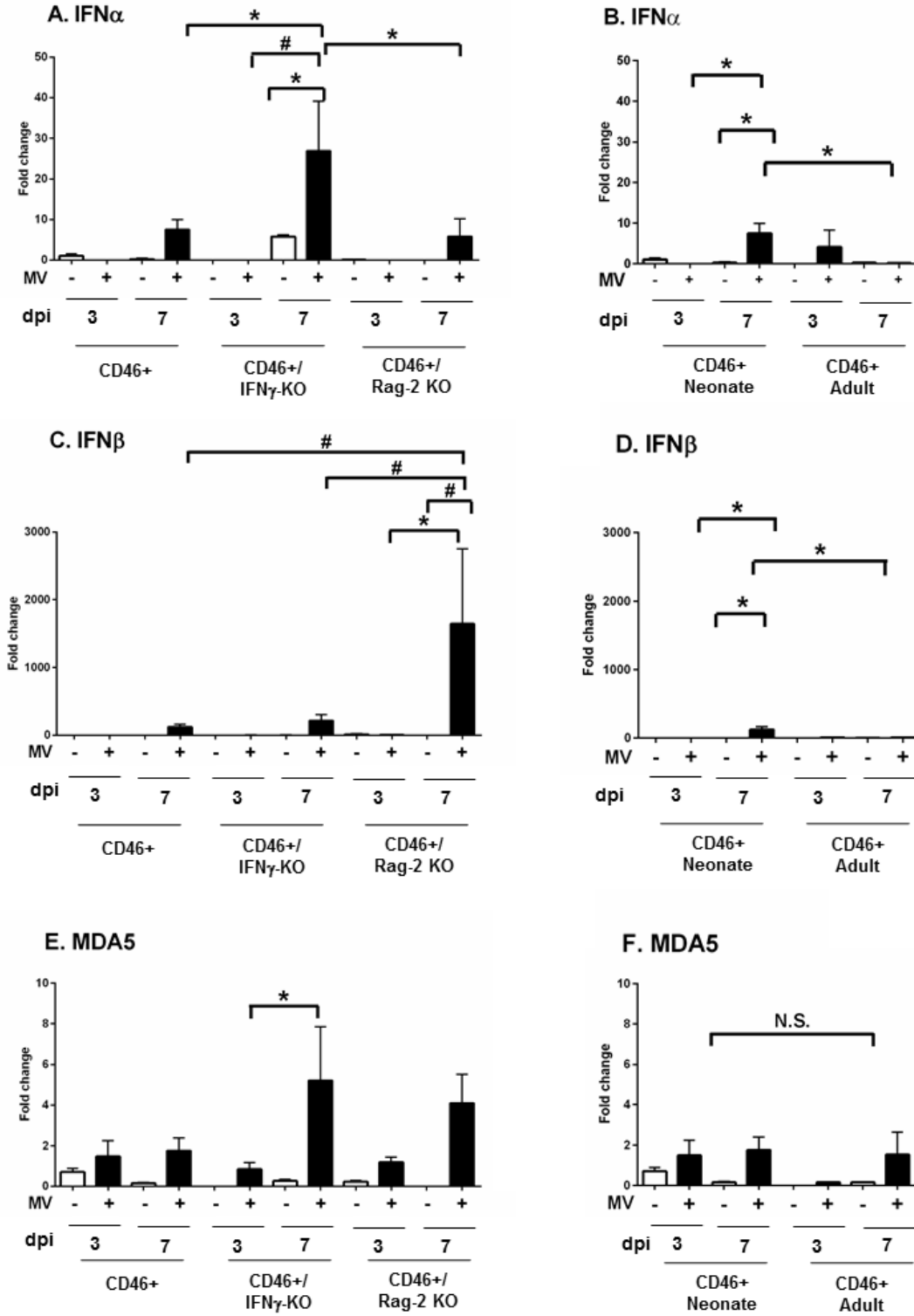
Figure 21. Neonatal mice induce greater expression of Type I interferons during MV infection in comparison to adults.

Brains of uninfected and MV-infected CD46+ mice were analyzed for the mRNA expression of Type I interferons at 3 dpi and 7 dpi. CD46+, CD46+/IFNγ-KO, and CD46+/RAG2-KO neonates (left column; A, C, E) and CD46+ neonates and adults (right column; B, D, F) were compared. qRT-PCR analysis was performed for IFNα4 (A, B), IFNβ (C, D) and MDA5 (E, F). Relative gene expression is shown as the fold-change normalized to the CD46+ uninfected controls (n=4-5 mice/condition). Each bar represents the mean fold-change and SEM. Statistical differences were determined by three-way ANOVA (* $p<0.05$, # $p<0.001$) with Bonferroni post hoc test.

4.3.3 MV-infection induces distinct expression of pattern recognition receptors in the neonatal and adult CNS.

Although it is possible that other IFNα isoforms are expressed in the infected adults or neonates, we further looked at other PRRs that sense RNA virus such as RIGI, TLR3, and TLR7 to explore age dependent differences upstream of Type I IFNs. As we did not observe an early induction of Type I response at 3 dpi, we explored the changes of other PRRs at the 7 dpi timepoint only **(Figure 22)**. For our analysis, we focused on RIGI, which is expressed in the brains of MV-infected transgenic mice expressing Hsp70, and TLR 3 and 7, which recognize viral RNAs (Kim et al. , 2013, Sorgeloos et al. , 2013). TLR3, in particular, has been shown to be induced by the MV-Edmonston strain in cell lines (Tanabe, Kurita-Taniguchi, 2003). During infection of CD46+ mice, both CD46+ and CD46+/RAG2-KO neonates upregulate RIGI (12.2-fold and 24.4-fold respectively, **Figure 22A**) in the brain, whereas infected CD46+ adults did not demonstrate significant upregulation of RIGI with infection (**Figures 22B**). CD46+ neonates did not upregulate either TLR3 or TLR7 (**Figure 22C and 22E**), while CD46+/IFNγ-KO neonates upregulated TLR3 (41-fold, **Figure 22C**) and CD46+/RAG2-KOs upregulated TLR7 (11-fold, **Figure 22E**). In contrast, CD46+ adults upregulate TLR3 (2.3×10^5-fold) and TLR7 (37.3-fold) to a greater extent than the any genotype of the MV-infected neonates (**Figure 22D and 22F**). These results suggest that the CD46+ adult mice may rely on the TLR family of proteins for recognition of the virus. Additionally, these results suggest that gene expression of Type I IFN and associated ISGs remain relatively low at the start of infection in both neonates and adults, when Type I IFN expression would be expected to dominate. Thus, we propose that the less effective immune response in neonates is not attributable to a diminished Type I IFN response.

Figure 22.
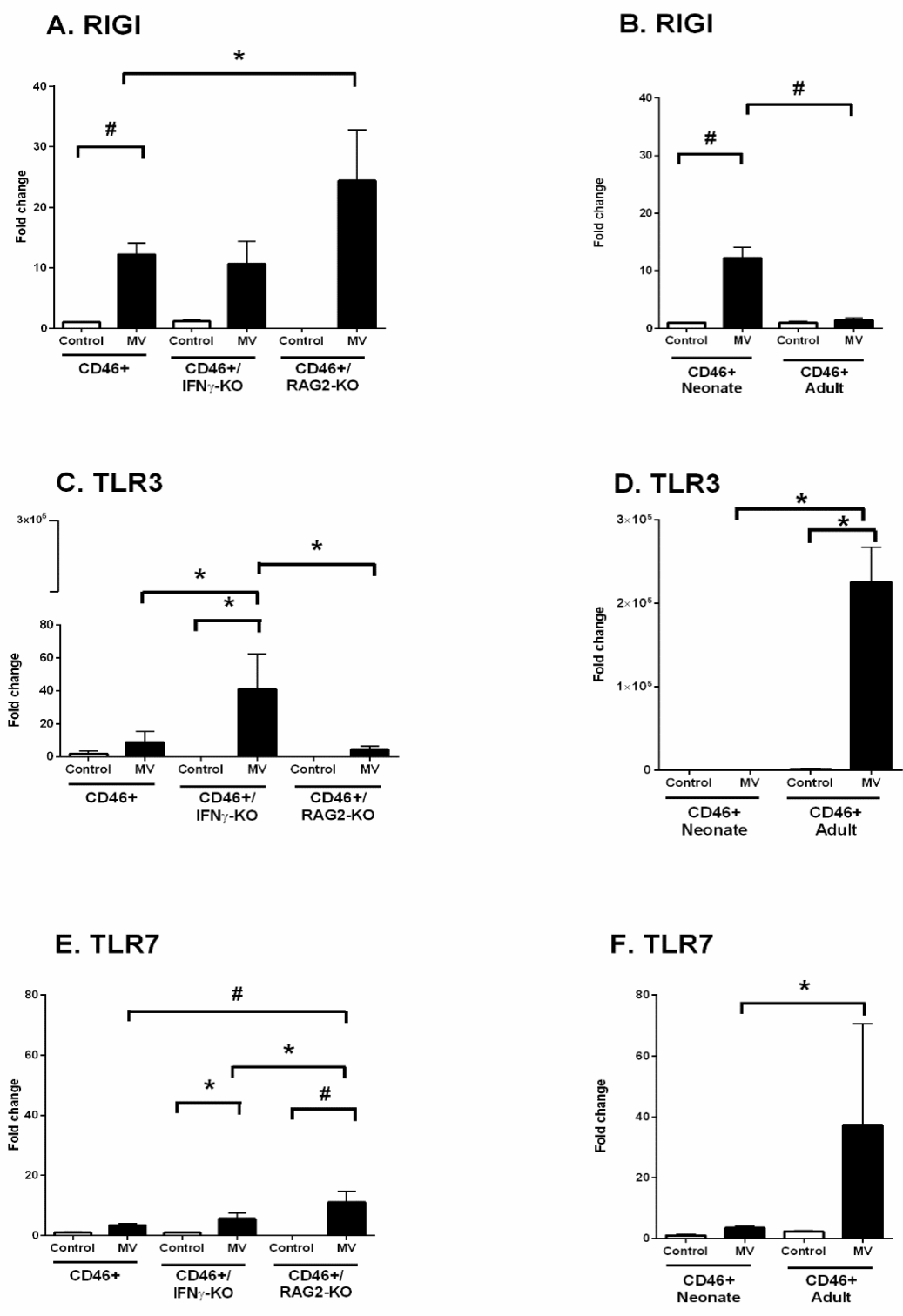
Figure 22. MV-infection induces distinct expression of pattern recognition receptors in the neonatal and adult CNS.

Brains of uninfected and MV-infected CD46+ mice were analyzed for the mRNA expression of pattern recognition receptors (PRRs) at 7 dpi. CD46+, CD46+/IFNγ-KO, and CD46+/RAG2-KO neonates (left column; A, C, E) and CD46+ neonates and adults (right column; B, D, F) were compared. qRT-PCR analysis was performed for RIGI (A, B), TLR3 (C, D), and TLR7 (E, F). Relative gene expression is shown as the fold-change normalized to the CD46+ uninfected controls (n=4-5 mice/condition). Each bar represents the mean fold-change and SEM. Statistical differences were determined by two-way ANOVA (* $p<0.05$, # $p<0.001$) with Bonferroni post hoc test.

4.3.4 IFNγ induction occurs independently of age, but activation of the IFNγ-responsive gene CIITA occurs only in adults.

Finally, to confirm the results of the RT array, we examined the mRNA induction of IFNγ in brain tissue through qRT-PCR at 7 dpi. Expression of IFNγ mRNA was higher in CD46+ neonates compared to CD46+/RAG2-KO neonates (**Figure 23A**). Induction of IFNγ mRNA was also greater in CD46+ neonates than in adults (**Figure 23B**). While we had observed the induction of some IFNγ-responsive genes in both age groups (Table 1), adult mice also expressed IFNγ-responsive genes that were not expressed in neonates (*e.g.* CXCL9), suggesting that neonatal mice may have impaired IFNγ signaling. To investigate the downstream effects of IFNγ signaling, we compared the mRNA expression of *CIITA (*Class II Major Histocompatibility Complex Transactivator), a critical regulator of MHC-II induction and a IFNγ-responsive gene (Reith, LeibundGut-Landmann, 2005). There was no difference in CIITA expression among the three genotypes of the neonates (**Figure 23C**), despite the expression of IFNγ in CD46+ (4-fold) and CD46+/RAG2-KOs (2-fold) neonates. However, CD46+ adults induced greater CIITA expression (11-fold) compared to uninfected controls and compared to infected CD46+ neonates (**Figure 23D**), despite less expression of both IFNγ and MV. These results suggest that although IFNγ may be induced in the brain during infection, there may be deficiencies in IFNγ signaling or transcriptional activation in the neonatal brain.

Figure 23.
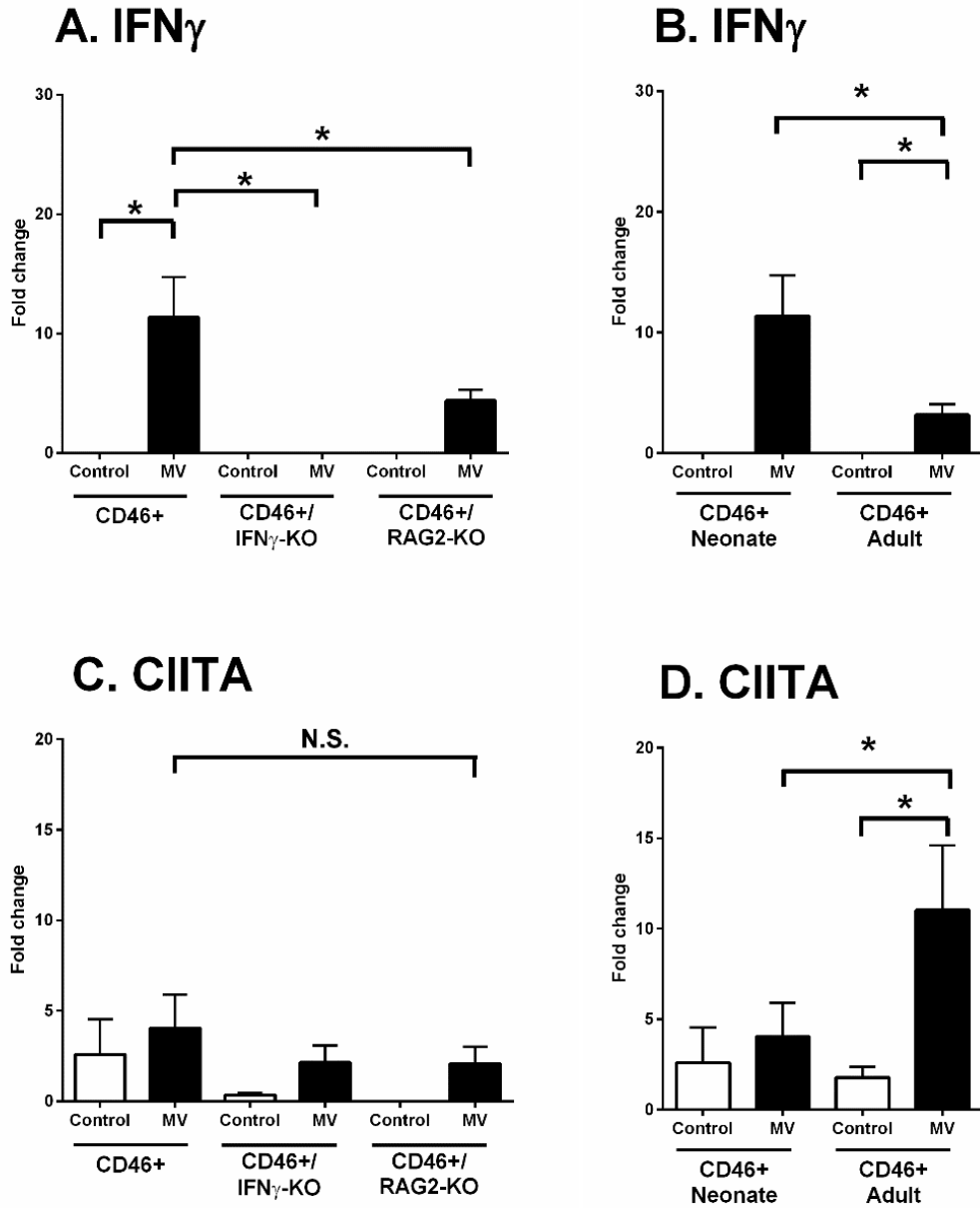
Figure 23. Despite elevated IFNγ expression during infection, transcription of IFNγ-responsive genes is age-dependent.

Brains of uninfected and MV-infected CD46+ mice were analyzed for the mRNA expression of IFNγ and CIITA at 7 dpi. CD46+, CD46+/IFNγ-KO, and CD46+/RAG2-KO neonates (left column; A, C) and CD46+ neonates and adults (right column, B, D) were compared. qRT-PCR analysis was performed for IFNγ (A, B) and CIITA (C, D). Relative gene expression is shown as the fold-change normalized to the CD46+ uninfected controls (n=4-5 mice/condition). Each bar represents the mean fold-change and SEM. Statistical differences were determined by two-way ANOVA (* $p<0.05$, $^{\#}$ $p<0.001$) with Bonferroni post hoc test.

4.4 Discussion

Recognition of viral RNA by PRRs such as the RIG-I and the membrane bound TLRs lead to the induction of Type 1 IFNs, which are significant early steps in viral control (Akira, Uematsu, 2006, Yoneyama, Kikuchi, 2004, Zalinger, Elliott, 2015). As we observed greater T cell infiltration in the adults despite a lower viral load than the neonates, we considered the possibility that enhanced expression of pattern recognition receptors (PRRs), and subsequent Type I IFN expression, could correlate with the relatively robust immune response that is induced in adults. The type I IFNs, IFNα and IFNβ, both signal through the same receptor (comprised of IFNAR1 and R2), but they exert different biological effects in the CNS. Several studies suggest that IFNβ expression is associated with anti-inflammatory effects in the CNS (Hua et al. , 1998, Lu et al. , 1995, McLaurin et al. , 1995). Whereas IFNα expression has been associated with neuroinflammatory disorders and brain injury such as HIV-associated brain injury and HIV-associated neurocognitive disorders (Sas et al. , 2009, Sas et al. , 2007). Studies also suggest that transgenic expression of IFNα in the mouse CNS results in progressive inflammatory encephalopathy and neurodegeneration (Akwa et al. , 1998). Thus, it is possible that high IFNα expression may contribute to inflammation and edema seen in CD46+/IFNγ-KO neonatal brains (**Figure 21**), which may lead to earlier death despite a lower viral load (**Figure 7 and 8**).

In canonical Type I IFN signalling, production of IFNβ leads to the subsequent induction of IFNα. But studies in SIV infection suggests that CCL2 binds to the CCR2 receptor on macrophages to selectively suppress IFNα induction without any effect on IFNβ and antiviral ISG expression (Zaritsky et al. , 2012). Thus, a pronounced upregulation of

CCL2 in CD46+/RAG2-KO CNS (**493-fold – Table 2**) may suppress IFNα in these brains

and inhibit IFNα-mediated neurotoxicity. Studies in HIV-gp120 transgenic mice and SIV

models suggest that IFNβ response is activated without the production of neurotoxic IFNα

(Thaney et al. , 2017). RIG-I, a PRR that is expressed in microglia, astrocytes, and neurons

and may contribute to endogenous production of IFNβ in the CNS (Furr et al. , 2008, Nazmi,

Dutta, 2011). We observe that CD46+/RAG2-KO neonates have highest RIG-1 expression in

the CNS which may correlate with higher IFNβ production in their brain (**Figure 21 and 22**).

Studies in human fetal microglia provide evidence that IRF3, a transcription factor, is required

for induction of IFNβ and contributes to the switch of microglia from pro- to anti-

inflammatory phenotype via the PI3K/AKT pathway (Tarassishin et al. , 2011). Thus, this

suggests that IFNβ may change the phenotype of microglia from proinflammatory to anti-

inflammatory/protective state. Therefore, it will be interesting to look at the differences in

IRF3 expression in the CD46+/RAG2-KO compared to CD46+ neonates post infection.

Additionally, a future direction for this project is to characterize the phenotype of microglia *in*

vivo to determine whether a predominant M1 or M2 phenotype occurs post neonatal MV

infection.

IFNβ also induces CCL4, a chemokine which is upregulated in the neonates (Figure

and Table 2). CD46+/RAG2-KO neonates show a robust upregulation of CCL4 post infection.

In vitro studies indicate the CCL4 protects cerebrocortical neurons against neurotoxicity

(Thaney, O'Neill, 2017). The IFN response is complex and hence, interplay of several factors

and ISGs such as CXCL10, CCL4, and CCL2 may contribute to neuronal rescue in

CD46+/RAG2-KO neonate compared to CD46+ neonates, which express low levels of IFNβ.

Another possibility is that higher expression of RIG-1 and IFNβ in the CD46+/RAG2-KO CNS than other neonates or adults (**Figure 21**) may lead to early viral sensing and subsequent IFNβ help. Thus, this may help control CD46+/RAG2-KOs neonates to control the infection better in the absence of adaptive immune cells. Furthermore, CD46+/RAG2-KO neonates expressed a broader of array of cytokines/chemokines during infection than CD46+ neonates or adults (**Table 2**). Among the factors that were upregulated only by the CD46+/RAG2-KO neonates, the expression of multiple BMP family members (BMP 2, 4, 6, and 7) was elevated during infection, although it is important to note that the BMP family members exhibited lower basal expression in the CD46+/RAG2-KO mice prior to infection. Studies of neonatal mice infected with reovirus show that BMP signaling is activated during CNS infection, and that BMP6 protects virally-infected neurons from apoptosis (Beckham et al. , 2009). We speculate that BMP expression in the CD46+/RAG2-KOs may confer a neuroprotective advantage against the virus, which may help the CD46+/RAG2-KOs to resist succumbing to the infection as readily as their wildtype counterparts.

CCL2, which functions as a chemoattractant for monocytes, macrophages, and T cells, was upregulated significantly in CD46+ MV-infected neonates but not in adults. Transgenic adult mice that express CCL2 in the CNS are ineffective at viral clearance and succumb when infected with a neurotropic strain of mouse hepatitis virus (Trujillo, Fleming, 2013). Overexpression of CCL2 is also associated with greater infiltration of regulatory T cells and reduced microglial/macrophage activation with a mixed M1/M2 phenotype, which also was associated with a suppressive phenotype (Trujillo, Fleming, 2013). Thus, overexpression of CCL2 can lead to a defective immune response that fails to clear the virus and is both

inflammatory and immunosuppressive. Although CCL2 is crucial for lymphocyte recruitment and clearance of some viruses from the brain (Chen et al. , 2001), it is possible that expression of CCL2 in MV-infected neonates contributes to a suppressive, M2-like phenotype in microglia.

CD46+ neonates upregulate RIGI expression post virus infection (Red) in the brain and may activate downstream signaling cascade that result in Type I IFN (Interferon) production. **(Figure 24A)** Macrophages, part of innate immunity sense viruses and engulf them by phagocytosis and produce several cytokines such as IFNα, IFNβ, IL-12 and IL-27. These cytokines further lead to activation of Natural killer cells. Both NK cells and macrophages may also produce IFNγ that binds to IFNγR on neurons and APCs. MHC-II encodes for genes that are essential for presentation of antigen to CD4+ T-cell. The induction of MHC-II expression in most cell types is modulated by exposure to IFNγ. In neonates, low expression of CIITA may lead to low MHC-II and lead to loss of control to viral infection in the neonatal CNS **(Figure 24A).** This contrasts to what occurs in the adult CNS, where IFNγ signaling leads to higher expression of CIITA **(Figure 24B)** that may lead to high MHC-II. Thus, adults exhibit effective antigen presentation and IFNγ-mediated viral clearance.
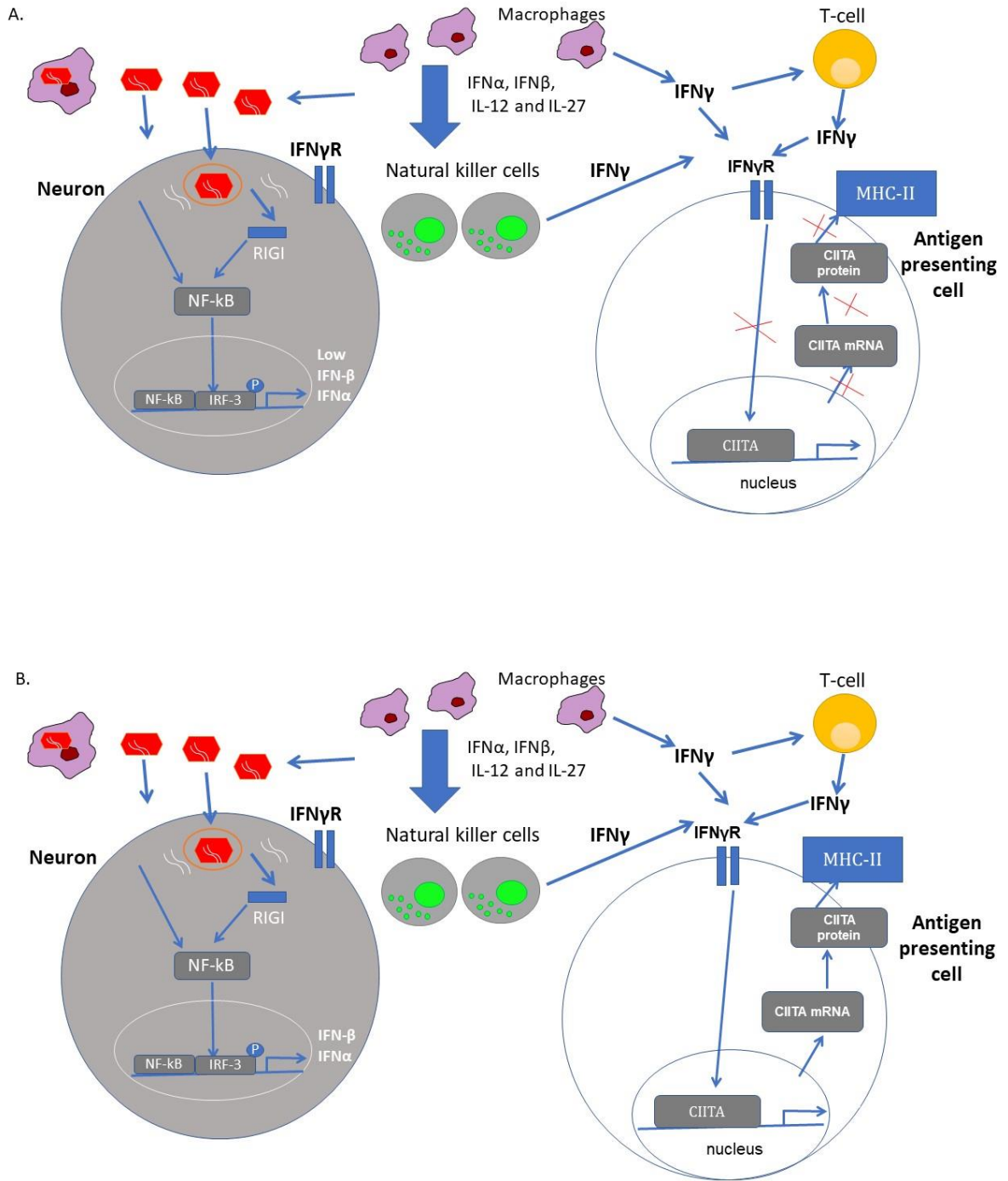
Figure 24.

Figure 24. Model of neonatal immune response in the brain

Multiple studies have shown that neonates have poor Th1 function and a strong Th2 response during microbial infections (Forsthuber et al. , 1996, Powell and Streilein, 1990, Singh et al. , 1996). This Th2 bias may be due to delayed maturation of accessory cells or intrinsic epigenetic factors in neonatal T cells. (Li et al. , 2004). Regardless of the cause, Th2-like responses are not typically associated with IFNγ production, which is a hallmark of Th1 responses. Given the significance of IFNγ in viral control in neurons, we predicted that the failure of CD46+ pups to control MV would be due towards a Th2-bias in the brain. Although distinct cytokine subsets were observed in infected CD46+ adults and neonates, the neonatal mice did not demonstrate a clear Th2 bias. CCL2 can be important for the development of a Th2 phenotype (Gu et al. , 2000), but other key Th2 factors (*e.g.* IL-4, IL-5) were not upregulated in infected neonates. Rather, both adult and neonatal CD46+ mice expressed Th1-associated cytokines and chemokines, including IFNγ, CXCL10, CCL3, and CCL5, during infection. IFNγ-inducible genes, including CXCL10 and CXCL11, were also upregulated in both infected neonates and adults, suggesting that there is a sufficient amount of IFNγ to activate downstream transcriptional changes. However, neonatal CD46+ mice failed to activate both CXCL9 and CIITA (**Table 1** and **Figure 11**), both of which are IFNγ-inducible genes. These findings suggest that IFNγ signaling may be limited in the neonatal CNS, at least in regard to the profile of genes that are activated **(Figure 24A)**. Previous studies in CD46+ neonates demonstrate elevated expression and phosphorylation of Signal transducer and activator of transcription 1 (STAT1), the major signaling molecule downstream of IFNγ, in the hippocampus during infection (Fantetti, Gray, 2016). This observation implies that IFNγ induces its canonical signaling cascade in the neonatal brain. However, both Type I and II interferons signal through STAT1, so it is possible that STAT1 activation in neonates does not

reflect robust IFNγ signaling per se. Regardless of the level of STAT1 activation, the disparity in the activation of IFNγ-inducible genes suggests that the outcomes of IFNγ signaling may be dictated by age-related factors **(Figure 24)**.

Although CD46+ neonates and adults upregulated similar Th1 cytokines and chemokines in the CNS, the expression of some cytokines during infection was age-dependent. In addition to unique expression of CCL2, neonatal mice express the anti-inflammatory cytokine IL-10, which is classically associated with Th2-like responses and repression of Th1 cytokine synthesis (Couper et al. , 2008). In the CNS, recombinant expression IL-10 is protective against virally-induced demyelination and lymphocyte infiltration (Trandem et al. , 2011a). Endogenous IL-10 also protects against neuropathology caused by coronaviruses and flaviviruses in murine models of adult infection (Trandem et al. , 2011b, Tun et al. , 2014). However, the lack of IL-10 induction in CD46+ adult mice suggests that IL-10 is dispensable for non-cytolytic viral clearance from neurons. Similarly, CD46+ neonates, but not CD46+ adults, upregulated TNF during infection. TNF is associated with neuroprotection in models of flavivirus encephalitis (Hayasaka et al. , 2013, Tun, Aoki, 2014). Thus, it is surprising that both IL-10 and TNF would be expressed in the neonatal CD46+ model, where viral clearance fails and neuronal dropout is apparent, but not in the adult CD46+ model, where viral control is successful. One possible explanation is that IL-10 induction in neonates dampens the expression of necessary anti-viral or neuroprotective cytokines but does not completely inhibit them, which may explain the extensive overlap in cytokine profiles between adults and neonates despite disparate outcomes in viral control and survival.

Age-dependent innate immune responses may also contribute to early viral control, even if innate immunity is not responsible for the ultimate resolution of the virus. Previous studies indicate that murine neonatal intestinal epithelial cells fail to express TLR3 in response to rotavirus infection through post-natal days 1-10, which overlaps with the time points reflected in our study (Pott, Stockinger, 2012). Similarly, human cord blood samples do not induce TLR3 in response to poly(I:C) treatment or HSV activation in comparison to adult NK cells (Slavica, Nordstrom, 2013). Although, we observed robust RIG-I expression in the CD46+ neonates, there is also evidence in human neonatal dendritic cells that RIG-I function is impaired and is associated with poor control of RSV (Marr et al. , 2014). In CNS infections of HSV, TLR3 signalling is critical to control both primary HSV infection and its reactivation. Humans with defects in TLR3 signaling are more susceptible to encephalitis (Guo et al. , 2011, Zhang et al. , 2007). Nevertheless, neonatal mice demonstrated greater induction of Type I IFN expression than adults at the time points examined, suggesting that the neonatal mice are capable of detecting MV through other PRRs.

CD46+/RAG2-KO neonates show high expression of IFNβ at 7dpi. Although, type I IFN may be dispensable for viral control in the adult CNS (Cavanaugh, Holmgren, 2015), IFNβ may contribute to early viral control in the neonatal CNS. To fully characterize age-dependent differences in Type I IFNs, the other isoforms of IFNα would also have to be analyzed. However, it is possible that in the absence of a fully developed T cell response, a Type I IFN response can be especially impactful in the neonatal CNS. Additionally, exploring the role of TLRs and their deficiencies in the neonatal CNS may provide future targets for therapeutic intervention.

5. Conclusions

The focus of this dissertation centered on dissecting the role of the neonatal immune response during a viral CNS infection. We found that (i) interferon-gamma (IFNγ), a key cytokine required for viral control in neurons in adults, delays mortality in neonates, (ii) neonates ultimately succumb despite IFNγ-independent infiltration of natural killer cells, neutrophils, inflammatory monocytes, and CD4 and CD8 T-cells (iii) neonates and adults differentially express pathogen recognition receptors and Type I interferons during infection, (iv) both neonates and adults express IFNγ, CXCL10, IL-1, and IL-1RA, among induction of other Th1-associated factors cytokines/chemokines, in the brain but only adults control the infection, and (v) neonates and adults also express non-overlapping sets of cytokines/chemokines. The results suggest age-dependent expression of cytokine profiles in the brain and distinct dynamic interplays between lymphocyte populations and cytokines/chemokines in MV-infected neonates.

We had anticipated that neonatal mice would demonstrate major deficits in T cell infiltration. Although we did observe lower T cell numbers in neonates at later time points, we did not observe as much of a quantitative deficit as we had anticipated. Thus, we also investigated potential deficits in innate immune cells. Here, we observed that NK cells, neutrophils and inflammatory monocytes infiltrate into the neonatal brain post MV infection. In the absence of IFNγ, highest numbers of NK cells, neutrophils, inflammatory monocytes, T-cells and B-cells accumulate into the CNS. These neonates succumb earliest to the neurotropic MV infection in the brain. We hypothesized that IFNγ expression may be lacking in the CD46+

neonatal CNS. However, surprisingly we found IFNγ expression in the brain but induction of downstream signalling of CIITA is decreased in neonates compared to adults.

Our findings highlight the complex, age-specific responses of immune cells to a CNS viral infection, and suggest that multiple cytokines likely contribute to successful viral clearance from neurons. A major focus of future work is to better understand how the cytokine milieu in adult mice affects viral clearance in neurons, and to determine if the cytokine profile in neonates can be directed toward more effective viral clearance. Given that IFNγ was expressed in both neonatal and adult mice, but distinct profiles of IFNγ-responsive genes were induced, it suggests that there may be age-dependent differences in IFNγ signaling. Prior studies by our laboratory have demonstrated cell type-specific differences in expression of the IFNγ receptor and of intracellular signaling molecules (*e.g.* STAT1) in neural cells. As the proportion and/or maturity of cells change in the CNS with age, it is conceivable that the signaling pathways induced by IFNγ also change over time. How such age-dependent changes affect the profile of the anti-viral program, and what cells are most affected by age-dependent changes, remain an open question.

Future studies may employ adoptive transfer approaches to transfer adult T-cells into the neonates to determine the age-dependent T-cell behaviour in the CNS. Additionally, the mechanism of early viral control in CD46+/RAG2-KO neonates may be explored. IFNβ was significantly upregulated at 7dpi in CD46+/RAG2-KO neonates. Therefore, further studies to elucidate the role of IFNβ and its downstream signalling in the neonatal CNS may enhance our understanding of Type I mediated viral control. BMPs were also upregulated only in the

CD46+/RAG2-KO neonatal brains. There is evidence for BMPs being neuroprotective in reovirus infections. Thus, the role of Bmp agonists in neurotrophic MV infections may shed light into the mechanisms of viral control in CD46+/RAG2-KO compared to CD46+ neonates. Hence, a better understanding of neonatal immunity will lead to effective therapeutic strategies and enable us to design better vaccines to protect the fetus, mother, and newborns.

6. References

Abromson-Leeman S, Bronson R, Luo Y, Berman M, Leeman R, Leeman J, et al. T-cell properties determine disease site, clinical presentation, and cellular pathology of experimental autoimmune encephalomyelitis. Am J Pathol. 2004;165:1519-33.

Adams Waldorf KM, McAdams RM. Influence of infection during pregnancy on fetal development. Reproduction. 2013;146:R151-62.

Adkins B, Leclerc C, Marshall-Clarke S. Neonatal adaptive immunity comes of age. Nat Rev Immunol. 2004;4:553-64.

Ajami B, Bennett JL, Krieger C, Tetzlaff W, Rossi FM. Local self-renewal can sustain CNS microglia maintenance and function throughout adult life. Nat Neurosci. 2007;10:1538-43.

Akira S, Uematsu S, Takeuchi O. Pathogen recognition and innate immunity. Cell. 2006;124:783-801.

Akwa Y, Hassett DE, Eloranta ML, Sandberg K, Masliah E, Powell H, et al. Transgenic expression of IFN-alpha in the central nervous system of mice protects against lethal neurotropic viral infection but induces inflammation and neurodegeneration. J Immunol. 1998;161:5016-26.

Al-Hertani W, Yan SR, Byers DM, Bortolussi R. Human newborn polymorphonuclear neutrophils exhibit decreased levels of MyD88 and attenuated p38 phosphorylation in response to lipopolysaccharide. Clin Invest Med. 2007;30:E44-53.

Allen C, Thornton P, Denes A, McColl BW, Pierozynski A, Monestier M, et al. Neutrophil cerebrovascular transmigration triggers rapid neurotoxicity through release of proteases associated with decondensed DNA. J Immunol. 2012;189:381-92.

An J, Zhou DS, Zhang JL, Morida H, Wang JL, Yasui K. Dengue-specific CD8+ T cells have both protective and pathogenic roles in dengue virus infection. Immunol Lett. 2004;95:167-74.

Araya N, Sato T, Yagishita N, Ando H, Utsunomiya A, Jacobson S, et al. Human T-lymphotropic virus type 1 (HTLV-1) and regulatory T cells in HTLV-1-associated neuroinflammatory disease. Viruses. 2011;3:1532-48.

Atallah N, Vasiu R, Bosca AB, Cretu DI, Georgiu C, Constantin AM, et al. Microglia--performers of the 21st century. Rom J Morphol Embryol. 2014;55:745-65.

Baba Y, Tsuboi Y, Inoue H, Yamada T, Wszolek ZK, Broderick DF. Acute measles encephalitis in adults. J Neurol. 2006;253:121-4.

Beckham JD, Tuttle K, Tyler KL. Reovirus activates transforming growth factor beta and bone morphogenetic protein signaling pathways in the central nervous system that contribute to neuronal survival following infection. J Virol. 2009;83:5035-45.

Bergmann CC, Parra B, Hinton DR, Ramakrishna C, Dowdell KC, Stohlman SA. Perforin and gamma interferon-mediated control of coronavirus central nervous system infection by CD8 T cells in the absence of CD4 T cells. J Virol. 2004;78:1739-50.

Bergmann CC, Ramakrishna C, Gonzales JM, Tschen SI, Stohlman SA. Coronavirus immunity: from T cells to B cells. Adv Exp Med Biol. 2006;581:341-9.

Biron CA, Nguyen KB, Pien GC, Cousens LP, Salazar-Mather TP. Natural killer cells in antiviral defense: function and regulation by innate cytokines. Annu Rev Immunol. 1999;17:189-220.

Black FL. Measles endemicity in insular populations: critical community size and its evolutionary implication. Journal of theoretical biology. 1966;11:207-11.

Borden EC, Sen GC, Uze G, Silverman RH, Ransohoff RM, Foster GR, et al. Interferons at age 50: past, current and future impact on biomedicine. Nat Rev Drug Discov. 2007;6:975-90.

Bozic CR, Kolakowski LF, Jr., Gerard NP, Garcia-Rodriguez C, von Uexkull-Guldenband C, Conklyn MJ, et al. Expression and biologic characterization of the murine chemokine KC. J Immunol. 1995;154:6048-57.

Braaten DC, Sparks-Thissen RL, Kreher S, Speck SH, Virgin HWt. An optimized CD8+ T-cell response controls productive and latent gammaherpesvirus infection. J Virol. 2005;79:2573-83.

Brice GT, Graber NL, Hoffman SL, Doolan DL. Expression of the chemokine MIG is a sensitive and predictive marker for antigen-specific, genetically restricted IFN-gamma production and IFN-gamma-secreting cells. J Immunol Methods. 2001;257:55-69.

Brooks DG, Walsh KB, Elsaesser H, Oldstone MB. IL-10 directly suppresses CD4 but not CD8 T cell effector and memory responses following acute viral infection. Proc Natl Acad Sci U S A. 2010;107:3018-23.

Burdeinick-Kerr R, Govindarajan D, Griffin DE. Noncytolytic clearance of sindbis virus infection from neurons by gamma interferon is dependent on Jak/STAT signaling. J Virol. 2009;83:3429-35.

Burdeinick-Kerr R, Wind J, Griffin DE. Synergistic roles of antibody and interferon in noncytolytic clearance of Sindbis virus from different regions of the central nervous system. J Virol. 2007;81:5628-36.

Callan MF, Steven N, Krausa P, Wilson JD, Moss PA, Gillespie GM, et al. Large clonal expansions of CD8+ T cells in acute infectious mononucleosis. Nat Med. 1996;2:906-11.

Carlson T, Kroenke M, Rao P, Lane TE, Segal B. The Th17-ELR+ CXC chemokine pathway is essential for the development of central nervous system autoimmune disease. J Exp Med. 2008;205:811-23.

Cavanaugh SE, Holmgren AM, Rall GF. Homeostatic interferon expression in neurons is sufficient for early control of viral infection. J Neuroimmunol. 2015;279:11-9.

Centers for Disease Control and Prevention. Measles Cases and Outbreaks. 2017.

Chen BP, Kuziel WA, Lane TE. Lack of CCR2 results in increased mortality and impaired leukocyte activation and trafficking following infection of the central nervous system with a neurotropic coronavirus. J Immunol. 2001;167:4585-92.

Chesler DA, Dodard C, Lee GY, Levy DE, Reiss CS. Interferon-gamma-induced inhibition of neuronal vesicular stomatitis virus infection is STAT1 dependent. J Neurovirol. 2004;10:57-63.

Coughlin MM, Bellini WJ, Rota PA. Contribution of dendritic cells to measles virus induced immunosuppression. Reviews in medical virology. 2013;23:126-38.

Couper KN, Blount DG, Riley EM. IL-10: the master regulator of immunity to infection. J Immunol. 2008;180:5771-7.

Cullell-Young M, Barrachina M, Lopez-Lopez C, Gonalons E, Lloberas J, Soler C, et al. From transcription to cell surface expression, the induction of MHC class II I-A alpha by interferon-gamma in macrophages is regulated at different levels. Immunogenetics. 2001;53:136-44.

Curtsinger JM, Valenzuela JO, Agarwal P, Lins D, Mescher MF. Type I IFNs provide a third signal to CD8 T cells to stimulate clonal expansion and differentiation. J Immunol. 2005;174:4465-9.

Das S, Basu A. Viral infection and neural stem/progenitor cell's fate: implications in brain development and neurological disorders. Neurochem Int. 2011;59:357-66.

de Swart RL, Ludlow M, de Witte L, Yanagi Y, van Amerongen G, McQuaid S, et al. Predominant infection of CD150+ lymphocytes and dendritic cells during measles virus infection of macaques. PLoS Pathog. 2007;3:e178.

de Vries RD, Lemon K, Ludlow M, McQuaid S, Yuksel S, van Amerongen G, et al. In vivo tropism of attenuated and pathogenic measles virus expressing green fluorescent protein in macaques. J Virol. 2010;84:4714-24.

de Vries RD, Mesman AW, Geijtenbeek TB, Duprex WP, de Swart RL. The pathogenesis of measles. Current opinion in virology. 2012;2:248-55.

Delhaye S, Paul S, Blakqori G, Minet M, Weber F, Staeheli P, et al. Neurons produce type I interferon during viral encephalitis. Proc Natl Acad Sci U S A. 2006;103:7835-40.

Downes CE, Crack PJ. Neural injury following stroke: are Toll-like receptors the link between the immune system and the CNS? Br J Pharmacol. 2010;160:1872-88.

Drescher B, Bai F. Neutrophil in viral infections, friend or foe? Virus Res. 2013;171:1-7.

Duhen T, Herschke F, Azocar O, Druelle J, Plumet S, Delprat C, et al. Cellular receptors, differentiation and endocytosis requirements are key factors for type I IFN response by human epithelial, conventional and plasmacytoid dendritic infected cells by measles virus. Virus Res. 2010;152:115-25.

Ehrengruber MU, Ehler E, Billeter MA, Naim HY. Measles virus spreads in rat hippocampal neurons by cell-to-cell contact and in a polarized fashion. J Virol. 2002;76:5720-8.

Eichinger KM, Egana L, Orend JG, Resetar E, Anderson KB, Patel R, et al. Alveolar macrophages support interferon gamma-mediated viral clearance in RSV-infected neonatal mice. Respir Res. 2015;16:122.

Erlandsson L, Blumenthal R, Eloranta ML, Engel H, Alm G, Weiss S, et al. Interferon-beta is required for interferon-alpha production in mouse fibroblasts. Curr Biol. 1998;8:223-6.

Fantetti KN, Gray EL, Ganesan P, Kulkarni A, O'Donnell LA. Interferon gamma protects neonatal neural stem/progenitor cells during measles virus infection of the brain. J Neuroinflammation. 2016;13:107.

Fernandes A, Miller-Fleming L, Pais TF. Microglia and inflammation: conspiracy, controversy or control? Cell Mol Life Sci. 2014;71:3969-85.

Ferreira CS, Frenzke M, Leonard VH, Welstead GG, Richardson CD, Cattaneo R. Measles virus infection of alveolar macrophages and dendritic cells precedes spread to lymphatic organs in transgenic mice expressing human signaling lymphocytic activation molecule (SLAM, CD150). J Virol. 2010;84:3033-42.

Fisher DL, Defres S, Solomon T. Measles-induced encephalitis. QJM. 2015;108:177-82.

Forest F, Duband S, Pillet S, Stachowicz ML, Cornillon J, Dumollard JM, et al. Lethal human herpesvirus-6 encephalitis after cord blood transplant. Transpl Infect Dis. 2011;13:646-9.

Forsthuber T, Yip HC, Lehmann PV. Induction of TH1 and TH2 immunity in neonatal mice. Science. 1996;271:1728-30.

Fragkoudis R, Ballany CM, Boyd A, Fazakerley JK. In Semliki Forest virus encephalitis, antibody rapidly clears infectious virus and is required to eliminate viral material from the brain, but is not required to generate lesions of demyelination. J Gen Virol. 2008;89:2565-8.

Frei R, Steinle J, Birchler T, Loeliger S, Roduit C, Steinhoff D, et al. MHC class II molecules enhance Toll-like receptor mediated innate immune responses. PLoS One. 2010;5:e8808.

Fugier-Vivier I, Servet-Delprat C, Rivailler P, Rissoan MC, Liu YJ, Rabourdin-Combe C. Measles virus suppresses cell-mediated immunity by interfering with the survival and functions of dendritic and T cells. J Exp Med. 1997;186:813-23.

Furr SR, Chauhan VS, Sterka D, Jr., Grdzelishvili V, Marriott I. Characterization of retinoic acid-inducible gene-I expression in primary murine glia following exposure to vesicular stomatitis virus. J Neurovirol. 2008;14:503-13.

Ginhoux F, Greter M, Leboeuf M, Nandi S, See P, Gokhan S, et al. Fate mapping analysis reveals that adult microglia derive from primitive macrophages. Science. 2010;330:841-5.

Gonzalez-Dosal R, Horan KA, Rahbek SH, Ichijo H, Chen ZJ, Mieyal JJ, et al. HSV infection induces production of ROS, which potentiate signaling from pattern recognition receptors: role for S-glutathionylation of TRAF3 and 6. PLoS Pathog. 2011;7:e1002250.

Goodbourn S, Didcock L, Randall RE. Interferons: cell signalling, immune modulation, antiviral response and virus countermeasures. J Gen Virol. 2000;81:2341-64.

Griffin D, Levine B, Tyor W, Ubol S, Despres P. The role of antibody in recovery from alphavirus encephalitis. Immunol Rev. 1997;159:155-61.

Griffin DE. Measles virus-induced suppression of immune responses. Immunol Rev. 2010;236:176-89.

Griffin DE, Pan CH, Moss WJ. Measles vaccines. Frontiers in bioscience : a journal and virtual library. 2008;13:1352-70.

Grosjean I, Caux C, Bella C, Berger I, Wild F, Banchereau J, et al. Measles virus infects human dendritic cells and blocks their allostimulatory properties for CD4+ T cells. J Exp Med. 1997;186:801-12.

Gu L, Tseng S, Horner RM, Tam C, Loda M, Rollins BJ. Control of TH2 polarization by the chemokine monocyte chemoattractant protein-1. Nature. 2000;404:407-11.

Guo Y, Audry M, Ciancanelli M, Alsina L, Azevedo J, Herman M, et al. Herpes simplex virus encephalitis in a patient with complete TLR3 deficiency: TLR3 is otherwise redundant in protective immunity. J Exp Med. 2011;208:2083-98.

Hahm B, Arbour N, Oldstone MB. Measles virus interacts with human SLAM receptor on dendritic cells to cause immunosuppression. Virology. 2004;323:292-302.

Hamo L, Stohlman SA, Otto-Duessel M, Bergmann CC. Distinct regulation of MHC molecule expression on astrocytes and microglia during viral encephalomyelitis. Glia. 2007;55:1169-77.

Harker JA, Lee DC, Yamaguchi Y, Wang B, Bukreyev A, Collins PL, et al. Delivery of cytokines by recombinant virus in early life alters the immune response to adult lung infection. J Virol. 2010;84:5294-302.

Hausmann J, Pagenstecher A, Baur K, Richter K, Rziha HJ, Staeheli P. CD8 T cells require gamma interferon to clear borna disease virus from the brain and prevent immune system-mediated neuronal damage. J Virol. 2005;79:13509-18.

Hayasaka D, Shirai K, Aoki K, Nagata N, Simantini DS, Kitaura K, et al. TNF-alpha acts as an immunoregulator in the mouse brain by reducing the incidence of severe disease following Japanese encephalitis virus infection. PLoS One. 2013;8:e71643.

Heise MT, Virgin HWt. The T-cell-independent role of gamma interferon and tumor necrosis factor alpha in macrophage activation during murine cytomegalovirus and herpes simplex virus infections. J Virol. 1995;69:904-9.

Hibbert L, Pflanz S, De Waal Malefyt R, Kastelein RA. IL-27 and IFN-alpha signal via Stat1 and Stat3 and induce T-Bet and IL-12Rbeta2 in naive T cells. J Interferon Cytokine Res. 2003;23:513-22.

Hoffmann B, Tappe D, Hoper D, Herden C, Boldt A, Mawrin C, et al. A Variegated Squirrel Bornavirus Associated with Fatal Human Encephalitis. N Engl J Med. 2015;373:154-62.

Holmgren AM, Miller KD, Cavanaugh SE, Rall GF. Bst2/Tetherin Is Induced in Neurons by Type I Interferon and Viral Infection but Is Dispensable for Protection against Neurotropic Viral Challenge. J Virol. 2015;89:11011-8.

Hooper DC, Phares TW, Fabis MJ, Roy A. The production of antibody by invading B cells is required for the clearance of rabies virus from the central nervous system. PLoS Negl Trop Dis. 2009;3:e535.

Horikami SM, Moyer SA. Synthesis of leader RNA and editing of the P mRNA during transcription by purified measles virus. J Virol. 1991;65:5342-7.

Hou W, Kang HS, Kim BS. Th17 cells enhance viral persistence and inhibit T cell cytotoxicity in a model of chronic virus infection. J Exp Med. 2009;206:313-28.

Howe CL, Lafrance-Corey RG, Sundsbak RS, Sauer BM, Lafrance SJ, Buenz EJ, et al. Hippocampal protection in mice with an attenuated inflammatory monocyte response to acute CNS picornavirus infection. Sci Rep. 2012;2:545.

Hua LL, Liu JS, Brosnan CF, Lee SC. Selective inhibition of human glial inducible nitric oxide synthase by interferon-beta: implications for multiple sclerosis. Ann Neurol. 1998;43:384-7.

Ito Y, Kimura H, Yabuta Y, Ando Y, Murakami T, Shiomi M, et al. Exacerbation of herpes simplex encephalitis after successful treatment with acyclovir. Clin Infect Dis. 2000;30:185-7.

Jang H, Boltz DA, Webster RG, Smeyne RJ. Viral parkinsonism. Biochim Biophys Acta. 2009;1792:714-21.

Jeong ES, Won YS, Kim HC, Cho MH, Choi YK. Role of IL-10 deficiency in pneumonia induced by Corynebacterium kutscheri in mice. J Microbiol Biotechnol. 2009;19:424-30.

Jones CA, Fernandez M, Herc K, Bosnjak L, Miranda-Saksena M, Boadle RA, et al. Herpes simplex virus type 2 induces rapid cell death and functional impairment of murine dendritic cells in vitro. J Virol. 2003;77:11139-49.

Kallfass C, Ackerman A, Lienenklaus S, Weiss S, Heimrich B, Staeheli P. Visualizing production of beta interferon by astrocytes and microglia in brain of La Crosse virus-infected mice. J Virol. 2012;86:11223-30.

Kawai T, Akira S. Toll-like receptor and RIG-I-like receptor signaling. Ann N Y Acad Sci. 2008;1143:1-20.

Khandaker GM, Zimbron J, Lewis G, Jones PB. Prenatal maternal infection, neurodevelopment and adult schizophrenia: a systematic review of population-based studies. Psychol Med. 2013;43:239-57.

Kierdorf K, Erny D, Goldmann T, Sander V, Schulz C, Perdiguero EG, et al. Microglia emerge from erythromyeloid precursors via Pu.1- and Irf8-dependent pathways. Nat Neurosci. 2013;16:273-80.

Kim MY, Shu Y, Carsillo T, Zhang J, Yu L, Peterson C, et al. hsp70 and a novel axis of type I interferon-dependent antiviral immunity in the measles virus-infected brain. J Virol. 2013;87:998-1009.

King NJ, Getts DR, Getts MT, Rana S, Shrestha B, Kesson AM. Immunopathology of flavivirus infections. Immunol Cell Biol. 2007;85:33-42.

Kollmann TR, Levy O, Montgomery RR, Goriely S. Innate immune function by Toll-like receptors: distinct responses in newborns and the elderly. Immunity. 2012;37:771-83.

Komatsu T, Bi Z, Reiss CS. Interferon-gamma induced type I nitric oxide synthase activity inhibits viral replication in neurons. J Neuroimmunol. 1996;68:101-8.

Kopp SJ, Ranaivo HR, Wilcox DR, Karaba AH, Wainwright MS, Muller WJ. Herpes simplex virus serotype and entry receptor availability alter CNS disease in a mouse model of neonatal HSV. Pediatr Res. 2014;76:528-34.

Lambert L, Sagfors AM, Openshaw PJ, Culley FJ. Immunity to RSV in Early-Life. Front Immunol. 2014;5:466.

Landreau F, Galeano P, Caltana LR, Masciotra L, Chertcoff A, Pontoriero A, et al. Effects of two commonly found strains of influenza A virus on developing dopaminergic neurons, in relation to the pathophysiology of schizophrenia. PLoS One. 2012;7:e51068.

Larena M, Regner M, Lobigs M. Cytolytic effector pathways and IFN-gamma help protect against Japanese encephalitis. Eur J Immunol. 2013;43:1789-98.

Larranaga CL, Ampuero SL, Luchsinger VF, Carrion FA, Aguilar NV, Morales PR, et al. Impaired immune response in severe human lower tract respiratory infection by respiratory syncytial virus. The Pediatric infectious disease journal. 2009;28:867-73.

Lauwerys BR, Garot N, Renauld JC, Houssiau FA. Cytokine production and killer activity of NK/T-NK cells derived with IL-2, IL-15, or the combination of IL-12 and IL-18. J Immunol. 2000;165:1847-53.

Lawrence DM, Vaughn MM, Belman AR, Cole JS, Rall GF. Immune response-mediated protection of adult but not neonatal mice from neuron-restricted measles virus infection and central nervous system disease. J Virol. 1999;73:1795-801.

Lee EY, Schultz KL, Griffin DE. Mice deficient in interferon-gamma or interferon-gamma receptor 1 have distinct inflammatory responses to acute viral encephalomyelitis. PLoS One. 2013;8:e76412.

Lee PT, Holt PG, McWilliam AS. Failure of MHC class II expression in neonatal alveolar macrophages: potential role of class II transactivator. Eur J Immunol. 2001;31:2347-56.

Lee YC, Lin SJ. Neonatal natural killer cell function: relevance to antiviral immune defense. Clinical & developmental immunology. 2013;2013:427696.

Lemon K, de Vries RD, Mesman AW, McQuaid S, van Amerongen G, Yuksel S, et al. Early target cells of measles virus after aerosol infection of non-human primates. PLoS Pathog. 2011;7:e1001263.

Lester SN, Li K. Toll-like receptors in antiviral innate immunity. J Mol Biol. 2014;426:1246-64.

Levine B, Hardwick JM, Trapp BD, Crawford TO, Bollinger RC, Griffin DE. Antibody-mediated clearance of alphavirus infection from neurons. Science. 1991;254:856-60.

Li L, Lee HH, Bell JJ, Gregg RK, Ellis JS, Gessner A, et al. IL-4 utilizes an alternative receptor to drive apoptosis of Th1 cells and skews neonatal immunity toward Th2. Immunity. 2004;20:429-40.

Libbey JE, Fujinami RS. Adaptive immune response to viral infections in the central nervous system. Handb Clin Neurol. 2014;123:225-47.

Licon Luna RM, Lee E, Mullbacher A, Blanden RV, Langman R, Lobigs M. Lack of both Fas ligand and perforin protects from flavivirus-mediated encephalitis in mice. J Virol. 2002;76:3202-11.

Ljunggren HG, Malmberg KJ. Prospects for the use of NK cells in immunotherapy of human cancer. Nat Rev Immunol. 2007;7:329-39.

Loo YM, Gale M, Jr. Immune signaling by RIG-I-like receptors. Immunity. 2011;34:680-92.

Lu HT, Riley JL, Babcock GT, Huston M, Stark GR, Boss JM, et al. Interferon (IFN) beta acts downstream of IFN-gamma-induced class II transactivator messenger RNA accumulation to block major histocompatibility complex class II gene expression and requires the 48-kD DNA-binding protein, ISGF3-gamma. J Exp Med. 1995;182:1517-25.

Ludlow M, Kortekaas J, Herden C, Hoffmann B, Tappe D, Trebst C, et al. Neurotropic virus infections as the cause of immediate and delayed neuropathology. Acta Neuropathol. 2016;131:159-84.

Ludlow M, Lemon K, de Vries RD, McQuaid S, Millar EL, van Amerongen G, et al. Measles virus infection of epithelial cells in the macaque upper respiratory tract is mediated by subepithelial immune cells. J Virol. 2013;87:4033-42.

Lull ME, Block ML. Microglial activation and chronic neurodegeneration. Neurotherapeutics. 2010;7:354-65.

Malvoisin E, Wild TF. Measles virus glycoproteins: studies on the structure and interaction of the haemagglutinin and fusion proteins. J Gen Virol. 1993;74 (Pt 11):2365-72.

Manchester M, Eto DS, Oldstone MB. Characterization of the inflammatory response during acute measles encephalitis in NSE-CD46 transgenic mice. J Neuroimmunol. 1999;96:207-17.

Manchester M, Rall GF. Model Systems: transgenic mouse models for measles pathogenesis. Trends Microbiol. 2001;9:19-23.

Mantovani A, Cassatella MA, Costantini C, Jaillon S. Neutrophils in the activation and regulation of innate and adaptive immunity. Nat Rev Immunol. 2011;11:519-31.

Mariscalco MM, Tcharmtchi MH, Smith CW. P-Selectin support of neonatal neutrophil adherence under flow: contribution of L-selectin, LFA-1, and ligand(s) for P-selectin. Blood. 1998;91:4776-85.

Marodi L. Neonatal innate immunity to infectious agents. Infect Immun. 2006;74:1999-2006.

Marr N, Wang TI, Kam SH, Hu YS, Sharma AA, Lam A, et al. Attenuation of respiratory syncytial virus-induced and RIG-I-dependent type I IFN responses in human neonates and very young children. J Immunol. 2014;192:948-57.

McArthur JC. HIV dementia: an evolving disease. J Neuroimmunol. 2004;157:3-10.

McCarthy MK, Procario MC, Twisselmann N, Wilkinson JE, Archambeau AJ, Michele DE, et al. Proinflammatory effects of interferon gamma in mouse adenovirus 1 myocarditis. J Virol. 2015;89:468-79.

McLaurin J, Antel JP, Yong VW. Immune and non-immune actions of interferon-beta-Ib on primary human neural cells. Mult Scler. 1995;1:10-9.

Melvan JN, Bagby GJ, Welsh DA, Nelson S, Zhang P. Neonatal sepsis and neutrophil insufficiencies. Int Rev Immunol. 2010;29:315-48.

Merrill JE, Kono DH, Clayton J, Ando DG, Hinton DR, Hofman FM. Inflammatory leukocytes and cytokines in the peptide-induced disease of experimental allergic encephalomyelitis in SJL and B10.PL mice. Proc Natl Acad Sci U S A. 1992;89:574-8.

Mesman AW, de Vries RD, McQuaid S, Duprex WP, de Swart RL, Geijtenbeek TB. A prominent role for DC-SIGN+ dendritic cells in initiation and dissemination of measles virus infection in non-human primates. PLoS One. 2012;7:e49573.

Mildner A, Mack M, Schmidt H, Bruck W, Djukic M, Zabel MD, et al. CCR2+Ly-6Chi monocytes are crucial for the effector phase of autoimmunity in the central nervous system. Brain. 2009;132:2487-500.

Miller KD, Schnell MJ, Rall GF. Keeping it in check: chronic viral infection and antiviral immunity in the brain. Nat Rev Neurosci. 2016;17:766-76.

Mina MJ, Metcalf CJ, de Swart RL, Osterhaus AD, Grenfell BT. Long-term measles-induced immunomodulation increases overall childhood infectious disease mortality. Science. 2015;348:694-9.

Mizuno T, Zhang G, Takeuchi H, Kawanokuchi J, Wang J, Sonobe Y, et al. Interferon-gamma directly induces neurotoxicity through a neuron specific, calcium-permeable complex of IFN-gamma receptor and AMPA GluR1 receptor. FASEB J. 2008;22:1797-806.

Moore KW, de Waal Malefyt R, Coffman RL, O'Garra A. Interleukin-10 and the interleukin-10 receptor. Annu Rev Immunol. 2001;19:683-765.

Moss WJ, Griffin DE. Global measles elimination. Nat Rev Microbiol. 2006;4:900-8.

Moss WJ, Griffin DE. Measles. Lancet. 2012;379:153-64.

Muhl H, Pfeilschifter J. Anti-inflammatory properties of pro-inflammatory interferon-gamma. Int Immunopharmacol. 2003;3:1247-55.

Muhlebach MD, Mateo M, Sinn PL, Prufer S, Uhlig KM, Leonard VH, et al. Adherens junction protein nectin-4 is the epithelial receptor for measles virus. Nature. 2011;480:530-3.

Munir S, Hillyer P, Le Nouen C, Buchholz UJ, Rabin RL, Collins PL, et al. Respiratory syncytial virus interferon antagonist NS1 protein suppresses and skews the human T lymphocyte response. PLoS Pathog. 2011;7:e1001336.

Murabayashi N, Kurita-Taniguchi M, Ayata M, Matsumoto M, Ogura H, Seya T. Susceptibility of human dendritic cells (DCs) to measles virus (MV) depends on their activation stages in conjunction with the level of CDw150: role of Toll stimulators in DC maturation and MV amplification. Microbes and infection / Institut Pasteur. 2002;4:785-94.

Muscat M, Bang H, Wohlfahrt J, Glismann S, Molbak K, Group EN. Measles in Europe: an epidemiological assessment. Lancet. 2009;373:383-9.

Mustafa MM, Weitman SD, Winick NJ, Bellini WJ, Timmons CF, Siegel JD. Subacute measles encephalitis in the young immunocompromised host: report of two cases diagnosed by polymerase chain reaction and treated with ribavirin and review of the literature. Clin Infect Dis. 1993;16:654-60.

Mutnal MB, Cheeran MC, Hu S, Little MR, Lokensgard JR. Excess neutrophil infiltration during cytomegalovirus brain infection of interleukin-10-deficient mice. J Neuroimmunol. 2010;227:101-10.

Mutnal MB, Hu S, Lokensgard JR. Persistent humoral immune responses in the CNS limit recovery of reactivated murine cytomegalovirus. PLoS One. 2012;7:e33143.

Myrick C, DiGuisto R, DeWolfe J, Bowen E, Kappler J, Marrack P, et al. Linkage analysis of variations in CD4:CD8 T cell subsets between C57BL/6 and DBA/2. Genes Immun. 2002;3:144-50.

Navaratnarajah CK, Leonard VH, Cattaneo R. Measles virus glycoprotein complex assembly, receptor attachment, and cell entry. Curr Top Microbiol Immunol. 2009;329:59-76.

Nazmi A, Dutta K, Basu A. RIG-I mediates innate immune response in mouse neurons following Japanese encephalitis virus infection. PLoS One. 2011;6:e21761.

Nishikomori R, Usui T, Wu CY, Morinobu A, O'Shea JJ, Strober W. Activated STAT4 has an essential role in Th1 differentiation and proliferation that is independent of its role in the maintenance of IL-12R beta 2 chain expression and signaling. J Immunol. 2002;169:4388-98.

Novelli F, Casanova JL. The role of IL-12, IL-23 and IFN-gamma in immunity to viruses. Cytokine & growth factor reviews. 2004;15:367-77.

Noyce RS, Richardson CD. Nectin 4 is the epithelial cell receptor for measles virus. Trends Microbiol. 2012;20:429-39.

O'Donnell LA, Conway S, Rose RW, Nicolas E, Slifker M, Balachandran S, et al. STAT1-independent control of a neurotropic measles virus challenge in primary neurons and infected mice. J Immunol. 2012;188:1915-23.

O'Donnell LA, Henkins KM, Kulkarni A, Matullo CM, Balachandran S, Pattisapu AK, et al. Interferon Gamma Induces Protective Non-Canonical Signaling Pathways in Primary Neurons. J Neurochem. 2015.

O'Donnell LA, Rall GF. Blue moon neurovirology: the merits of studying rare CNS diseases of viral origin. Journal of neuroimmune pharmacology : the official journal of the Society on NeuroImmune Pharmacology. 2010;5:443-55.

O'Keefe GM, Nguyen VT, Benveniste EN. Regulation and function of class II major histocompatibility complex, CD40, and B7 expression in macrophages and microglia: Implications in neurological diseases. J Neurovirol. 2002;8:496-512.

Olson MR, Hartwig SM, Varga SM. The number of respiratory syncytial virus (RSV)-specific memory CD8 T cells in the lung is critical for their ability to inhibit RSV vaccine-enhanced pulmonary eosinophilia. J Immunol. 2008;181:7958-68.

Olson MR, Varga SM. CD8 T cells inhibit respiratory syncytial virus (RSV) vaccine-enhanced disease. J Immunol. 2007;179:5415-24.

Paludan SR, Bowie AG, Horan KA, Fitzgerald KA. Recognition of herpesviruses by the innate immune system. Nat Rev Immunol. 2011;11:143-54.

Paolini R, Bernardini G, Molfetta R, Santoni A. NK cells and interferons. Cytokine Growth Factor Rev. 2015;26:113-20.

Parra B, Hinton DR, Marten NW, Bergmann CC, Lin MT, Yang CS, et al. IFN-gamma is required for viral clearance from central nervous system oligodendroglia. J Immunol. 1999;162:1641-7.

Patterson CE, Lawrence DM, Echols LA, Rall GF. Immune-mediated protection from measles virus-induced central nervous system disease is noncytolytic and gamma interferon dependent. J Virol. 2002;76:4497-506.

Perry AK, Chen G, Zheng D, Tang H, Cheng G. The host type I interferon response to viral and bacterial infections. Cell Res. 2005;15:407-22.

Perry RT, Halsey NA. The clinical significance of measles: a review. J Infect Dis. 2004;189 Suppl 1:S4-16.

Phares TW, Stohlman SA, Hwang M, Min B, Hinton DR, Bergmann CC. CD4 T cells promote CD8 T cell immunity at the priming and effector site during viral encephalitis. J Virol. 2012;86:2416-27.

Poli A, Kmiecik J, Domingues O, Hentges F, Blery M, Chekenya M, et al. NK cells in central nervous system disorders. J Immunol. 2013;190:5355-62.

Pott J, Stockinger S, Torow N, Smoczek A, Lindner C, McInerney G, et al. Age-dependent TLR3 expression of the intestinal epithelium contributes to rotavirus susceptibility. PLoS Pathog. 2012;8:e1002670.

Powell TJ, Jr., Streilein JW. Neonatal tolerance induction by class II alloantigens activates IL-4-secreting, tolerogen-responsive T cells. J Immunol. 1990;144:854-9.

Prinz M, Priller J, Sisodia SS, Ransohoff RM. Heterogeneity of CNS myeloid cells and their roles in neurodegeneration. Nat Neurosci. 2011;14:1227-35.

Rall GF, Manchester M, Daniels LR, Callahan EM, Belman AR, Oldstone MB. A transgenic mouse model for measles virus infection of the brain. Proc Natl Acad Sci U S A. 1997;94:4659-63.

Ransohoff RM, Brown MA. Innate immunity in the central nervous system. J Clin Invest. 2012;122:1164-71.

Reith W, LeibundGut-Landmann S, Waldburger JM. Regulation of MHC class II gene expression by the class II transactivator. Nat Rev Immunol. 2005;5:793-806.

Renno T, Krakowski M, Piccirillo C, Lin JY, Owens T. TNF-alpha expression by resident microglia and infiltrating leukocytes in the central nervous system of mice with experimental allergic encephalomyelitis. Regulation by Th1 cytokines. J Immunol. 1995;154:944-53.

Richard JL, Masserey Spicher V. Large measles epidemic in Switzerland from 2006 to 2009: consequences for the elimination of measles in Europe. Euro Surveill. 2009;14.

Rima BK, Duprex WP. The measles virus replication cycle. Curr Top Microbiol Immunol. 2009;329:77-102.

Rock RB, Hu S, Deshpande A, Munir S, May BJ, Baker CA, et al. Transcriptional response of human microglial cells to interferon-gamma. Genes Immun. 2005;6:712-9.

Rosendahl Huber S, van Beek J, de Jonge J, Luytjes W, van Baarle D. T cell responses to viral infections - opportunities for Peptide vaccination. Front Immunol. 2014;5:171.

Rouse BT, Sehrawat S. Immunity and immunopathology to viruses: what decides the outcome? Nat Rev Immunol. 2010;10:514-26.

Sas AR, Bimonte-Nelson H, Smothers CT, Woodward J, Tyor WR. Interferon-alpha causes neuronal dysfunction in encephalitis. J Neurosci. 2009;29:3948-55.

Sas AR, Bimonte-Nelson HA, Tyor WR. Cognitive dysfunction in HIV encephalitic SCID mice correlates with levels of Interferon-alpha in the brain. AIDS. 2007;21:2151-9.

Schneider-Schaulies J, Meulen V, Schneider-Schaulies S. Measles infection of the central nervous system. J Neurovirol. 2003;9:247-52.

Schoggins JW, Wilson SJ, Panis M, Murphy MY, Jones CT, Bieniasz P, et al. A diverse range of gene products are effectors of the type I interferon antiviral response. Nature. 2011;472:481-5.

Shibeshi ME, Masresha BG, Smit SB, Biellik RJ, Nicholson JL, Muitherero C, et al. Measles resurgence in southern Africa: challenges to measles elimination. Vaccine. 2014;32:1798-807.

Shingai M, Ebihara T, Begum NA, Kato A, Honma T, Matsumoto K, et al. Differential type I IFN-inducing abilities of wild-type versus vaccine strains of measles virus. J Immunol. 2007;179:6123-33.

Singh RR, Hahn BH, Sercarz EE. Neonatal peptide exposure can prime T cells and, upon subsequent immunization, induce their immune deviation: implications for antibody vs. T cell-mediated autoimmunity. J Exp Med. 1996;183:1613-21.

Slavica L, Nordstrom I, Karlsson MN, Valadi H, Kacerovsky M, Jacobsson B, et al. TLR3 impairment in human newborns. J Leukoc Biol. 2013;94:1003-11.

Solomos AC, O'Regan KJ, Rall GF. CD4+ T cells require either B cells or CD8+ T cells to control spread and pathogenesis of a neurotropic infection. Virology. 2016;499:196-202.

Sorgeloos F, Kreit M, Hermant P, Lardinois C, Michiels T. Antiviral type I and type III interferon responses in the central nervous system. Viruses. 2013;5:834-57.

Stifter SA, Bhattacharyya N, Pillay R, Florido M, Triccas JA, Britton WJ, et al. Functional Interplay between Type I and II Interferons Is Essential to Limit Influenza A Virus-Induced Tissue Inflammation. PLoS Pathog. 2016;12:e1005378.

Stohlman SA, Bergmann CC, Lin MT, Cua DJ, Hinton DR. CTL effector function within the central nervous system requires CD4+ T cells. J Immunol. 1998;160:2896-904.

Stout-Delgado HW, Du W, Shirali AC, Booth CJ, Goldstein DR. Aging promotes neutrophil-induced mortality by augmenting IL-17 production during viral infection. Cell Host Microbe. 2009;6:446-56.

Stowe AM, Adair-Kirk TL, Gonzales ER, Perez RS, Shah AR, Park TS, et al. Neutrophil elastase and neurovascular injury following focal stroke and reperfusion. Neurobiol Dis. 2009;35:82-90.

Stubblefield Park SR, Widness M, Levine AD, Patterson CE. T cell-, interleukin-12-, and gamma interferon-driven viral clearance in measles virus-infected brain tissue. J Virol. 2011;85:3664-76.

Suh HS, Brosnan CF, Lee SC. Toll-like receptors in CNS viral infections. Curr Top Microbiol Immunol. 2009;336:63-81.

Takeuchi O, Akira S. Innate immunity to virus infection. Immunol Rev. 2009;227:75-86.

Tanabe M, Kurita-Taniguchi M, Takeuchi K, Takeda M, Ayata M, Ogura H, et al. Mechanism of up-regulation of human Toll-like receptor 3 secondary to infection of measles virus-attenuated strains. Biochem Biophys Res Commun. 2003;311:39-48.

Tarassishin L, Suh HS, Lee SC. Interferon regulatory factor 3 plays an anti-inflammatory role in microglia by activating the PI3K/Akt pathway. J Neuroinflammation. 2011;8:187.

Thaney VE, O'Neill AM, Hoefer MM, Maung R, Sanchez AB, Kaul M. IFNbeta Protects Neurons from Damage in a Murine Model of HIV-1 Associated Brain Injury. Sci Rep. 2017;7:46514.

Thompson C, Whitley R. Neonatal herpes simplex virus infections: where are we now? Adv Exp Med Biol. 2011;697:221-30.

Tishon A, Lewicki H, Andaya A, McGavern D, Martin L, Oldstone MB. CD4 T cell control primary measles virus infection of the CNS: regulation is dependent on combined activity with either CD8 T cells or with B cells: CD4, CD8 or B cells alone are ineffective. Virology. 2006;347:234-45.

Trandem K, Jin Q, Weiss KA, James BR, Zhao J, Perlman S. Virally expressed interleukin-10 ameliorates acute encephalomyelitis and chronic demyelination in coronavirus-infected mice. J Virol. 2011a;85:6822-31.

Trandem K, Zhao J, Fleming E, Perlman S. Highly activated cytotoxic CD8 T cells express protective IL-10 at the peak of coronavirus-induced encephalitis. J Immunol. 2011b;186:3642-52.

Tripp RA, Hou S, McMickle A, Houston J, Doherty PC. Recruitment and proliferation of CD8+ T cells in respiratory virus infections. J Immunol. 1995;154:6013-21.

Trujillo JA, Fleming EL, Perlman S. Transgenic CCL2 expression in the central nervous system results in a dysregulated immune response and enhanced lethality after coronavirus infection. J Virol. 2013;87:2376-89.

Tun MM, Aoki K, Senba M, Buerano CC, Shirai K, Suzuki R, et al. Protective role of TNF-alpha, IL-10 and IL-2 in mice infected with the Oshima strain of Tick-borne encephalitis virus. Sci Rep. 2014;4:5344.

Utley TF, Ogden JA, Gibb A, McGrath N, Anderson NE. The long-term neuropsychological outcome of herpes simplex encephalitis in a series of unselected survivors. Neuropsychiatry Neuropsychol Behav Neurol. 1997;10:180-9.

van den Pol AN, Reuter JD, Santarelli JG. Enhanced cytomegalovirus infection of developing brain independent of the adaptive immune system. J Virol. 2002;76:8842-54.

Vivier E, Tomasello E, Baratin M, Walzer T, Ugolini S. Functions of natural killer cells. Nat Immunol. 2008;9:503-10.

Volpe JJ. Neurology of the Newborn: Saunders/Elsevier; 2008.

Wensky AK, Furtado GC, Marcondes MC, Chen S, Manfra D, Lira SA, et al. IFN-gamma determines distinct clinical outcomes in autoimmune encephalomyelitis. J Immunol. 2005;174:1416-23.

Willenborg DO, Fordham SA, Staykova MA, Ramshaw IA, Cowden WB. IFN-gamma is critical to the control of murine autoimmune encephalomyelitis and regulates both in the periphery and in the target tissue: a possible role for nitric oxide. J Immunol. 1999;163:5278-86.

Yoneyama M, Kikuchi M, Natsukawa T, Shinobu N, Imaizumi T, Miyagishi M, et al. The RNA helicase RIG-I has an essential function in double-stranded RNA-induced innate antiviral responses. Nat Immunol. 2004;5:730-7.

Yount JS, Moran TM, Lopez CB. Cytokine-independent upregulation of MDA5 in viral infection. J Virol. 2007;81:7316-9.

Zaghouani H, Hoeman CM, Adkins B. Neonatal immunity: faulty T-helpers and the shortcomings of dendritic cells. Trends Immunol. 2009;30:585-91.

Zalinger ZB, Elliott R, Rose KM, Weiss SR. MDA5 Is Critical to Host Defense during Infection with Murine Coronavirus. J Virol. 2015;89:12330-40.

Zaritsky LA, Gama L, Clements JE. Canonical type I IFN signaling in simian immunodeficiency virus-infected macrophages is disrupted by astrocyte-secreted CCL2. J Immunol. 2012;188:3876-85.

Zhang SY, Jouanguy E, Ugolini S, Smahi A, Elain G, Romero P, et al. TLR3 deficiency in patients with herpes simplex encephalitis. Science. 2007;317:1522-7.

Zhou J, Stohlman SA, Hinton DR, Marten NW. Neutrophils promote mononuclear cell infiltration during viral-induced encephalitis. J Immunol. 2003;170:3331-6.

Zhou Y, Ye L, Wan Q, Zhou L, Wang X, Li J, et al. Activation of Toll-like receptors inhibits herpes simplex virus-1 infection of human neuronal cells. J Neurosci Res. 2009;87:2916-25.